The Dissertation Committee for Kara Rachelle Barber Certifies that this is the approved version of the following dissertation:

The Role of Presynaptic Par-1 Kinase in Regulating the Localization of Active Zone Protein BRP

Committee:

Thomas Green

Giulio Taglialatela

Shao Jun Tang

Yan Chen

Catherine Collins

Yogesh Wairkar

Dean, Graduate School

The Role of Presynaptic Par-1 Kinase in Regulating the Localization of Active Zone Protein BRP

by

Kara Rachelle Barber, B.S.

Dissertation

Presented to the Faculty of the Graduate School of

The University of Texas Medical Branch

in Partial Fulfillment

of the Requirements

for the Degree of

Doctor of Philosophy

The University of Texas Medical Branch

August, 2018

Dedication

This dissertation is dedicated to my husband Mohanad Al-Obaidi for his love and support throughout this process. Love you.

Acknowledgments

I want to thank my family, Dad, Rhonda, Mom, Rick, Kory, and Katie for their love, support, and encouragement. Also, I would like to thank my husband Mohanad and my parents-in-law Mohammed and Ibtisam.

Secondly, I would like to thank all members of the Wairkar lab past and present. Jade Martinez and Keegan Bush, thank you for sticking with me until the end.

Aurora Galvan and Owen Hamill, thank you for all you do for the Neuroscience Graduate Program. Also, all my fellow graduate students and friends at UTMB, especially Claudia Marino. Thank you for your company on long days and weekends in the lab and our many shopping trips to unwind.

Martin Hrusak, Matthew Dalva, Irwin Levitan, Hong Fei, Michael Sherman, and Michael Woodson thank you for collaborating and your inputs into my manuscripts.

I would also like to acknowledge those who served on my advisory committee, Drs., Thomas Green, Giulio Taglialatela, Shao Jun Tang, Yan Chen, and Catherine Collins. Thank you for always being supportive and guiding me through my project.

Lastly, I would like to thank my mentor, Yogi Wairkar. Your mentorship, expertise, and persistence have been the key to my success. You inspire me to pursue science diligently and to become a dedicated mentor to future scientists.

The Role of Presynaptic Par-1 Kinase in Regulating the Localization of Active Zone Protein BRP

Publication No._____

Kara Rachelle Barber, Ph.D.

The University of Texas Medical Branch, 2018

Supervisor: Yogesh Wairkar

Precise localization of synaptic proteins is required for proper synaptic function, which is compromised in many neurodevelopmental and neurodegenerative diseases. Since proteins that reside at the active zones are used most frequently during synaptic transmission, they must be continuously replenished to maintain active zones. Therefore, the trafficking of these proteins plays an essential role in replenishing these vital components necessary for the health of active zones. While the trafficking and localization of synaptic vesicles and mitochondria are relatively well understood, little is known about the mechanisms that regulate the localization of protein components localized to active zones.

In this dissertation, I show that mechanisms involved in transporting proteins destined to active zones are distinct from those that transport synaptic vesicles or mitochondria. Further, imprecise levels of presynaptic Par-1 kinase disrupt the transport of Bruchpilot- an essential active zone scaffolding protein in *Drosophila* and leads to its accumulation of BRP in axons at the expense of BRP at active zones. Ultimately, the loss of BRP at active zones results in reduced synaptic transmission. Temporal analysis

demonstrated that accumulation of BRP within the axons precedes the loss of synaptic function and its depletion from the active zones. Mechanistically, my data suggest that Par-1 co-localizes with BRP and is present in the same complex as BRP, raising the possibility of a novel mechanism for selective localization of BRP. Taken together, these data suggest an intriguing possibility that mislocalization of active zone proteins like BRP might be one of the earliest signs of perturbation of synapses that precede many neurological disorders.

TABLE OF CONTENTS

List of Figures

List of Abbreviations

Aβ:	Amyloid beta
AD:	Alzheimer's Disease
AMPK:	Adenosine monophosphate-activated protein kinase
ASD:	Autism Spectrum Disorders
AZ:	Active Zone
BRP:	Bruchpilot
CAST:	Cytomatrix at the Active Zone Protein
CAZ:	Cytomatrix at the AZ
Dlg:	Disc Large
EJP:	Excitatory Junction Potential
FTD:	Frontotemporal Dementia
HRP:	Horse Radish Peroxidase
KA1:	Kinase-associated Domain
KXGS:	Lys-X-Gly-Ser
$LKB1^{OE}$:	Overexpression of LKB1
MAPs:	Microtubule Associated Proteins
MARK:	Microtubule Affinity Regulating Kinases
mEJPs:	Mini Excitatory Junction Potentials
NFT:	Neurofibrillary tangles
NMJ:	Neuromuscular Junction
Par-1:	Partitioning-defective 1

Par-1^{OE}:	Overexpression of Par-1
Par-1^{T408A}:	Overexpression of inactive Par-1
Par-1^{RNAi}:	RNAi knockdown of Par-1
PLA:	Proximity Ligation Assay
PSD:	Postsynaptic Density
PTVs:	Piccolo-Bassoon transport vesicles
RIMs:	Rab3-interacting molecules
RIM-BPs:	RIM- binding proteins
RRP:	Readily Releasable Pool of SVs
Slmb:	Slimb
STED:	Stimulated emission deletion microscopy
UBA:	Ubiquitin-association domain
VNC:	Ventral Nerve Cords

CHAPTER 1: INTRODUCTION

THE SYNAPSE

Synapses are sites of cell-to-cell contact and are fundamental for efficient communication between a neuron and its target cell(Sudhof, 2012). At chemical synapses, this communication, or neurotransmission, is triggered by the influx of calcium into the presynaptic nerve terminal, which induces the fusion of synaptic vesicles (SVs) filled with neurotransmitters (NTs) to specialized regions called the presynaptic active zone (AZ)(Sudhof, 2012). Synapses can be both excitatory and inhibitory, depending on the type of NTs synthesized in the neurons, which are loaded into SVs by specific transporters. Once SVs release their content into the synaptic cleft the neurotransmitters must rapidly diffuse across the synaptic cleft and subsequently bind to specific neurotransmitter receptors on the postsynaptic target cell(Sudhof, 2012). Since this process is so vital to synaptic communication, protein localization and transport of cargo to these sites, including the AZs is highly regulated(tom Dieck et al., 1998, Gasparini et al., 2001, Li et al., 2007). Changes in the localization of essential components of the AZs, often results in changes in synaptic morphology(Zhai and Bellen, 2004, Ackermann et al., 2015), which is altered in a plethora of neurological disorders(Selkoe, 2002, Bae and Kim, 2017, Bourgeron, 2009, van Spronsen and Hoogenraad, 2010). While many studies have focused on the transport of synaptic cargoes such as synaptic vesicles(Pack-Chung et al., 2007, Goldstein et al., 2008, Okada et al., 1995) and mitochondria(Saxton and Hollenbeck, 2012, Stowers et al., 2002, Russo et al., 2009), very little is known about the regulation of presynaptic AZs. In this section, I will describe the presynaptic AZ, how

alterations in AZs may be linked to neurological diseases, and advantages of using the *Drosophila* NMJ as a model to study the localization and function of AZ components. Lastly, I will introduce Par-1/MARK kinase which was identified in a screen to affect the localization of AZ protein BRP and has implications in synapse instability in neurological diseases.

The Presynaptic Active Zone

Structurally, the architecture of presynaptic terminals is similar between excitatory and inhibitory synapses. Presynaptic terminals are characterized by the presence of synaptic vesicles and the presence of a specialized electron-dense presynaptic membrane called the AZ. AZs are large (50-500nm) specialized presynaptic sites where neurotransmitter-filled vesicles are released via exocytosis (Sudhof, 2012). Synaptic vesicle release from the AZs can be broken down into priming, clustering, docking at the AZ membrane, followed by the release of their content(Sudhof, 2004). Since AZs specialize in neurotransmitter release, they are enriched with voltage-gated Ca^{2+} channels(Kawasaki et al., 2004, Stanley, 1997, Catterall, 1998) and are precisely apposed to PSD via transsynaptic cell-adhesion molecules(Uchida et al., 1996). Based on electron microscopic studies, all AZs can be morphologically divided into three distinct regions: **1**- Presynaptic electron-dense membrane apposed to the postsynaptic density **2**- A distinct proteinaceous cytomatrix also called cytomatrix at the AZ (CAZ) (Gundelfinger and Fejtova, 2012) that presents in electron micrographs as a diffuse electron-dense material and **3**- An electron-dense structure that emanates from the cytomatrix and projects into the cytoplasm (a.k.a. dense bars/bodies) (Atwood et al., 1993).

The protein-rich CAZ serves as an organizational platform for proteins that localize to the AZ. CAZ consists of a meshwork of multi-domain scaffolding proteins including Rab3-interacting molecules (RIMs)(Wang et al., 1997), the RIM-binding proteins (RIM-BPs), Bassoon and Piccolo/Aczonin/Fife(Wang et al., 1999, tom Dieck et al., 1998, Fenster et al., 2000, Bruckner et al., 2012), the cytomatrix at the AZ protein (CAST)/ELKS/Bruchpilot proteins(Wagh et al., 2006, Wang et al., 2002, Nakata et al., 1999), and the Liprin- α and the UNC-13/Munc-13 proteins(Kaufmann et al., 2002, Taru and Jin, 2011, Zhen and Jin, 1999, Dai et al., 2006, Brose et al., 1995). Thus, CAZ proteins are large, structural, scaffolding proteins and are evolutionarily conserved from *C. elegans* and *Drosophila* to vertebrate (Ackermann et al., 2015, Zhai and Bellen, 2004). The core proteins at the CAZ regulate the release of neurotransmitter by recruiting and retaining synaptic vesicles and Ca^{2+} channels at the AZ(Sudhof, 2012).

It is not surprising that changes in CAZ protein expression are used to maintain presynaptic homeostatic plasticity or modulate response to a stimulus(Frank et al., 2006, Lazarevic et al., 2011). Presynaptic homeostasis is a mechanism of synaptic plasticity that is evolutionarily conserved from *Drosophila* to humans(Frank et al., 2006) and has been extensively studied at the *Drosophila* NMJ (Davis and Muller, 2015, Frank, 2014). Two presynaptic mechanisms that have been postulated for modulating presynaptic homeostasis: increase in presynaptic calcium influx through calcium channels and modulation of the readily releasable pool of synaptic vesicles (RRP)(Davis and Muller, 2015, Frank, 2014). Generally, activity leads to the strengthening of synapses, which is a more significant response to stimulation(Tessier and Broadie, 2009). Modulation in the expression of CAZ proteins results in alteration of neurotransmitter release and affect

overall changes in network-wide neuronal activity(Lazarevic et al., 2011, De Gois et al., 2005).

BRUCHPILOT AN ACTIVE ZONE ORGANIZER AT THE *DROSOPHILA* NMJS

Drosophila larval neuromuscular junctions (NMJs) are a well-characterized model synapse(Harris and Littleton, 2015, Collins and DiAntonio, 2007), which has been extensively used to study AZ organization and its regulation (Collins and DiAntonio, 2007, Bellen et al., 2010, Keshishian et al., 1996). At *Drosophila* NMJs, motor neuron terminals innervate target muscle to form presynaptic bouton that contains as many as 40 AZs per bouton, which can be identified using an antibody against the presynaptic AZ marker, **Br**uch**p**ilot (BRP)(Wagh et al., 2006)(Figure 1.1).

BRP was first discovered in *Drosophila* using the monoclonal antibody nc82(Wagh et al., 2006). Initial studies found that nc82 localized to the presynaptic membranes in a punctate pattern and precisely apposed the postsynaptic glutamate receptors(Wagh et al., 2006), suggesting that nc82 localized to AZs, which was later confirmed(Fouquet et al., 2009). The N-terminus of this protein is homologous to CAZ scaffolding protein(Wagh et al., 2006) ELKS/CAST and ERC2 in humans(Kaeser et al., 2009, Wagh et al., 2006, Chia et al., 2013, Hida and Ohtsuka, 2010) and was named Bruchpilot or BRP. Pan-neuronal knockdown of BRP in *Drosophila* leads to a complete loss of electron-dense bodies (a.k.a T-bars) at AZs and disrupts synaptic transmission and is lethal(Wagh et al., 2006), demonstrating that BRP is an essential component of AZs. Furthermore, BRP plays a pivotal role in the clustering and retention of Ca^{2+} channels

beneath the T-bar(Kittel et al., 2006) and determines the size of the readily releasable pool (RRP) of SVs(Matkovic et al., 2013).

During synaptogenesis, BRP arrives at the AZ much later than other structural proteins such as Liprin- α (Fouquet et al., 2009). While it is not clear why this is the case, the arrival of BRP is timed in such a way that Ca^{2+} channels are retained and in place for synaptic transmission(Fouquet et al., 2009). After synaptogenesis, BRP also plays a critical role in the maturation of synapses. BRP's role in synapse maturation is supported by studies in *C. elegans* and mice (Dai et al., 2006, Chia et al., 2013), where maturation of AZs is dependent on interaction BRP homolog, ELKS and other essential AZ proteins such as SYD2/ Liprin-α(Dai et al., 2006) and RIM/Unc10(Stigloher et al., 2011).

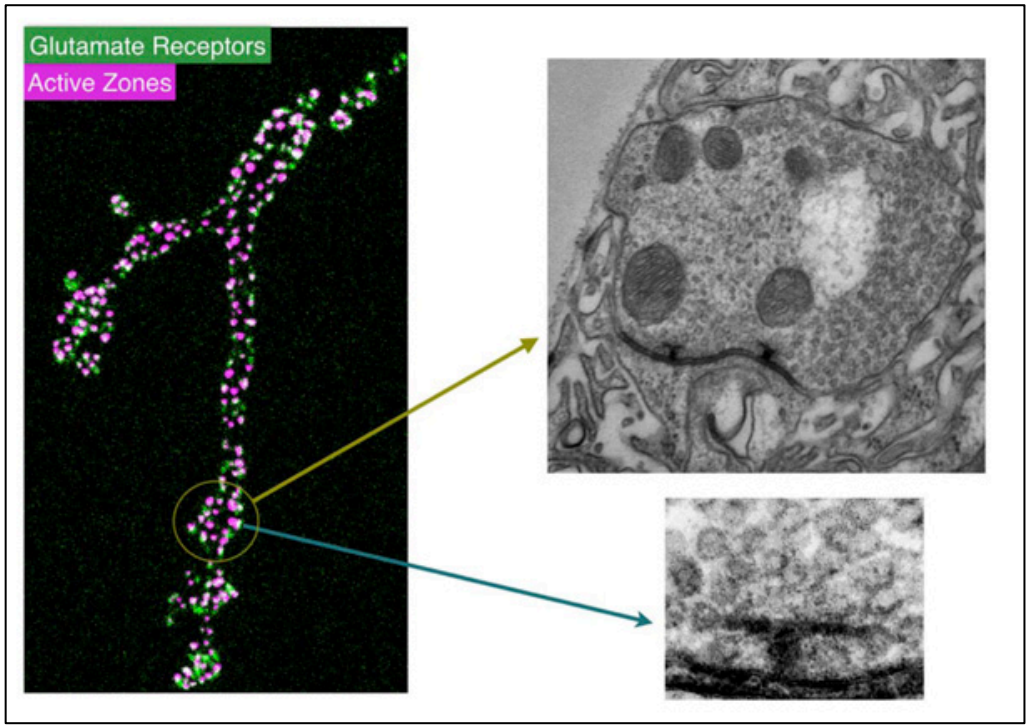

Figure 1.1 Anatomy of the *Drosophila* NMJ (Adapted from (Harris and Littleton, 2015))

A muscle 4 NMJ is shown with immunolabeling for the AZ protein Brp (magenta) and a postsynaptic GluR subunit (green). EM images of a bouton and a T-bar AZ are shown on the right.

Structural organization of T-bars at the Drosophila NMJ

Recent advances in imaging have revealed that T-bars, which likely consist mostly of BRP, has an elongated confirmation that stretches from the AZ membrane and extends into the cytoplasm, which looks like a T, hence the name (Figure 1.1) (Ehmann et al., 2015, Ehmann et al., 2014). An elegant study using super-resolution microscopy revealed that the T-bars form a doughnut-like structure at the AZs(Figure 1.2) (Maglione and Sigrist, 2013) and that each T-bar is composed of ~137 BRP molecules that are assembled into ~15 heptameric clusters(Ehmann et al., 2014). Interestingly, this organization appears to be highly dynamic and may be linked to the functional state of the AZs(Ehmann et al., 2014, Wichmann and Sigrist, 2010). Indeed, the plasticity of AZs is observed in mutations affecting synaptic apposition (Graf et al., 2009), synaptic homeostasis(Weyhersmuller et al., 2011) and circadian rhythms(Gorska-Andrzejak et al., 2013) all of which require the AZs to be plastic. However, mechanisms that regulate the plasticity of the T-bar and importantly, the transport of the components needed for building the T-bars remains to be determined.

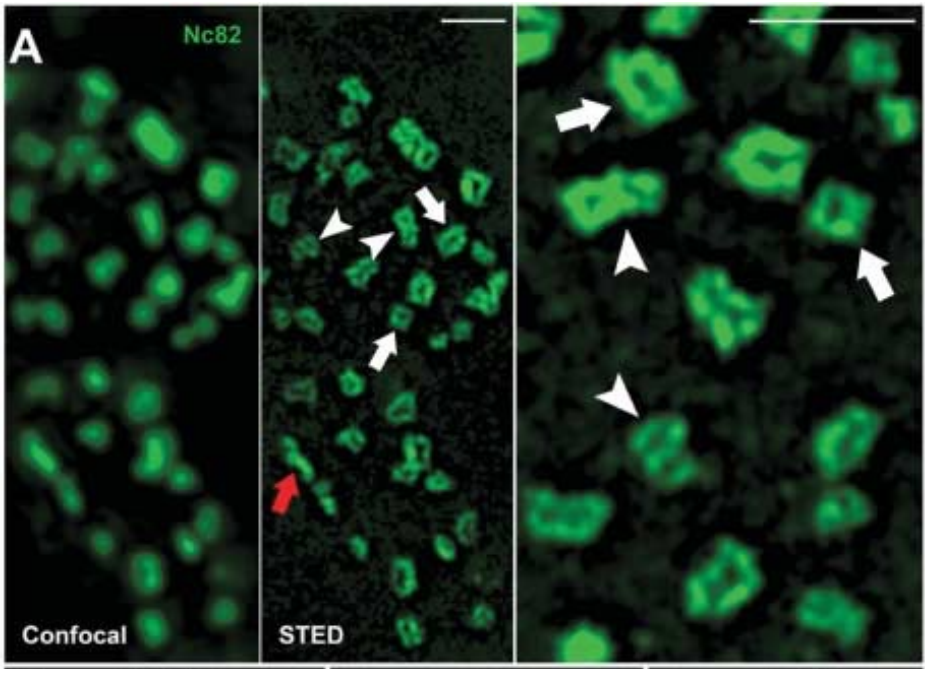

Figure 1.2 T-bars form doughnut like structure at active zones (Adapted from (Kittel et al., 2006))

Unlike confocal, STED microscopy revealed doughnut-shaped structures recognized by Nc82. Viewed from above, both single (white arrows) and clusters of multiple rings (arrowheads) were identified. The red arrow indicates a synapse viewed parallel to the synaptic plane.

TRANSPORT OF ACTIVE ZONE PROTEINS

Neurotransmission relies on proper trafficking of synaptic proteins from neuronal cell bodies to the synapses via axonal transport. This is important because some synapses can be very far away from the cell body, and in human can be located up to a meter away from the soma (Goldstein et al., 2008, Holzbaur and Scherer, 2011). Majority of long-distance axonal transport of protein of organelle cargoes is accomplished using two microtubule-based motors; namely the kinesin family that moves cargo towards the plus ends of microtubules (toward synapses) and the dynein family that moves cargo towards the minus ends of microtubules (toward cell bodies)(Caviston and Holzbaur, 2006).

While many studies have demonstrated the unique motors, adapters, and regulators of axonal transport for mitochondria(Glater et al., 2006, Russo et al., 2009) and synaptic vesicles(Pack-Chung et al., 2007, Goldstein et al., 2008, Okada et al., 1995), very little is known about the transport of AZ proteins.

Neuronal cell culture studies have suggested that AZs are assembled during synaptogenesis by the transport of AZ proteins in bulk carrier vesicles called piccolo-bassoon transport vesicles (PTVs)(Zhai et al., 2001, Shapira et al., 2003). PTVs are transported via kinesin superfamily motors (KIFs)(Hirokawa et al., 2009) to the growth cones and are likely attached to KIFs via adaptor proteins(Schlager and Hoogenraad, 2009). While very little is known about these initial events in the transport and assembly of nascent AZs, even less is known about how AZ components are transported during the maintenance phase. Thus, while AZs are present at all synapses and play essential functions(Sudhof, 2012), the mechanisms by which they are transported and how the multimeric scaffolding proteins are assembled and integrated into the AZs maintained remains poorly understood.

ALTERED SYNAPSES AND AXONAL TRANSPORT IN NEURODEGENERATIVE DISEASE

Changes to the protein composition and structure of synapses often lead to changes in synaptic function(Sudhof, 2012). Abnormalities in morphology and function of synapses have been consistently observed in many neurological diseases including Alzheimer's diseases (AD) and Autism Spectrum Disorders (ASD)(Bourgeron, 2009, Selkoe, 2002, Bae and Kim, 2017, van Spronsen and Hoogenraad, 2010). Furthermore, decreased synaptic density usually precedes the death of neurons and is likely a key

determinate of cognitive impairments observed in neurodevelopmental and neurodegenerative disease(Bourgeron, 2009, Selkoe, 2002, Bae and Kim, 2017, van Spronsen and Hoogenraad, 2010).

Altered Synapses in Neurodegenerative Disease

Neurodegenerative disorders of which, AD is the most common(Hebert et al., 2013), are characterized by substantial and progressive loss of selective neurons and astrogliosis(Scheff et al., 1990, DeKosky and Scheff, 1990, Scheff et al., 2013). Cell death observed in AD occurs first in vulnerable brain regions such as the hippocampus, nucleus basalis, and entorhinal cortex(1997, Serrano-Pozo et al., 2011). Decades of research have suggested that accumulations of toxic proteins play a vital role in the pathogenesis of the disease and neuronal death. Moreover, in AD accumulations of Aβ and Tau are implicated in the widespread neuronal cell death found in later stages of neurodegeneration(Braak and Del Tredici, 2011, Spires-Jones and Hyman, 2014, Tai et al., 2012). Unfortunately, therapies developed for AD, targeting the aberrant protein aggregations has proved to be unsuccessful in reversing the cognitive decline observed in the disease(Klein, 2002, Herrup, 2015, Castello et al., 2014). It is now becoming increasingly apparent that early intervention before neurons are lost, will prove most beneficial(Barnett et al., 2014, DeKosky, 2003) to stop or slow the cognitive impairment associated with these disorders. Unfortunately, very little is known about early stages, but there is evidence to suggest that loss of synapses is key in the early progression of AD(DeKosky and Scheff, 1990, Scheff et al., 2013, Arendt, 2009, Terry et al., 1991). In fact, synapse loss correlates best with the cognitive decline that is characteristic of AD and is thought to precede neuronal loss(Terry et al., 1991, DeKosky and Scheff, 1990).

Recent studies suggest that AD could take decades to develop starting as early as young adulthood or even childhood and once the process of neurodegeneration begins, it is irreversible(Serrano-Pozo et al., 2011). These data suggest that targeting early events in AD progression such as those that lead to the loss of synapses, could be beneficial for patients and strong targets for future therapies.

How are synapses lost in AD and how does this lead to cognitive decline? One hypothesis is the breakdown of processes that maintain synaptic structure triggers their demise(Palop and Mucke, 2010a, Palop and Mucke, 2010b, Selkoe, 2002). Moreover, the loss of synapses can result in failure of synaptic networks resulting in cognitive decline widely associated with neurodegenerative disease(Palop and Mucke, 2010a, Palop and Mucke, 2010b). Studies focusing on transgenic mouse models of AD have provided further insights into the role of synaptic dysfunction and pathogenesis of AD. For example, there is strong evidence that soluble Aβ oligomers may lead to dysfunction and loss of synapse by directly acting on postsynaptic receptors such as NMDA-type glutamate receptors(Snyder et al., 2005, Roselli et al., 2005, Li et al., 2009). Another study found that reducing the neuronal maintenance factor Nerve Growth Factor (NGF) can result in neurodegeneration and induce a phenotype similar to AD(Capsoni et al., 2000). Interestingly, specific reductions of NGF are found in the entorhinal cortex(Calissano et al., 2010), one of the brain regions that is affected early in AD(Serrano-Pozo et al., 2011). Finally, mutations in cysteine string protein (CSP), another key player in synaptic maintenance, it was found to lead to a progressive motor neuron disorder characterized by neurodegeneration(Sharma et al., 2012).

What events lead to synapse loss in AD? Synapse loss is likely preceded by an increase in synapse instability(Shahidullah et al., 2013, Eaton et al., 2002, Jackson et al., 2017). When synapses become unstable there is an imbalance between pre- and postsynaptic components that coincide with changes in neuronal activity(Jackson et al., 2017). Synapse instability is also marked by an increase in the gap between the pre- and postsynaptic membranes(Eaton et al., 2002). Such instabilities have been observed in normal aged rats/mice(Mostany et al., 2013) as well as in aMCI patient brains(Scheff et al., 2013). Synapse instability can manifest (at the level of AZs) by the removal of dense bars(Eaton et al., 2002). Taken together, these studies suggest that impairing synaptic maintenance can result in synaptic instability and ultimately lead to the degeneration of neurons. However, understanding mechanisms that regulate synaptic maintenance, and how they break down in disease, remains to be determined.

Axonal transport and Neurodegenerative Disease

Disruption of axonal transport has been implicated in neurodegenerative diseases(Stokin and Goldstein, 2006, Chevalier-Larsen and Holzbaur, 2006, Millecamps and Julien, 2013). Indeed, mutations that affect axonal transport lead to neurodegenerative diseases and deficits in axonal transport have been reported early in AD pathogenesis(Ishihara et al., 1999, Pigino et al., 2003, Puls et al., 2003, Hafezparast et al., 2003, Stokin et al., 2005, Lazarov et al., 2007, Zhang et al., 2004). Another cause of axonal transport deficits observed in AD is thought to be mediated by hyperphosphorylation of Tau(Ishihara et al., 1999, Iijima-Ando et al., 2012, Ebneth et al., 1998). In AD, Tau becomes highly phosphorylated and phosphorylation of Tau has been to show to disrupt microtubules leading to microtubule instability, followed by the

accumulation of many essential cargoes, such as mitochondria and post-synaptic receptors(Chin et al., 2000, Drewes et al., 1995, Ebneth et al., 1998, Biernat et al., 1993). While little is known about how mitochondria and synaptic vesicles are transported, even less is known about the extent to which presynaptic cargoes, such as AZ proteins, transport is affected in neurodegenerative disease.

What is known about AZ protein transport and neurodegenerative disease? In vertebrates, AZ density is maintained during the developmental stages but is significantly decreased with aging (Chen et al., 2012). Interestingly, axonal transport also declines with aging (Milde et al., 2015) suggesting that a combination of decreased axonal transport of AZ proteins along with aging may lead to a gradual decrease in the maintenance of AZs. The decreased maintenance of AZs may eventually lead to a failure to maintain synaptic function and ultimately lead to synapse degeneration. While this hypothesis is generally accepted, it has proven difficult to determine whether axonal transport is the cause or consequence of synapse loss.

RATIONALE FOR STUDY

Since AZs make up the vital presynaptic regions that are responsible for the rapid and efficacious release of neurotransmitters and synapses are important in many neurological diseases(Ackermann et al., 2015, Sudhof, 2012, Zhai and Bellen, 2004), understanding the assembly/disassembly of AZs may provide much needed insights into the mechanism of many disorders, like AD. Understanding these mechanisms is critical because most synapses are long-lived(Harris and Littleton, 2015) and therefore, assembly/disassembly of AZ critical for the survival and function of neurons(Harris and

Littleton, 2015). While little is known about how AZs are assembled/ disassembled during synaptogenesis, even less is known about how they are maintained.

I was interested in answering the following questions: How are AZs maintained and what regulates their localization? Does mislocalization of AZ components, such as BRP in *Drosophila*, cause synapses to become unstable and ultimately degenerate? The fly neuromuscular junction (NMJ) synapses provide an excellent way to investigate these studies and provide further insights. By taking advantage of the power of *Drosophila* genetics and combining it with super-resolution imaging, ultrastructural and electrophysiological studies(Collins and DiAntonio, 2007, Ghannad-Rezaie et al., 2012, Saxton, 2001), synapse stability can be studied at single AZ resolution. Furthermore, the long axons that supply NMJs in *Drosophila* are similar to the long axons that project from the locus coeruleus neurons to the cortical transentorhinal cortex(Braak et al., 2011), which is one of the most vulnerable regions of the brain in the initial phases of AD. Thus, the mechanisms of early synapse vulnerability might be applicable to neurodegenerative diseases.

To answer these questions and discover novel signaling pathways that regulate the localization of AZ proteins, the Wairkar laboratory performed an unbiased screen of about 500 loss-of-function mutants and RNAi lines of kinases and phosphatases. Accumulation of BRP(Wagh et al., 2006) within axon bundles was used as a readout to test if the disruption of these kinases and phosphatases selectively regulated the transport or assembly of AZ cargo. Of the approximately 500 lines that we screened, and loss of casein kinase 2α (CK2α) and Partitioning-defective 1 (Par-1) kinase resulted in selective accumulations of BRP within axons. Since the laboratory had previously demonstrated a role for CK2α in the transcription of BRP(Wairkar et al., 2013), for my dissertation, I

chose to focus on Par-1 kinase for two reasons. First, very little is known about the presynaptic role of Par-1 kinase and second, altered levels of Par-1 kinase are associated with many diseases (Beghini et al., 2003, Henderson et al., 2017), including ASD (Maussion et al., 2008) and AD (Seshadri et al., 2010, Chin et al., 2000).

PAR-1 KINASE

Par-1 kinase is a highly conserved serine/threonine kinase that has many diverse cellular functions like asymmetrical cell division(Kemphues et al., 1988) and the establishment of the anterior/posterior axis(Doerflinger et al., 2006, Shulman et al., 2000). *Drosophila* Par-1 is homologous to *C. elegans* PAR-1 and the mammalian **M**icrotubule **a**ffinity-**r**egulating **k**inases (MARK)(Drewes et al., 1997). Par-1/MARK kinases are members of the adenosine monophosphate-activated protein kinase (AMPK) family of CamKII kinases and share a conserved architecture with other AMPK family members(Marx et al., 2010). In *C. elegans* and *Drosophila* Par-1 is encoded by a single gene, while in mammals four genes encode four different proteins: MARK1, MARK2, MARK3, and MARK4(Drewes et al., 1998).

Par-1 kinase possesses a kinase domain near the N-terminus, a ubiquitin-association (UBA) domain adjacent to the kinase domain, a kinase-associated (KA1) membrane-binding domain near the C-terminus and a large uncharacterized spacer domain between the UBA and KA1 domains (Figure 1.3) (McDonald, 2014, Wu and Griffin, 2017). Many mechanisms have been implicated in the regulation of activity for Par-1 kinase (McDonald, 2014, Wu and Griffin, 2017). Both the UBA and KA1 domains appear to have important roles in this regulation(Marx et al., 2010, Timm et al., 2008,

Panneerselvam et al., 2006, Murphy et al., 2007). For example, the UBA domain is required for phosphorylation by LKB1(Jaleel et al., 2006), a conserved master regulator of all AMPK family kinases, at a conserved site in the activation loop of the kinase domain leading to maximal activation of Par-1 (Figure 1.3)(Wang et al., 2007).

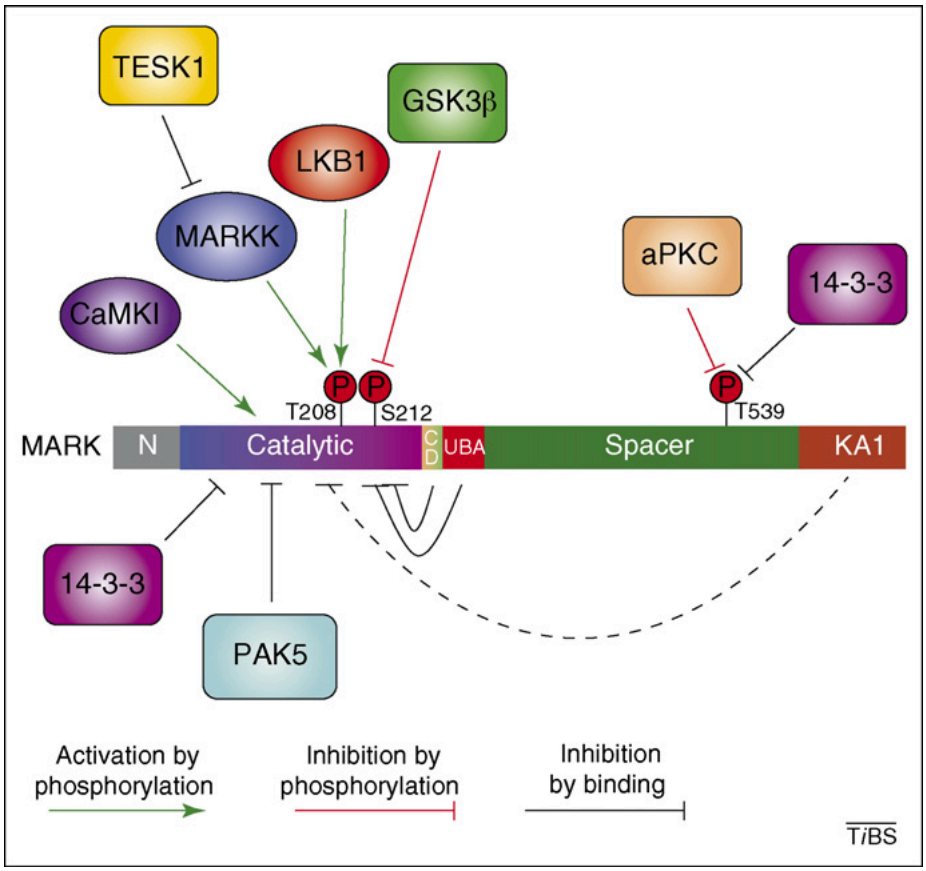

Figure 1.3 Summary of regulatory pathways of MARK. (From (Matenia and Mandelkow, 2009))

Role of Par-1 Kinase in Regulating Microtubule Stability

While the role of Par-1 in polarity is relatively well described(Doerflinger et al., 2006, Shulman et al., 2000, Wu and Griffin, 2017). I will focus on the role of Par-1 in regulating microtubule stability, which is critical to its presynaptic role in neurons. So,

what is known about Par-1 in regulating synapses development of disassembly? Par-1 regulates microtubules through phosphorylating microtubule-associated proteins (MAPs) such as Tau, MAP2, and MAP4(Drewes et al., 1997). MAPs play critical roles in regulating the growth, stability, and disassembly of microtubules. Par-1 phosphorylates MAPs at a conserved Lys-X-Gly-Ser (KXGS) motif(Drewes et al., 1998, Drewes et al., 1997). Phosphorylation of MAPs at these sites promotes the disassociation of MAPs from microtubules leading to destabilization of microtubules (Drewes et al., 1997). Tissue culture study confirmed that overexpression of Par-1/MARK leads to the destruction of the microtubule network(Drewes et al., 1995). Disruption of microtubules has been implicated as a critical event leading to synapse loss in many diseases including AD. This suggests that destabilization of microtubules by Par-1 phosphorylation could be contributing to synapse instability and loss in neurological disorders.

PAR-1 KINASES IN DISEASE

Neurodevelopmental Disorders

Increased expression of Par-1/MARK is implicated in both neurodevelopmental (Maussion et al., 2008, Hu et al., 2009, Carayol et al., 2011) and neurodegenerative diseases(Nishimura et al., 2004, Yu et al., 2012, Chin et al., 2000, Lee et al., 2012). In ASDs MARK1 levels were found to be selectively increased in prefrontal cortex in postmortem samples (Maussion et al., 2008). Interestingly, the disruption of synapses in the prefrontal cortex is highly implicated in ASDs (Maussion et al., 2008) but if increased levels of MARK is directly contributing to this disruption remain unknown.

Additionally, Par-1 also regulates the postsynaptic density during development(Zhang et al., 2007). In *Drosophila*, Par-1 regulates the localization of Disc Large (Dlg)(Zhang et al., 2007) - a scaffolding protein that is a known organizer of post-synaptic proteins which is homologous to PSD-95(Budnik et al., 1996). Regulation of Dlg occurs through its direct phosphorylation by Par-1 at a conserved S797 site(Zhang et al., 2007). Thus, Par-1 via its downstream targets and can influence synaptic development and function.

Neurodegenerative Disease

As opposed to the role of MARK in ASD, its role in neurodegenerative disease has been relatively better understood due to its function as a Tau kinase(Drewes, 2004). Tau is a MAP that lines the outer wall of microtubules and phosphorylation of Tau by kinases can lead to its disassociation from microtubules and promote disassembly of microtubule networks(Drewes et al., 1997). In pathological conditions such as AD, once disassociated from microtubules Tau might accumulate in somatodendritic compartments and form neurofibrillary tangles (NFTs), which is a hallmark of these diseases(Spires-Jones and Hyman, 2014). Further studies have shown Tau is phosphorylated at a conserved S262 by Par-1/MARK(Drewes et al., 1997) and this hyperphosphorylated form of Tau is present in NFTs in AD post-mortem samples(Augustinack et al., 2002). Furthermore, S262 phosphorylated Tau is also found in post-mortem brains of patients with frontotemporal dementia (FTD)(Chin et al., 2000) suggesting that Par-1/MARK phosphorylation may play a role in a variety of neurodegenerative disorders.

Consistent with the vertebrate studies, *Drosophila*, Par-1 can also phosphorylate Tau (Fortini, 2004, Wu and Griffin, 2017). Additionally, phosphorylation of Tau by Par-

1 primes Tau for further phosphorylation by other kinases like GSK-3β(Nishimura et al., 2004). Thus, Par-1 is thought to be the initiator kinase and trigger tau-mediated toxicity (Nishimura et al., 2004). In fact, postsynaptic overexpression of Par-1 leads to a stronger degeneration phenotype than overexpression of wild-type Tau by itself(Wang et al., 2007). Par-1 through Tau has also been shown to mediate Aβ toxicity on dendritic spines (Lee et al., 2012, Nishimura et al., 2004, Wang et al., 2007). While most studies have focused on the postsynaptic role of Par-1 at synapses, it is clear that Par-1 localizes to the presynaptic compartments(Zhang et al., 2007); however, little is known about its presynaptic function.

Par-1/MARK in Early Alzheimer's Disease Pathogenesis

Genome-wide association studies have implicated MARK in AD(Seshadri et al., 2010). Interestingly, increased expression of Par-1/MARK is associated with early stages of AD pathology(Chin et al., 2000, Lund et al., 2014, Yu et al., 2012) when synapse instability is thought to precede overt synapse loss(Jackson et al., 2017). However, the role of MARK in synapse stability and the role of synapse instability in neurodegenerative diseases are poorly understood. To confirm this observation, we assessed the expression of MARK in patient samples with a confirmed diagnosis of AD using a well-characterized anti-MARK antibody(Lund et al., 2014). Consistent with the previous study(Lund et al., 2014) there was very little detectable MARK in the age-matched control group. However, AD patient brains showed an increased MARK staining in a punctate pattern within the neurons, marked by NeuN (Mullen et al., 1992) (Figure 1.4). Furthermore, post-mortem brain slices from patients with a diagnosis of amnestic **M**ild **C**ognitive **I**mpairment (aMCI), a stage widely believed to precede

AD(Wilson et al., 2011)- showed that MARK was increased in these patient brains as well (Fig. 1.4) and is consistent with my hypothesis that MARK might function early during the process of synapse degeneration.

Moreover, while increased MARK levels have been shown in AD patients(Chin et al., 2000, Lund et al., 2014), its association with aMCI has not been reported. For the first time, this preliminary data reveal increases in MARK in aMCI patients, indicating that MARK may play a novel role in early during synapse pathology. Interestingly, my preliminary data also show that similar to age-matched controls; MARK is undetectable in Non-Demented with Alzheimer's Neuropathology (NDAN) individuals whose synapses resist the binding of toxic Aβ aggregates and remain functional(Bjorklund et al., 2012). The fact the NDAN individuals have undetectable levels of MARK raises the novel possibility that increased MARK levels when present along with Aβ or Tau aggregates could be an early indicator of cognitive decline. Importantly, the increases in MARK that were observed in human post-mortem samples were specific to entorhinal cortex, a region of the brain that is affected early during disease pathology(Braak and Del Trecidi, 2015). These observations suggest that MARK overexpression might be one of the early and necessary contributors for the cognitive impairments observed in AD patients.

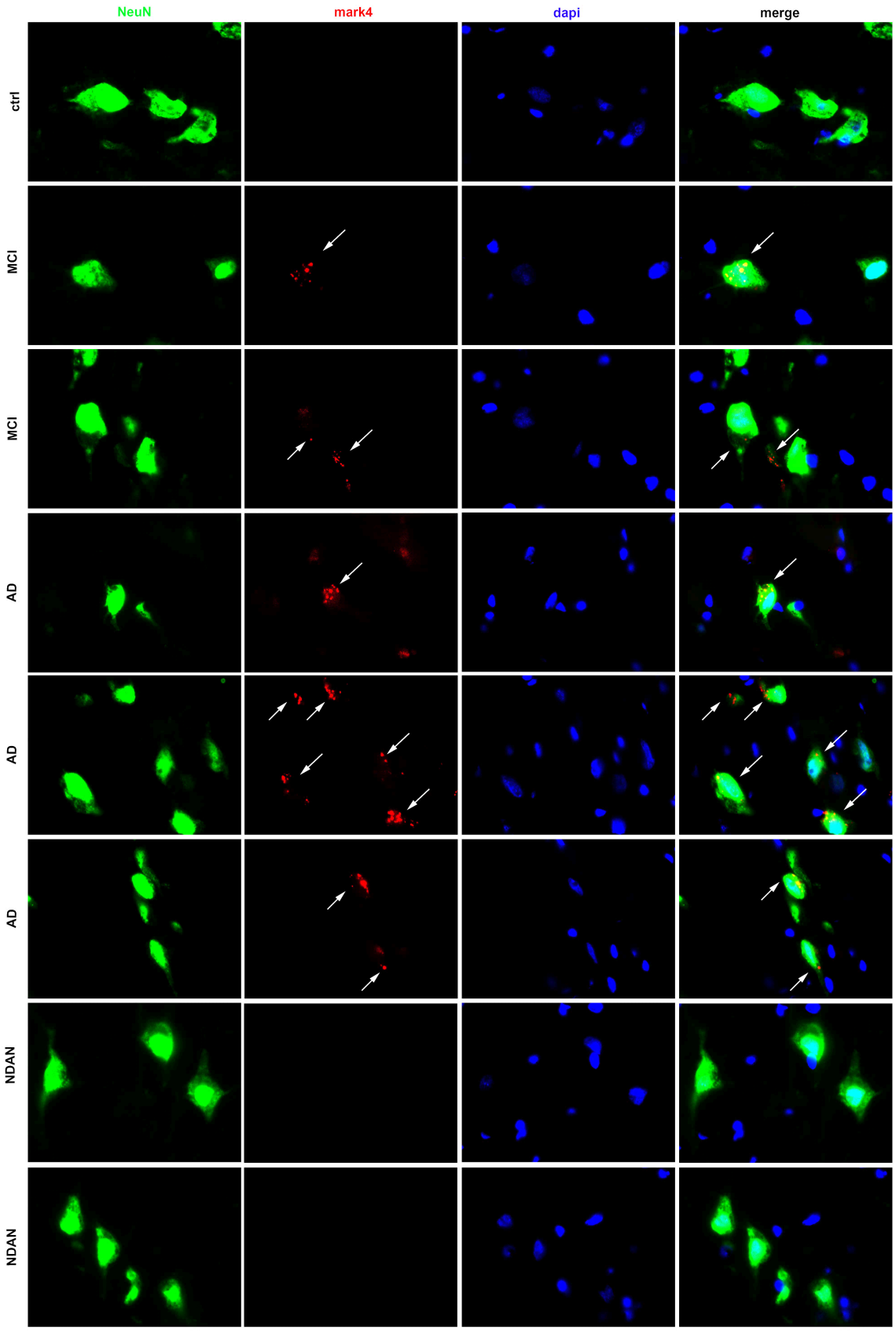
NeuN
mark4
dapi
merge
ctrl
MCI
MCI
AD
AD
AD
NDAN
NDAN

Figure 1.4 Par-1/MARK4 levels are increased in aMCI and AD entorhinal cortex

Representative images of brain slices stained with antibodies against anti- NeuN (Green), anti-MARK4 (Red), and anti-Dapi (Blue) from the following groups: Control (Ctrl), amnestic Mild cognitive impairment (aMCI), Alzheimer's Disease (AD), and Non-demented with Alzheimer's Disease Neuropathology (NDAN). Average age 85 years or more.

SUMMARY

While the association of Par-1/MARK with AD is exciting and needs to be worked out further, it is clear that it must have some role in the regulation of synapses and its function. Therefore, the work outlined in this dissertation is an effort to determine novel mechanisms that regulate the localization of AZ components and ultimately if misregulation leads to synaptic degeneration. I found using an unbiased genetic screen that presynaptic Par-1 kinase regulates the localization of AZ components, specifically BRP, to the AZs at Drosophila NMJs. In particular, my work suggests that mechanisms involved in trafficking BRP are distinct from those that transport synaptic vesicles and mitochondria. Furthermore, my data identify a role for Par-1 that is independent of Tau in localizing BRP(Drewes et al., 1998, Drewes et al., 1997). Finally, my work suggests that there is an important spatiotemporal relationship between Par-1 expression and localization of BRP. Increased level of Par-1 /MARK are associated with neurodegenerative diseases such as AD and in particular, are found to be elevated early in the disease. Overall, these observations suggest that Par-1 overexpression might be an early event in neurodegenerative diseases that hasten the demise of synapses by triggering the mislocalization of AZ proteins and initiating synaptic instability.

CHAPTER 2: MATERIALS AND METHODS

DROSOPHILA STOCKS AND FLY HUSBANDRY

Flies were reared in medium containing Nutri-Fly™ Bloomington formulation (Genesee Scientific, San Diego, CA), Jazz mix (Fisher Scientific, Waltham, MA, USA), sugar and powdered yeast (Genesee Scientific) in an 8:5:1:1 ratio and made according to standard procedures. The following fly stocks were used in this study: UAS-Par-1, UAS-Par-1^{T408A},UAS-Par-1^{RNAi}, UAS-LKB1(Lee et al., 2012) (All gifts from Bingwei Lu, Stanford School of Medicine, Stanford, CA, USA, (Lee et al., 2012)), *slmb*^{2A1} (Skwarek et al., 2014), UAS-Tau-GFP(Doerflinger et al., 2003), UAS-tau^{KO} (Burnouf et al., 2016), and UAS-mito-GFP(Pilling et al., 2006) (from Bloomington Stock Center), Df(3R)tauMR22(Bolkan and Kretzschmar, 2014, Doerflinger et al., 2003) (from Daniel St. Johnston, University of Cambridge (UK)), *olk*^{1} and *olk*^{3} (a gift from Doris Kretzschmar, Oregon Health and Science University, Portland, OR, USA)(Bettencourt da Cruz et al., 2005). The following GAL4 lines were used: BG380-Gal4 (Budnik et al., 1996) (A gift from Aaron DiAntonio, Washington University Medical School, St. Louis, MO, USA), elav-Gal4(Yao and White, 1994), nSyb-Gal4(Pauli et al., 2008), G7-Gal4(Zhang et al., 2001), and ELAV-*GeneSwitch* (Bloomington Stock Center) (Osterwalder et al., 2001).

RU486-GENESWITCH EXPERIMENTS

All experiments using the RU486-GeneSwitch system were performed according to Osterwalder et al., 2001 (Osterwalder et al., 2001). For overexpression of Par-1, UAS-

Par-1 and ELAV-GeneSwitch adults were placed on normal food and allowed to mate for two days at 25°C. Late second instar larvae or early third instar larvae were then placed on RU486 containing food (20 μg/ml RU486 diluted in EtOH)(Mifepristone; Sigma, St. Louis, MO) and dissected at time points following RU486 exposure, T_0, T_9, T_{12}, T_{24}, T_{48}, and T_{72}. Dissections, imaging, electrophysiology and analyses for these experiments are described in the following sections.

IMMUNOHISTOCHEMISTRY

Larvae were dissected in cold 1X PBS solution followed by fixation in Bouin's fixative for 5 minutes. Larvae were washed 3X with PBS-Triton (0.1% solution) and blocked using 5% NGS solution in PBS. Following primary antibodies were used: anti-BRP (1:250)(Wagh et al., 2006), anti-Tubulin (E7) (1:100), anti-Futsch (1:100)(Developmental Studies Hybridoma Bank), anti-GFP (1:500)(Gallio et al., 2011) (abcam), anti-DVGLUT (1:10,000)(Daniels et al., 2004)(gift from Aaron Diantonio, Washington University Medical School), anti-DGluRIII (1:1000)(Natarajan et al., 2013), and anti-Par-1 (1:10,000)(Zhang et al., 2007)(gift from Bingwei Lu, Stanford School of Medicine), anti-Liprin-α (1:500)(Fouquet et al., 2009)(gift from Stephan Sigrist, Free University Berlin), anti-DAB (Kawasaki et al., 2011)(gift from Richard Ordway, Pennsylvania State University), and anti-dTau (1:1000)(Doerflinger et al., 2003, Bolkan and Kretzschmar, 2014)(gift from Doris Kretzschmar, Oregon Health and Science University and Daniel St. Johnston, University of Cambridge). Dylight conjugated goat anti-HRP antibody (1:1,000), Goat Cy3-, and Alexa 488 conjugated secondary antibodies against mouse, rabbit, and chicken IgG (1:1000) were obtained from Jackson

ImmunoResearch, West Grove, PA.

IMAGING AND ANALYSIS

Larvae were imaged using a Nikon C1 confocal microscope. To compare different genotypes, samples were processed simultaneously. Imaging was performed on the same day and same slide, with an appropriate control, and the same confocal gain setting was used to image each genotype. Each staining was repeated at least three times with at least four larvae per genotype and at east 10 NMJs per individual experiment were included in the analyses.

For quantification of intensities within axon bundles and NMJs, a complete z-series stack collected at intervals of .4 μm was projected using the maximum intensity method. Staining intensities of various proteins within the axon bundles and the NMJs were quantified by using MetaMorph software (Molecular Devices, Sunnyvale, CA, USA). For axon bundles and synaptic boutons, HRP was used to set the color threshold. Only the axonal compartment and the region of synaptic bouton determined by HRP staining were used to measure the intensity of the red, green and blue channels. Intensity measurements at boutons were taken across the entire NMJ arbor. At axon bundles, intensity measurements were taken from axon bundles passing over the segments A3-A4(Graf et al., 2011, Wairkar et al., 2013). Measurements were taken from a box of 50 μm^2 and 3 random samples were taken per images, with a total of at least 10 images per genotype per experiment, which was repeated three times(Wairkar et al., 2013, Graf et al., 2011). Intensity measurements at boutons and within axon bundles were normalized to HRP intensity.

Quantification of active zones (BRP) at synaptic boutons were manually by counting the puncta stained by an anti-BRP antibody and the count was tracked using Fiji (Schindelin et al., 2012, Wairkar et al., 2009). Bouton area, Mitochondrial area, and BRP puncta size was quantified manually using Fiji (Schindelin et al., 2012). Bouton size was performed from the entire NMJ arbor and the number of BRP was counted manually and the count was tracked using Fiji (Schindelin et al., 2012, Wairkar et al., 2009). For Figure 4.5 bouton number and synaptic span were normalized to the mean muscle surface area of each genotype. Synaptic span was quantified using Simple Neurite Tracer plugin in Fiji (Schindelin et al., 2012). Experimenter was blinded to the genotypes of the larvae while performing and analyzing the experiments.

PROXIMITY LIGATION ASSAY (PLA)

Third instar larvae were dissected in cold HL3 solution (Stewart et al., 1994) and were incubated with anti-BRP (1:250, DSHB, Iowa city, IA)(Wagh et al., 2006) and anti-Par-1 antibodies (1:10,000, gift from Bingwei Lu, Stanford School of Medicine, CA) overnight at 4°C. Cy5-conjugated anti-HRP antibody raised in Goat was used (Jackson ImmunoResearch) at 1:500 to label the neuronal membranes. For PLA, Duolink Mouse Rabbit *in situ* PLA kit (Sigma-Aldrich, St. Louis, MO) was used and the PLA assay was performed as previously described(Lepicard et al., 2014, Wang et al., 2015). Synaptic boutons and axon bundles passing over A3-4 were imaged using Nikon C1 confocal microscope and analyzed as described above. At least 4 larvae from each time point and 10 NMJs were analyzed. Analysis of average PLA signal intensity was performed using

MetaMorph software (Molecular Devices, Sunnyvale, CA, USA) as described in the confocal microscopy analysis section (above) and normalized to HRP intensity.

STIMULATED EMISSION DEPLETION MICROSCOPY AND ANALYSIS

Stimulated emission deletion microscopy (STED) on NMJ preparations and analysis of BRP structure was done as previously described in Shahidullah et al., 2013 (Shahidullah et al., 2013). Images were taken of type 1b boutons from muscle 4 segments A3-4. BRP doughnuts at synaptic boutons were defined as having a "doughnut shape" when a hole could be visualized in the center of BRP puncta and were counted manually and the count was tracked using Fiji (Schindelin et al., 2012). Images analyzed were maximum projections. Perimeter and area of BRP puncta at synaptic boutons were quantified using particle analysis in Fiji (Schindelin et al., 2012). At least 4 larvae and 10 NMJs were used in this analysis.

ELECTROPHYSIOLOGY

Intracellular electrophysiological recordings were performed on muscle 6, segment A3-A4(Natarajan et al., 2013) on third-instar larvae. Dissections and intracellular recording were performed in HL3 saline(Stewart et al., 1994) containing 0.45 mM Ca^{2+}. Sharp electrodes were made of borosilicate glass and filled with 3 m KCl**.** The cells with input resistance of at least 5 MΩ and resting membrane potentials between -60mV and -80mV were used for analyses. Mean EJP amplitudes, mEJP amplitudes and frequency, were calculated from 75 consecutive traces or events using *pClamp* 9 *software* (Molecular Devices). Quantal content was estimated by dividing the

mean EJP amplitude by the mean mEJP amplitude (EJP/ mEJP) from the same synapse. For GeneSwitch experiments recordings were performed within a 2-hour window around the time point indicated in figures. A total of 5 recordings from 5 larvae per genotype were made per experiment and the experiment was repeated three times.

ELECTRON MICROSCOPY

Samples for ultrastructural analysis were performed as previously described(Wairkar et al., 2009). The larval head and tail were pinned and a dorsal slit was made lengthwise, thus filleting the larvae – in Tannic acid. The larvae were then post-fixed in 1% osmium tetroxide for 1 hr at 4°C. The larvae were dehydrated through 60, (1x, 7 min) 70, 80, 95 and 100% EtOH (2x, 10 min each step), transferred into propylene oxide (2x, 10 min), then into a 1:1 mixture of propylene oxide and Eponate, and left o/n, capped and at room temp. The larvae were then placed into fresh Eponate and into a mould, oriented and allowed to polymerize at 70°C. Thin sections were made and placed on superfrost/plus micro slide and stained with Toluidine Blue "O". Type 1b boutons from NMJ6/7 in segment A2-A4 from WT and Par-1^{OE} larval neuromuscular junctions were identified from the thin sections. Sections were cut at 50 nm with a diamond knife, picked up on formvar coated, copper slot grids, and stained with 2% aqueous uranyl acetate for 15 min followed by lead citrate stain for 1 min. Samples were observed and photographed in a JEM-1400 (JOEL, Japan) or JEOL 1200EX (JOEL, Japan) transmission electron microscope.

Sections analyzed were all mid bouton sections from 1b boutons and showed clear SSR and synaptic vesicles. T-bars, AZ count, AZ length, and AZ width were quantified

using Fiji distribution in ImageJ (Schindelin et al., 2012). Quantification for each genotype was performed on N of 20 or more synaptic boutons from at least 4 larvae per genotype. Floating T-bars were counted manually, and the experimenter was blinded to the genotype. Floating T-bars were defined as having at least a few synaptic vesicles localizing between the T-bar structure and the electron-dense AZ.

WESTERN BLOTS

Western blots were performed as described in(Wairkar et al., 2009) and run on 8% SDS-PAGE gels. Briefly, heads of flies were separated manually, and 20 heads were used to extract lysates using 1x SDS buffer. 6 head equivalent lysate was loaded into each well and probed for dTau using anti-dTau antibody (1:10,000) (Bolkan and Kretzschmar, 2014, Doerflinger et al., 2003) (gift from Doris Kretzschmar, Oregon Health and Science University and Daniel St. Johnston, University of Cambridge). 30 head equivalent lysate against anti- BRP (1:100)(Wagh et al., 2006) (Developmental Studies Hybridoma Bank) and anti-Tau (phospho S262) (1:1000) (abcam)(Nishimura et al., 2004) were performed according to Gorska-Andrzejak et al (Gorska-Andrzejak et al., 2009). In all experiments Syx1A Antibody (8C3) (1:100)(Burgess et al., 1997)(Developmental Studies Hybridoma Bank) was used as a loading control. Image J was used to analyze the intensity of bands on the western blots and the "Gel analysis" function in the program was used to quantify the intensity of the bands. Ratios of the intensities of WT, Par-1^{OE}, or Par-1^{T408A} bands to that of Syntaxin bands were measured and used for calculating the statistical differences between the genotypes.

CO-IMMUNOPRECIPITATION

Frozen (-80°C) WT, Par-1^{OE} and Par-1^{T408A} adult flies were vortexed and the vortexed (Separated parts) while still frozen, were passed through a sieve (No. 40) to separate the heads. At least 100 heads were collected per genotype and used for the Co-IP experiment. Heads were homogenized mechanically in 200µl of lysis buffer (Damulewicz et al., 2017) and incubated at 4°C for one hour. The head lysate was then incubated with anti-BRP antibody (1:25) overnight at 4°C. BRP along with its binding partners were isolated by incubating with Dynabeads (Invitrogen) for 1–3 hours at 4°C. After washing and elution, the samples were resolved using 4-20% gradient SDS-PAGE gel followed by western blotting. Blots were then probed using anti-Par-1 antibody (1:8,000) followed by HRP-conjugated goat α-rabbit (Jackson ImmunoResearch) secondary antibodies (1:3000). The blot was immersed in BIORAD clarity western ECL blotting substrate and images were acquired using *Bio-Rad's ChemiDoc* XRS+ system.

STATISTICAL ANALYSIS

Analyses were performed on at least 4 larvae per genotype for a single experiment and each experiment was repeated at least 3 times. Statistical analyses and graphs were generated using GraphPad Prism (GraphPad Software, Inc.). Student's T-test was used to compare within two groups or one-way ANOVA followed by Dunnett's or Tukey's post-hoc tests were performed to compare means between three or more groups. Fisher's exact test was used to test the occurrence of detached T-bars in WT and Par-1^{OE}. P values less than 0.05 were considered significant.

CHAPTER 3: ACTIVE ZONE PROTEINS ARE TRANSPORTED VIA DISTINCT MECHANISMS REGULATED BY PAR-1 KINASE

Adapted from Barber, Tanquary, Bush, Shaw, Woodson, Tangavelou, Sherman, Wairkar 2017

"Active Zone Proteins are Regulated by Distinct Mechanisms Regulated by Par-1 Kinase"

Published February 2017 in PLOS Genetics, DOI: 10.1371/journal.pgen.1006621

INTRODUCTION

Effective communication between neurons is maintained by synapses via their pre- and postsynaptic specializations called active zones and postsynaptic densities respectively. Active zones are composed of many proteins that are important for the efficient release of synaptic vesicles- a pre-requisite for efficacious neuronal communication(Sudhof, 2012, Zhai and Bellen, 2004). Proteins present at the active zones form an important presynaptic network for the regulation of vesicle release at all chemical synapses. Indeed, many proteins that regulate synapses are disrupted in both neurodevelopmental as well as neurodegenerative diseases(Zoghbi and Bear, 2012, Bourgeron, 2009, Spires-Jones and Hyman, 2014). One such protein, MARK/ Par-1 is implicated in both neurodevelopmental (Maussion et al., 2008, Hu et al., 2009, Carayol et al., 2011)and neurodegenerative diseases(Nishimura et al., 2004, Yu et al., 2012, Chin et al., 2000, Lee et al., 2012) but the mechanisms by which it disrupts synapses is unclear.

MARK1 levels are elevated in ASDs, a neurodevelopmental disorder(Maussion et al., 2008). Interestingly, MARK1 is overexpressed specifically in the prefrontal cortex- a region highly implicated in ASDs (Maussion et al., 2008). On the other hand, MARK4 is overexpressed in neurodegenerative diseases and is thought to hyperphosphorylate(Lund et al., 2014). Indeed, the site that is phosphorylated by the MARK is hyperphosphorylated in post-mortem brains of patients with frontotemporal dementia (FTD)(Chin et al., 2000). Thus, elevated levels or activity of Par-1/MARK is implicated in both neurodevelopmental and neurodegenerative diseases. While there is good evidence for the role of Par-1/MARK in regulating postsynaptic density during development(Zhang et al., 2007), it is unclear whether it has any presynaptic role.

In this chapter, I show for the first time that presynaptic overexpression of Par-1 regulates the axonal transport of an active zone protein- Bruchpilot (BRP). Decreased axonal transport of BRP due to presynaptic overexpression of Par-1 lead to a significant decrease in the number of BRP marked active zones at the synaptic terminals. Furthermore, consistent with a decrease in BRP protein at the synapse(Wagh et al., 2006), ultrastructural analysis demonstrated a decrease in the number of dense bars and deficits in synaptic transmission. Finally, our data show that Par-1/MARK affects the axonal transport of BRP independent of endogenous *Drosophila* Tau (dTau), implicating that a novel substrate of Par-1/MARK mediates the axonal transport of BRP. Together, these data suggest that different components of active zones are transported separately by distinct mechanisms, and that these processes are likely to be tightly regulated by kinases.

RESULTS

Overexpression of Par-1 in the presynaptic neurons leads to specific accumulation of BRP in axons.

Increase in levels or activity of Par-1/MARK is associated with both neurodevelopmental disorders like ASD(Maussion et al., 2008, Hu et al., 2009, Carayol et al., 2011) and neurodegenerative disorders like FTD(Chin et al., 2000). Since synapse is the common underlying unit disrupted in both these disorders(Bourgeron, 2009, Zoghbi and Bear, 2012, Spires-Jones and Hyman, 2014) I wanted to test the effects of elevated levels of presynaptic Par-1 on synapses. To test this, I overexpressed Par-1 presynaptically using the UAS-GAL4 binary system(Brand and Perrimon, 1993). BG380-GAL4(Budnik et al., 1996) driver was used to overexpress of Par-1 (Par-1^{OE}) specifically in presynaptic neurons. Neuromuscular Junction (NMJ) preparations were then stained with antibodies against the active zone marker (Bruchpilot (BRP), (Wagh et al., 2006)), synaptic vesicle marker (DVGLUT(Daniels et al., 2004)) and neuronal membrane marker (Horse Radish Peroxidase(HRP)(Jan and Jan, 1982)) to visualize synapses. Overexpression of Par-1 in presynaptic neurons resulted in significant accumulation of BRP in axons (Figure 3.1 A, B). This was observed using multiple presynaptic drivers (Supplemental Figure 3.1 A, B). While all the tested presynaptic drivers showed qualitatively similar increases in accumulation of BRP in axons, driving the same transgene postsynaptically using postsynaptic driver G7-Gal4(Zhang et al., 2001) did not result in the accumulation of BRP within axons (Figure 3.2 C), suggesting that this was a cell-autonomous effect.

Surprisingly, DVGLUT or HRP did not accumulate within the axons (Figure 3.1A, C), indicating that overexpression of Par-1 may result in specific accumulation of

only a subset of synaptic cargo in the axons. Importantly, overexpression of inactive Par-1 (Par-1^{T408A}, (Wang et al., 2007)) did not result in accumulation of BRP within axons (Figure 3.1 A, B), indicating that BRP accumulations were unlikely to be an unintended consequence of overexpression of Par-1 kinase.

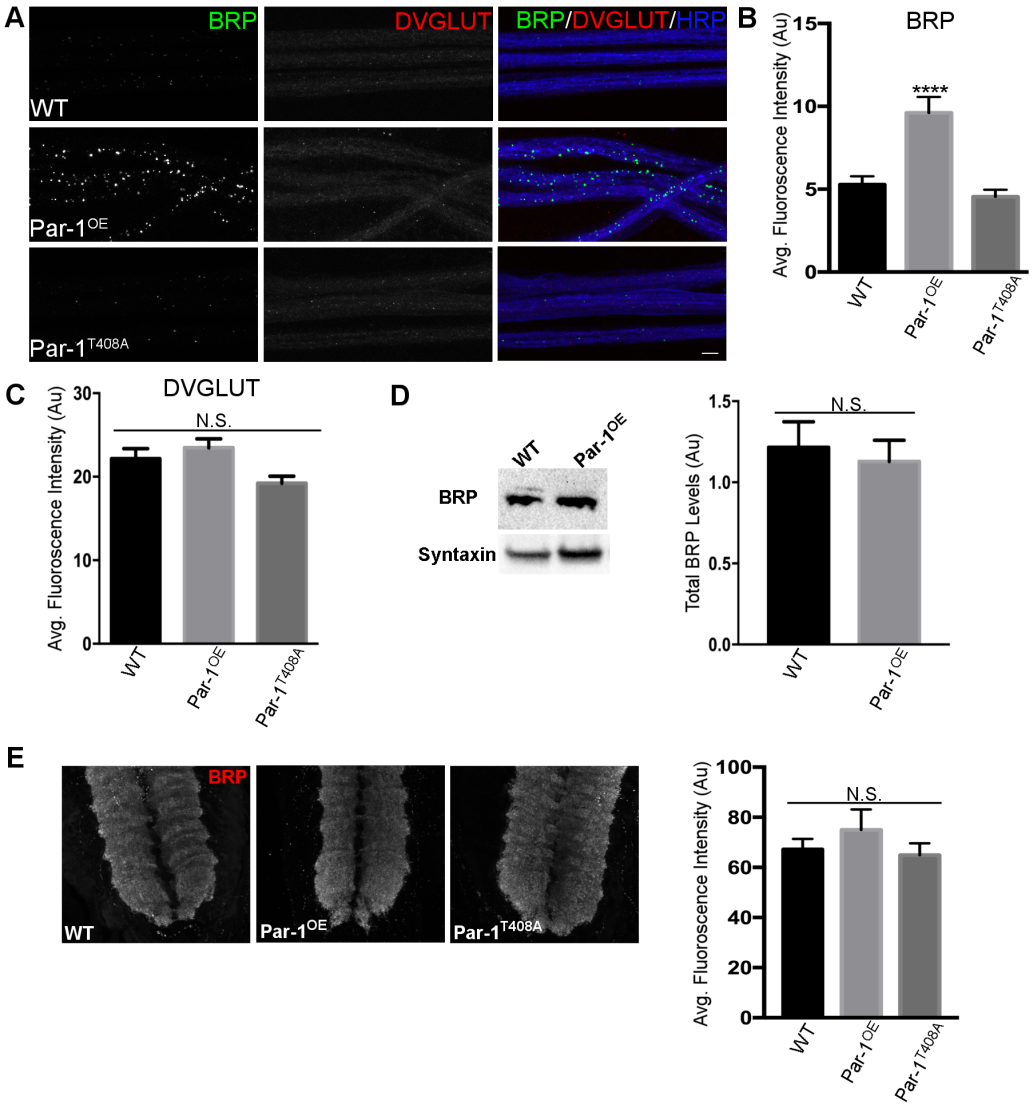

Figure 3.1 Overexpression of Par-1 leads to an accumulation of BRP in axon bundles

A) Representative confocal image stacks showing axons from WT, presynaptic overexpression of Par-1 (Par-1^{OE}) and inactive Par-1 (Par-1^{T408A}) using BG380-Gal4. Third instar larvae were stained with antibodies against BRP (Green), DVGLUT (Red) and HRP (Blue). Scale bar=10µm B) Quantification of BRP intensity from axons in A. n=12, ****=p<0.0001. C) Quantification of DVGLUT intensity from axons in A. n=12, p=0.12. D) Representative Western blots and bar graphs showing quantification of BRP levels in WT and Par-1^{OE} brains. Syntaxin was used as a loading control. N=3 p=0.7124. E) Representative images and bar graphs showing quantification of VNCs stained with BRP (Red) from identical genotypes as in 1A. N=12 p=0.46. Scale bar=10µm. Error bars represent S.E.M.

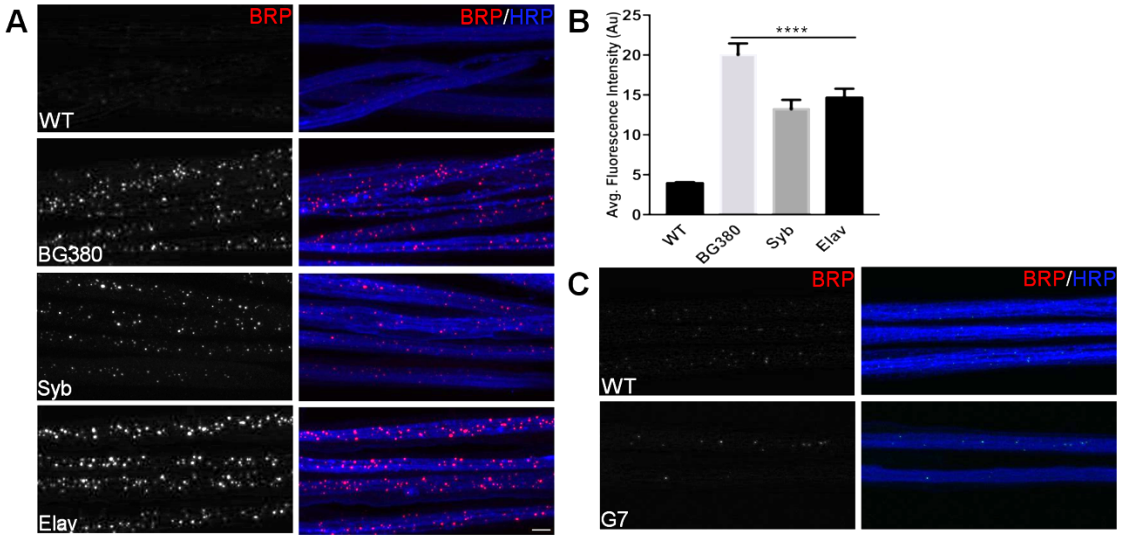

Figure 3.2 All tested presynaptic drivers lead to accumulation of BRP in axon bundles

A) Representative confocal image stacks showing axons from WT and Par-1OE third instar larvae stained with antibodies against BRP (red) and HRP (Blue) using different presynaptic Gal-4 drivers (indicated on figure). B) Quantification of BRP intensity from axons from genotypes in A. n=10, ****=p<0.0001. Scale Bar = 10µm. Error bars represent S.E.M. C) Representative confocal image stacks showing axons from WT and Par-1OE third instar larvae stained with antibodies against BRP (red) and HRP (Blue) using postsynaptic drive G7-Gal-4. N=10, p=0.47. Scale Bar = 10µm.

To further test my hypothesis that overexpression of Par-1 may lead to a specific axonal transport defect of BRP; we labeled the axons using markers of various cargoes that are transported within the axons. We used the following markers: Liprin-α (another marker of active zones,(Dai et al., 2006)), and disabled (DAB, a marker for endocytic

zones,(Kawasaki et al., 2011)). The levels of Liprin-α and DAB in the axons of flies overexpressing Par-1 were similar to the levels of these proteins in WT flies (Figure 3.3 A-C), providing further evidence that overexpression of Par-1 results in specific accumulation of BRP in axons. Next, we tested the transport of mitochondria, which is mediated by Milton and Miro(Glater et al., 2006). To test this, we generated flies that express mito-GFP in the presynaptic neurons along with overexpression of Par-1. To account for the possible "dilution" of GAL4 due to two UAS promoters (UAS-mito-GFP and UAS-Par-1^{OE}), we generated flies that carry UAS-GFP and UAS-Par-1 as a control. Expression of mito-GFP in wild type flies showed many mitochondria within the axons. Consistent with my hypothesis, flies overexpressing mito-GFP in Par-1 overexpression background showed no significant changes in the levels (Figure 3.3 A-C) or size (Figure 3.4 E) of mitochondria within the axons while still showing accumulations of BRP, indicating that overexpression of Par-1 does not affect mitochondrial transport.

Finally, to test the possibility that increased transcription of BRP may lead to accumulation of BRP in axons(Wairkar et al., 2013), I compared the BRP protein levels in the ventral nerve cords (VNC) between WT, Par-1^{OE} and Par-1^{T408A} flies. No significant differences were noted between the levels of BRP protein in the VNCs of these genotypes (Figure 3.1 E). To confirm these data, I also performed western blots using anti-BRP antibody on WT and Par-1^{OE} flies and did not observe any significant difference in the levels of BRP protein (Figure 3.1 D). These data indicate that increased accumulations of BRP in axons of flies overexpressing Par-1 are unlikely to be due to increased levels of

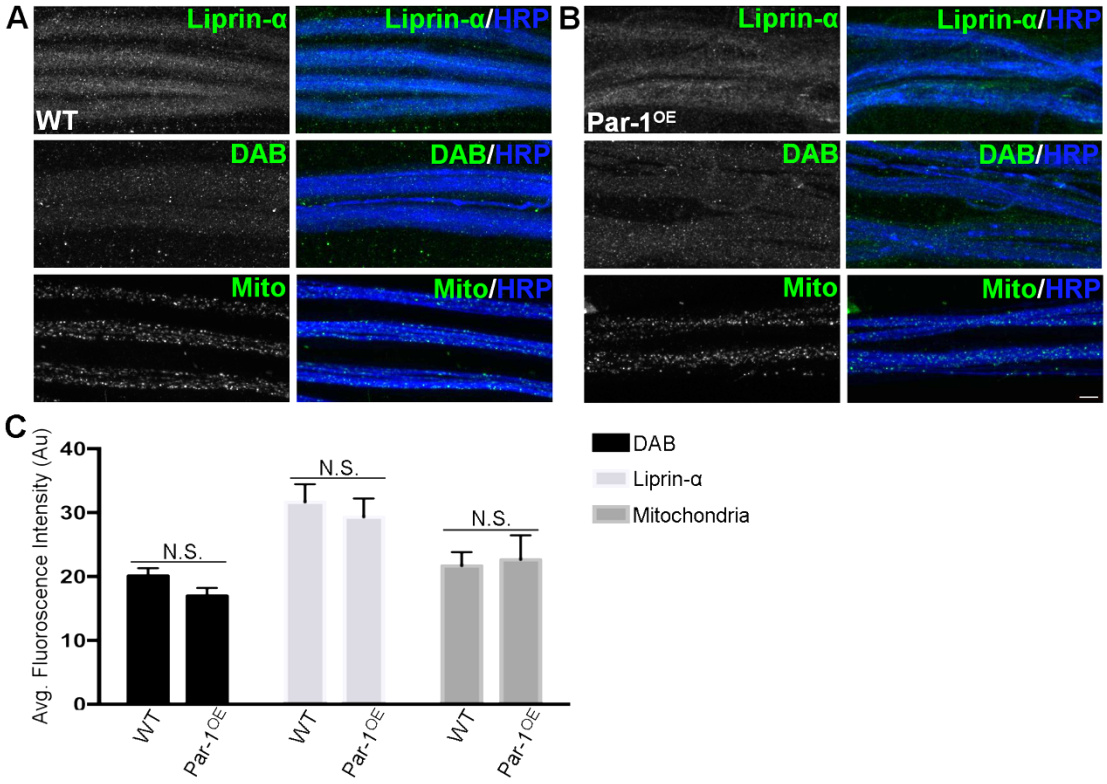

BRP protein. Taken together, my results strongly suggest that overexpression of Par-1 specifically affects the transport of BRP in the axons.

Figure 3.3 Overexpression of Par-1 leads to a specific accumulation of BRP

A) Representative confocal image stacks showing axons from WT and B) Par-1OE third instar larvae stained against Liprin-α (Green), DAB (Green), mito-GFP (Green) and HRP (Blue). Scale bar=10μm. C) Quantification of Liprin-α, DAB, mito-GFP intensities from axons. N=12, Liprin-α p =0.49, DAB p=0.09, and mito-GFP p=0.82. Error bars represent S.E.M.

Overexpression of Par-1 results in reduced T-bars and impaired synaptic transmission.

To test whether block in axonal transport of BRP would lead to decreased levels of BRP at the synapses, I labeled the NMJ synapses with BRP(Wagh et al., 2006) and HRP. Although I expected to see only a reduction in BRP at the synaptic terminals, I was

surprised to find that there were some interesting differences between WT synapses and those overexpressing Par-1. First, as expected, there were significant reductions in the number of active zones marked by BRP (Figure 3.5 A, B). Second, while the synaptic span was not significantly different in the flies overexpressing Par-1, the size of synaptic boutons was significantly reduced (Figure 3.6 A-C). However, these changes did not affect the apposition of synapses quantified using number of BRP puncta apposed to DGluRIII patches, a marker of postsynaptic density (Figure 3.6 A)(Marrus et al., 2004). These data show that although overexpression of Par-1 may cause specific defects in BRP transport, these defects may possibly lead to other changes at the synapse. It is not clear whether all of these changes are caused due to a block in axonal transport of BRP but levels of other synaptic proteins like Liprin-α and DAB are unaffected in flies overexpressing Par-1 (Figure 3.4 A-D). Interestingly, overexpression of Par-1^{T408A} does not show an increase in BRP within the axons or a reduction in BRP at the synapse arguing that these effects are not merely a consequence of overexpression of Par-1 (Figure 3.1 A,B and Figure 3.5 A,B).

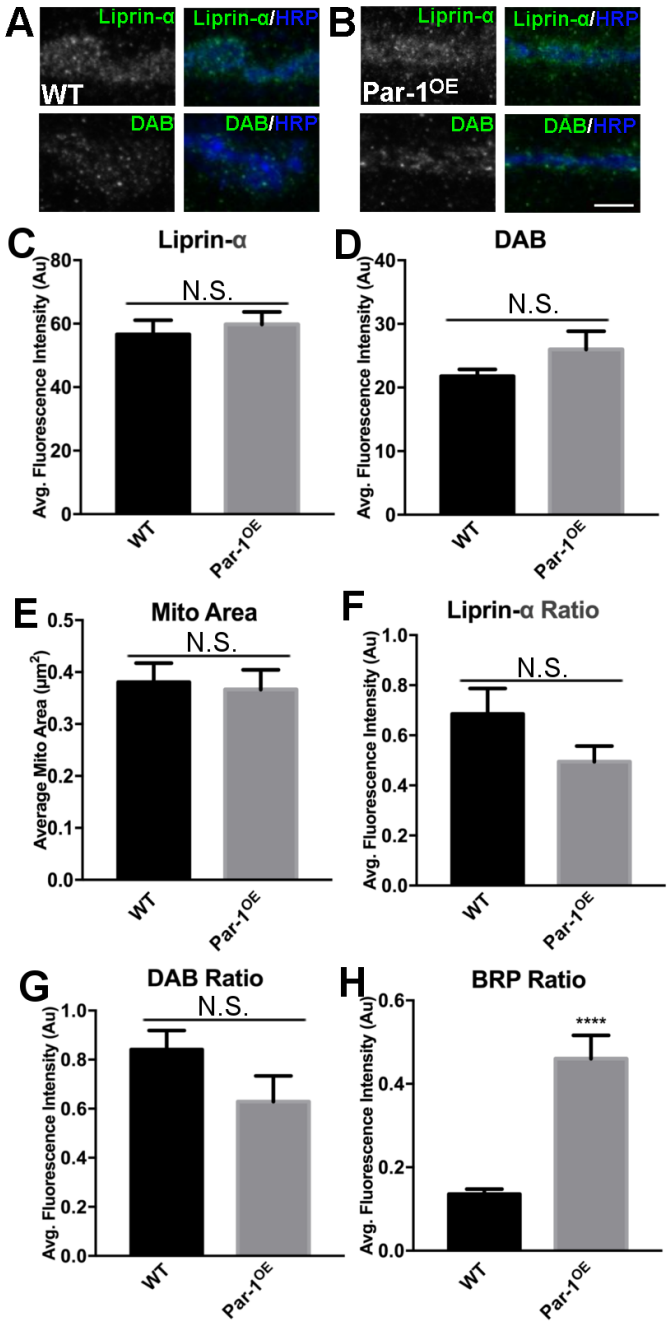

Figure 3.4 Overexpression of Par-1 does not affect other markers tested at synapses

A) Representative confocal image stacks showing NMJ synapses from WT and B) Par-1^{OE} third instar larvae stained against Liprin-α, DAB (Green) and HRP (Blue). Scale bar=10μm. C) Quantification of Liprin-α (Green) intensity from axons. N=12, p=0.49. Error bars represent S.E.M. D) Quantification of DAB (Green) intensity from axons. N=12, p=0.09. Error bars represent S.E.M. E) Quantification of Mitochondria area within axons (see Figure 2) of WT and Par-1^{OE} larvae. N=10, p=0.7893. Error bars represent

S.E.M. F-H) The ratio of signal in synapses to axons of Liprin-α (F), DAB (G), and BRP (H).

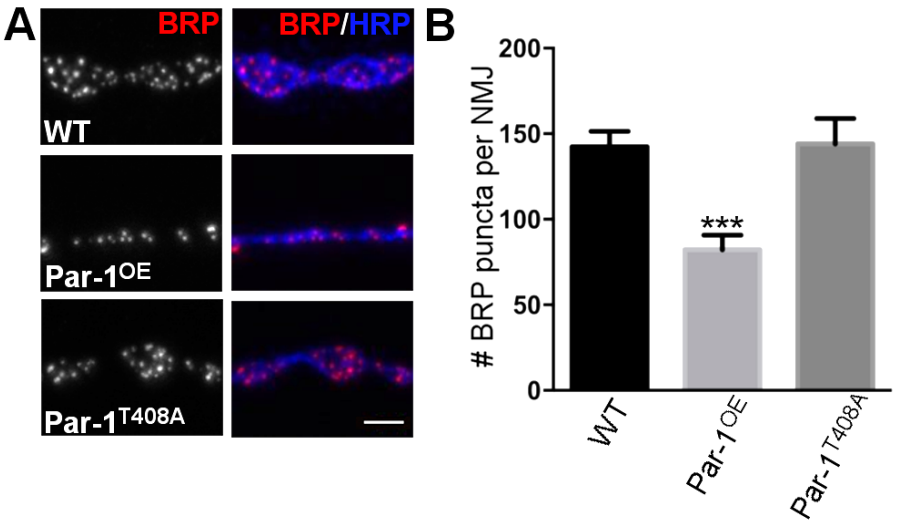

Figure 3.5 Par-1 overexpression leads to loss of BRP at synaptic boutons

A) Representative images from WT, Par-1OE and Par-1T408A showing the NMJ synapses labeled with anti-BRP (Red) and anti-HRP (Blue) antibodies B) Quantification of BRP puncta per NMJ. N=10, ***=p≤0.0001. Scale bar=10μm. Error bars represent S.E.M.

To confirm my light-level findings, I performed ultrastructural studies at WT and Par-1^{OE} synapses. Consistent with previous reports showing that a reduction in BRP causes a decrease in number of T-bars(Wagh et al., 2006, Wairkar et al., 2009), I found a significant decrease in the total number of T-bars per active zones at the synapses of flies overexpressing Par-1 as compared to WT (Figure 3.7 A, B). Taken together, my data so far demonstrate that overexpression of Par-1 in neurons leads to a specific block in axonal transport of BRP, which is the likely caused due to the reduction in T-bars at synapses.

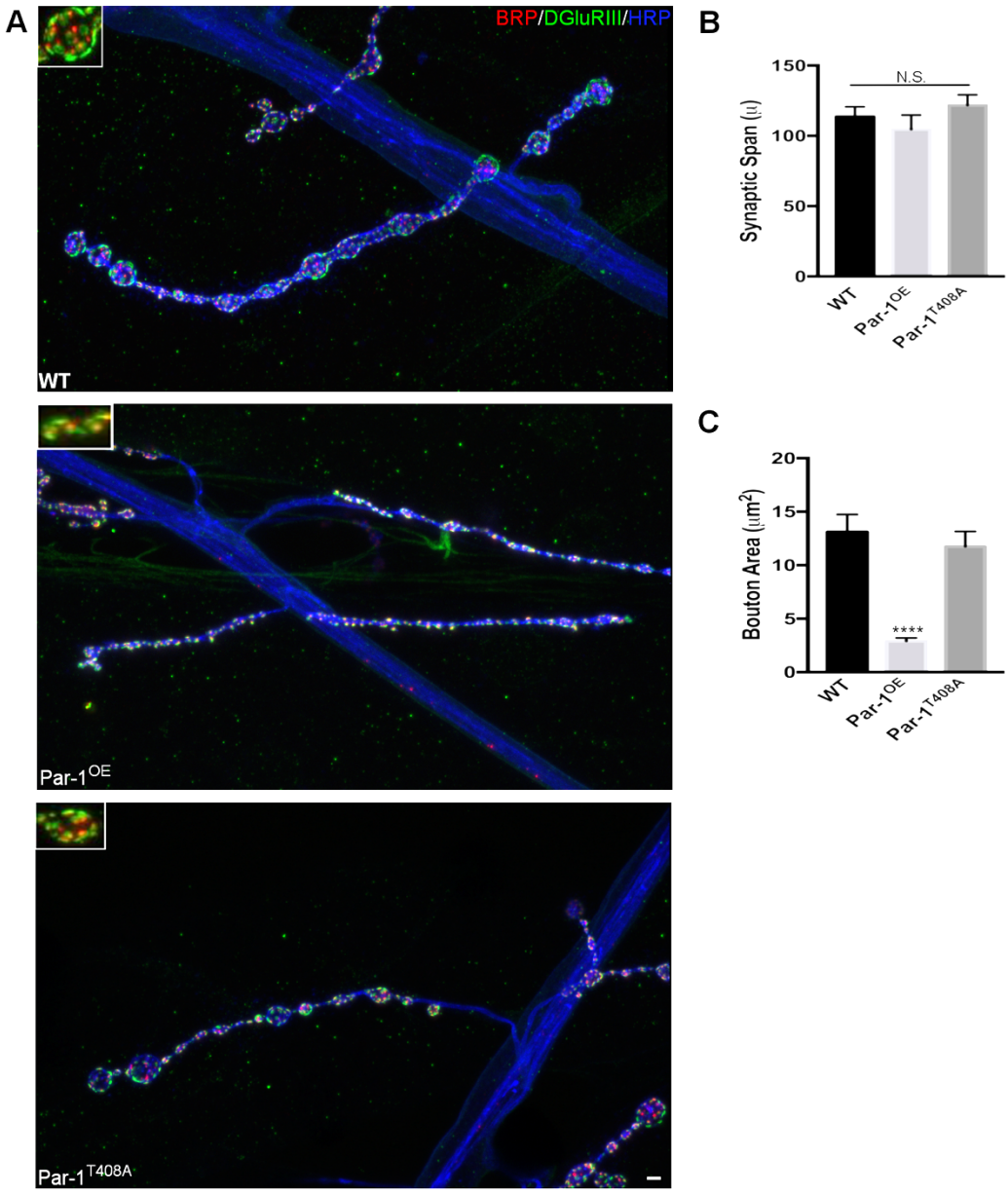

Figure 3.6 Par-1 overexpression leads to changes in morphology

A) Representative confocal image stacks showing NMJs from WT, Par-1OE and Par-1T408A third instar larvae stained with antibodies against BRP (red), DGluRIII (Green) and HRP (Blue). Synaptic apposition as marked by the apposition of BRP and DGluRIII (Inset) was unchanged. Scale Bar=5μm. B) Quantification of Synaptic Span. N=10, p=0.39. C) Quantification of bouton area. N=10, ****= p<0.0001. Error bars represent S.E.M.

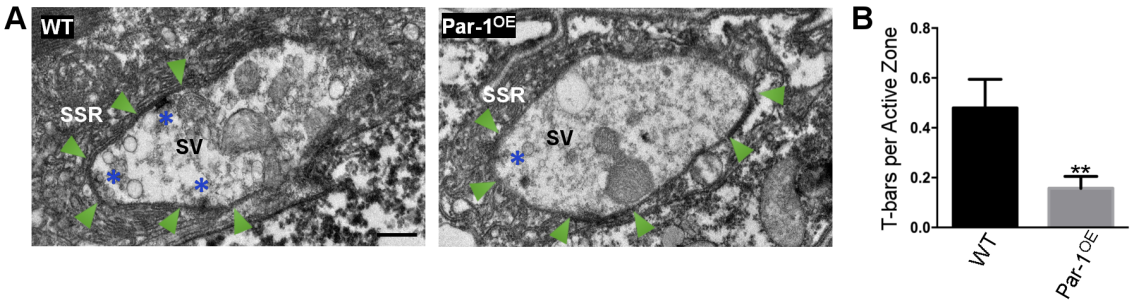

Figure 3.7 Par-1 overexpression leads to loss of T-bars

A) Representative electron micrographs from WT and Par-1OE third instar larvae showing electron dense active zones (Arrows), T-bars (Asterisks), synaptic vesicles (SV) and sub-synaptic reticulum (SSR) in a single synaptic bouton. B) Quantification of T-bars from WT and Par-1OE larvae. N=17, **=p=0.0048. Scale Bar = 0.5µm. Error bars represent S.E.M.

To test whether these synaptic changes result in defects in neurotransmission, Io performed intracellular electrophysiological recordings from WT, Par-1^{OE} and Par-1^{T408A} flies. I did not observe any change in the amplitude (Figure 3.8 A, C) of mini excitatory junction potentials (mEJPs), suggesting that the postsynaptic apparatus was unperturbed in Par-1^{OE} flies. However, the frequency of mEJPs was significantly reduced consistent with the decrease in number of release sites marked by BRP in Par-1^{OE} (Figure 3.8 A, D). Furthermore, there was a dramatic reduction in the excitatory junction potential (EJP) amplitude in Par-1^{OE} flies (Figure 3.8 B, E) pointing to a presynaptic defect. Calculation of the quantal content (EJP amplitude/mEJP amplitude) (Petersen et al., 1997) showed a decrease in quantal content (Figure 3.8 F) in flies overexpressing Par-1. These data are consistent with presynaptic deficits and are likely a consequence of fewer T-Bars(Wairkar et al., 2009, Wagh et al., 2006) and reduced size of synaptic boutons. Taken together, my data suggest that presynaptic elevation in the levels of Par-1 has both structural and functional consequences for the synapse.

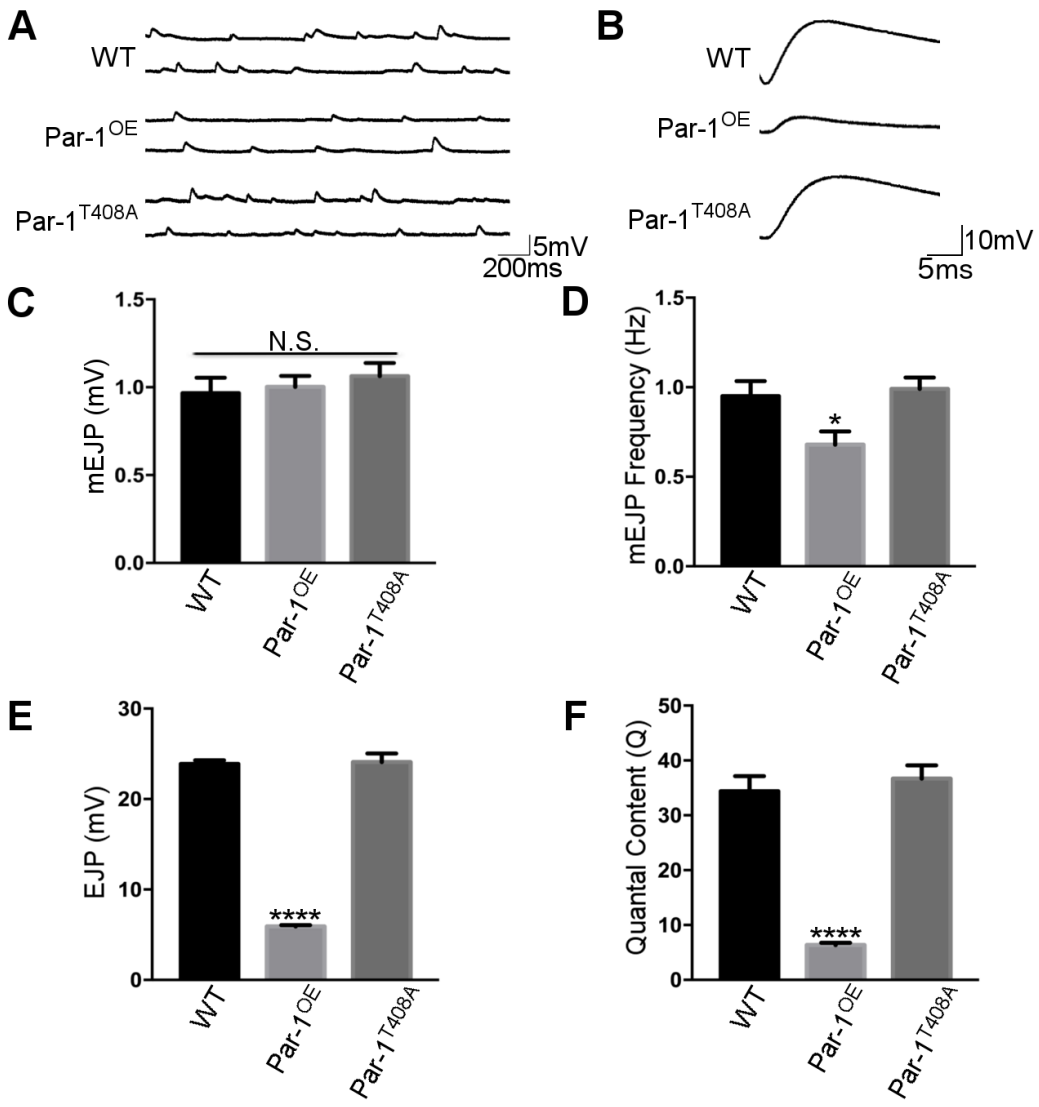

Figure 3.8 Par-1 overexpression leads to functional deficits

A) Representative mEJPs from WT, Par-1^{OE}, and Par-1^{T408A}. **B**) Representative EJPs from WT, Par-1^{OE}and Par-1^{T408A}. **C**) Quantification of mEJP amplitude. N=10, p=0.65. **D**) Quantification of frequency of mEJPs N=10, *=p<0.05. **E**) Quantification of EJP amplitude. N=10, ****=p<0.0001. **F**) Quantification of Quantal Content. N=10, ****=p<0.0001. Error bars represent S.E.M.

dTau does not mediate the specific transport of BRP.

Microtubules play an important role in axonal transport of synaptic cargo(Goldstein et al., 2008). Par-1/MARK kinase phosphorylates Tau(Drewes et al., 1995)-a microtubule associated protein that binds and helps stabilize microtubules.

Phosphorylation of Tau has been postulated to lead to its detachment from the microtubules leading to their destabilization(Drewes et al., 1997, Mandelkow et al., 2004). Thus, overexpression of Par-1 is expected to hyperphosphorylate Tau and lead to its detachment from microtubules making them unstable. To begin testing these possibilities, I first tested the levels of dTau using Western blot analysis on protein extracts from the ventral nerve cords (VNCs) of WT, Par-1^{OE} and Par-1^{T408A} flies using two previously characterized antibodies(Bolkan and Kretzschmar, 2014, Doerflinger et al., 2003). The levels of dTau were not significantly different between these genotypes (Figure 3.9 B, C), suggesting that Par-1 overexpression does not alter the levels of Tau in neurons. This raises the possibility that overexpressed Par-1 does not localize to the microtubules and is therefore unable to phosphorylate it. To test this possibility, I stained the axons of Par-1^{OE} flies with anti-Par-1 antibodies and compared its localization in WT axons. In Par-1^{OE} flies, Par-1 localized prominently within axons along with microtubules (Figure 3.10) indicating that Par-1 localization to the microtubules was not hampered. I also tested the possibility that Par-1^{T408A} may not localize to axons and therefore would not phosphorylate its substrate (Tau). However, Par-1^{T408A} localized similar to that of overexpressed wild type Par-1 (Figure 3.10). These experiments suggest that activity of Par-1 kinase is important to affect the transport of BRP within the axons.

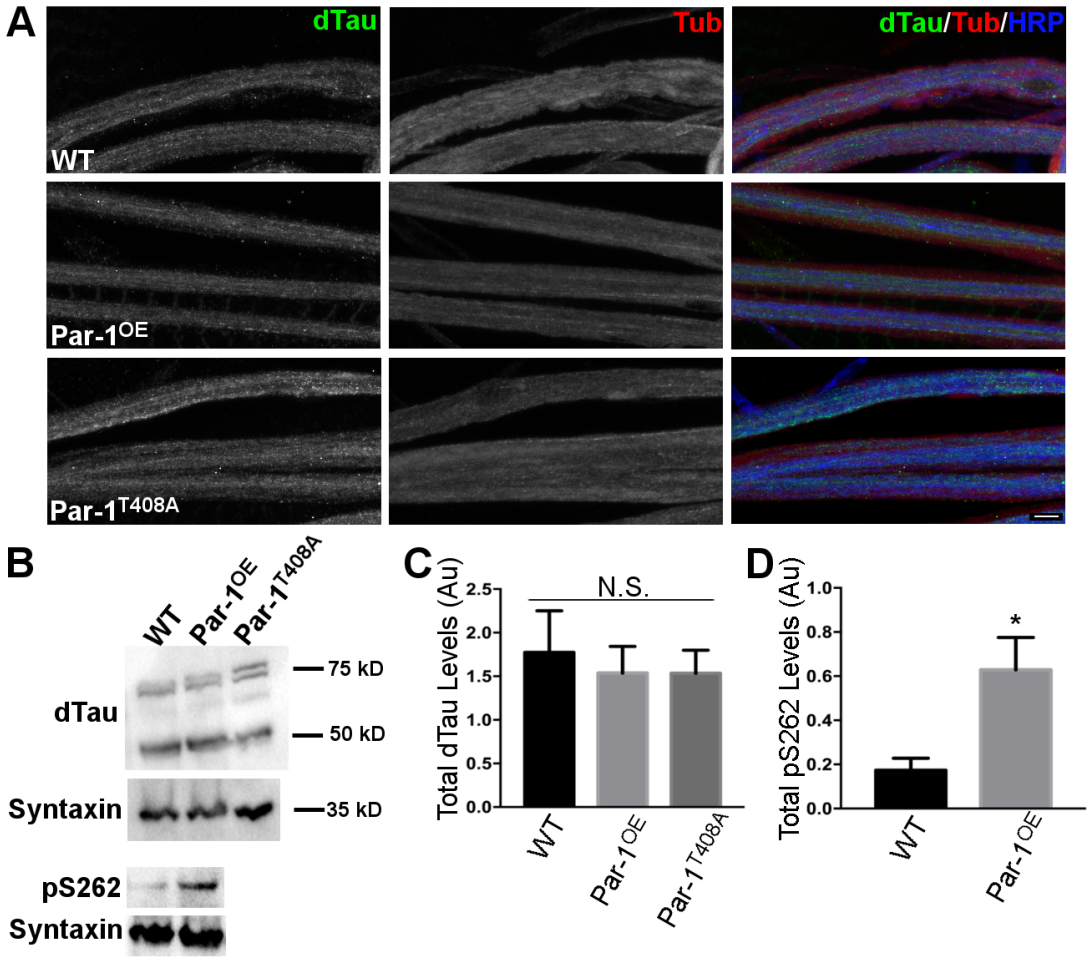

Figure 3.9 *Drosophila* Tau localizes to microtubules and levels are unchanged when Par-1 is overexpressed

A) Representative confocal image stack showing axons of WT, Par-1^{OE}, and Par-1^{T408A} third instar larvae stained with anti-dTau (Green), anti-Tubulin (Tub) (red) and anti-HRP antibodies (Blue). N=10. Scale bar=10µm. **B**) Representative Western blots from WT, Par-1^{OE} and Par-1^{T408A} using anti-dTau antibodies (upper panel). Western blot showing Tau phosphorylation at S262 site (pS262) of WT and Par-1^{OE} is shown in the bottom panel. Syntaxin was used as a loading control. **C**) Quantification of Western blots showing total dTau levels in the head lysates. N=3 independent experiments, p=0.87. Error bars represent S.E.M. **D**) Quantification of Western blots showing levels of pS262 levels of Tau. N=3 independent experiments, *= p =0.04. Error bars represent S.E.M.

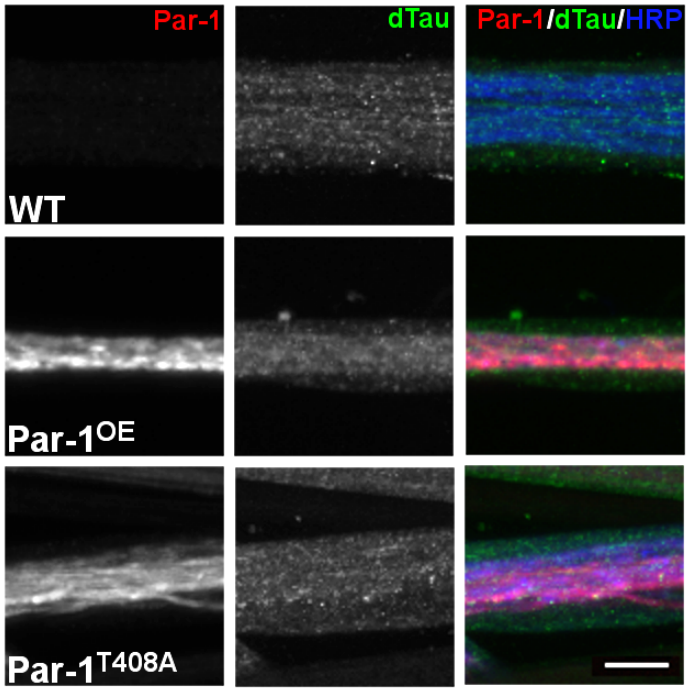

Figure 3.10 Par-1 and dTau localize to microtubules when both the active and inactive form of Par-1 is overexpressed

Representative images from WT and Par-1^{OE} and Par-1^{T408A} flies showing localization of overexpressed Par-1 (Red), endogenous tau (Green), and HRP (Blue) in axons.

Having established that overexpressed Par-1 can localize to the microtubules, I next wanted to test whether excess phosphorylation of Tau might cause its detachment from microtubules rendering them unstable(Drewes et al., 1997, Mandelkow et al., 2004). To test this, I first confirmed that overexpression of Par-1 could phosphorylate endogenous dTau. For this, I used an antibody that specifically recognizes the phospho-Ser262 on Tau (pS262) that is phosphorylated by Par-1(Iijima-Ando et al., 2012). I found that overexpression of Par-1 leads to an increase in dTau phosphorylation at Ser262 site (Figure 3.9 B, D). I then stained the axons of WT, Par-1^{OE}, and Par-1^{T408A} flies using the marker for stable microtubules-acetylated tubulin(Wolf et al., 1988). Distribution and levels of acetylated tubulin were unchanged in Par-1 overexpressing flies as compared to

WT (Figure 3.11 A, B), indicating that microtubule stability was uncompromised in flies overexpressing Par-1. Finally, I wanted to test whether dTau was mislocalized because of overexpression of Par-1. To test this, I used the previously generated anti-dTau antibody(Bolkan and Kretzschmar, 2014) but because this antibody has not been used for staining axons or synapses, I first tested its specificity. For this, I performed co-localization experiments with overexpressed tau^{GFP} (Figure 3.12 A). I found that overexpressed Tau^{GFP} co-localizes with anti-Tau antibody in axons. Furthermore, *tau*^{ko}(Burnouf et al., 2016) larval axons did not show any specific Tau staining within axons, (Figure 3.12 B) demonstrating the specificity of anti-dTau antibody. Next, to test whether dTau localizes to microtubules I performed co-localization experiments of dTau with Tubulin-a marker for microtubules (Figure 3.9 A). As expected, dTau and Tubulin co-localized in the axons indicating that dTau localizes to the microtubules in the axons.

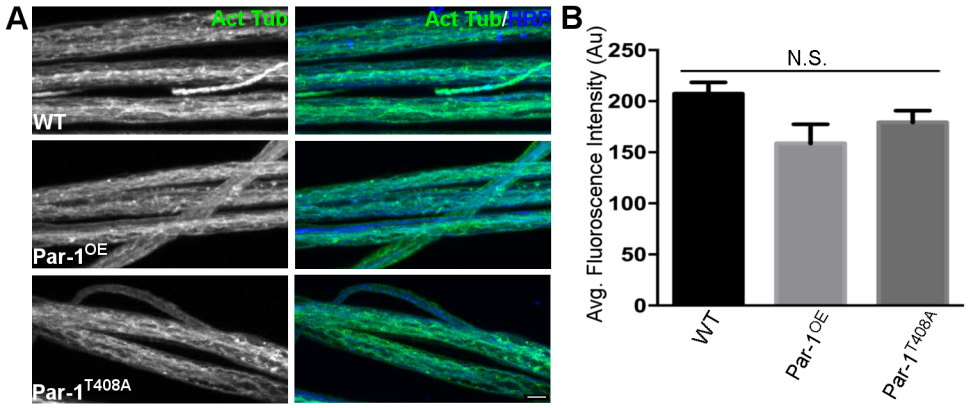

Figure 3.11 Par-1 overexpression does not lead to unstable microtubules

A) Representative images from WT, Par-1^{OE}, and Par-1^{T408A} flies showing axons stained against the marker for stable microtubules- acetylated tubulin (Green) and HRP (Blue). **B**) Quantification of acetylated tubulin (Green) intensity in axons. N=12, p=0.064. Scale bar=10µm.

I then tested whether dTau was mislocalized because of overexpression of Par-1 but did not find any evidence of mislocalization of dTau in flies overexpressing Par-1 (Figure 3.9 A) within the axons. I also double labeled the axons for Tubulin and dTau to ascertain that dTau was still localized to the microtubules in flies overexpressing Par-1 (Figure 3.9 A). These experiments suggest that instability of microtubule due to hyperphosphorylation of Tau is an unlikely reason for accumulations of BRP in axons of Par-1^{OE} flies.

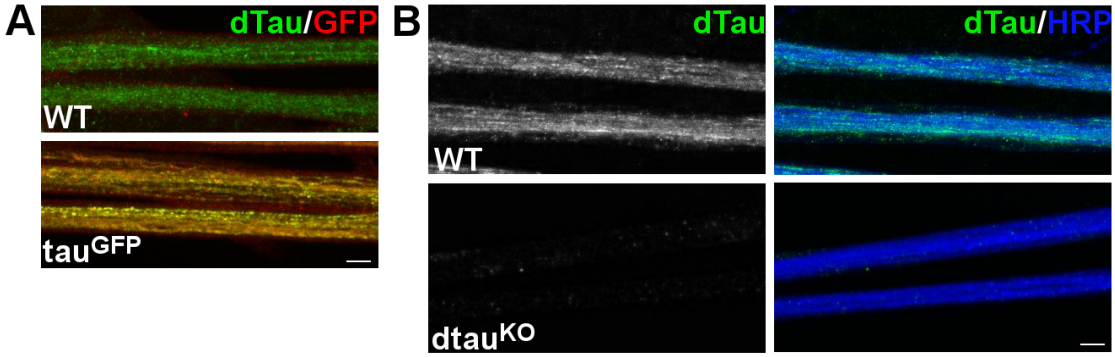

Figure 3.12 Validation of dTau antibody within axon bundles

A) Representative images from WT and Par-1^{OE} flies showing localization of overexpressed Tau^{GFP} (using anti-GFP antibody, Red) and dTau antibody (Green) in axons. Scale Bar = 10µm. **B**) Representative images from WT and d*tau*^{KO} flies showing localization of dTau (Green) in axons and HRP (Blue). Scale Bar = 10µm.

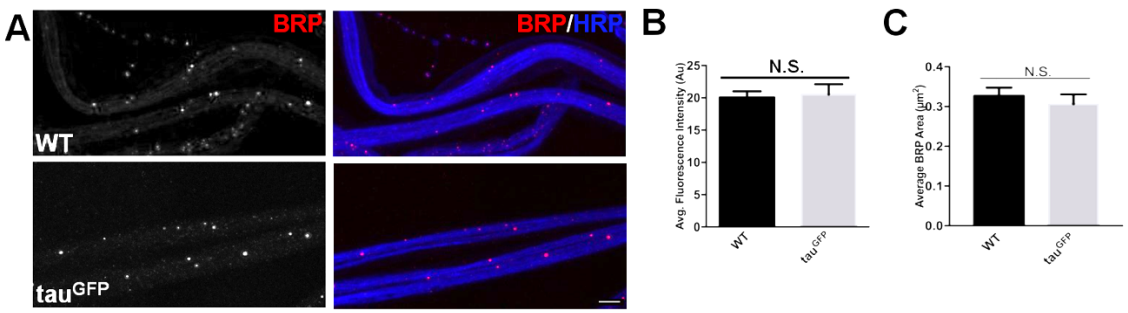

Figure 3.13 Overexpression of dTau does not lead to accumulation of BRP within axons

A) Representative confocal image stacks showing axons from WT and tau^{GFP} stained with antibodies against BRP (Red) and HRP (Blue). B) Quantification of BRP intensity in axons of identical genotypes as in A. N=10, p=0.30. Error bars represent S.E.M.

Having shown that the levels of endogenous Tau were not altered in flies overexpressing Par-1, and that stability of microtubules was uncompromised, I wondered whether overexpression of Tau, which has been shown to cause neurodegeneration(Andorfer et al., 2003, Adams et al., 2009), might have an effect on axonal transport of BRP. To test this possibility, I overexpressed tau^{GFP} in the presynaptic neurons. First, to confirm that dTau was overexpressed, I stained the axons with the anti-GFP antibody(Gallio et al., 2011) (Figure 3.12 A) and found that dTau was overexpressed. I then stained the axons of tau^{GFP} flies with antibodies against BRP to test whether dTau overexpression affected the axonal transport of BRP. I did not observe any significant difference in the levels of BRP within the axons (Figure 3.13 A, B) in flies overexpressing dTau as compared to WT. These data show that dTau overexpression does not cause accumulation of BRP within the axons.

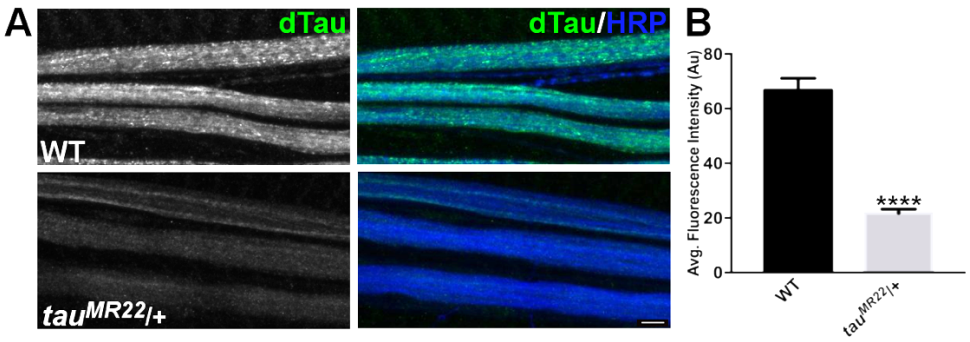

Figure 3.14 *dtau* transheterozygote has a significant reduction of endogenous dTau

A) Representative images from WT and *tau*^{MR22}/+flies showing axons stained against dTau (Green) and HRP (Blue). **B**) Quantification of dTau intensity in WT and *tau*^{MR22}/+ axons. N=8, ****=p<0.0001. Scale bar=10µm. Error bars represent S.E.M.

Finally, to test whether dTau may not be the endogenous substrate of Par-1 that mediates axonal transport of BRP, I generated a fly that overexpressed Par-1 in a *dtau* transheterozygote (Df(3R)tauMR22/+, (Doerflinger et al., 2003)) (Par-1^{OE}, tau^{MR22}/+) because *tau*^{MR22} mutants are embryonic lethal(Bolkan and Kretzschmar, 2014, Doerflinger et al., 2003). To confirm that *tau*^{MR22} heterozygotes had at least a 50% decrease because of deletion of one copy of dTau, I stained the *tau*^{MR22} heterozygous larvae with anti-dTau antibody. Levels of dTau in axons were reduced by ~70% (Figure 3.14 A, B) in *tau*^{MR22} heterozygotes. If dTau were to mediate the effects of Par-1 overexpression on the axonal transport of BRP, I expect to see at least a partial suppression of BRP accumulations within the axons of flies that have reduced dTau levels.

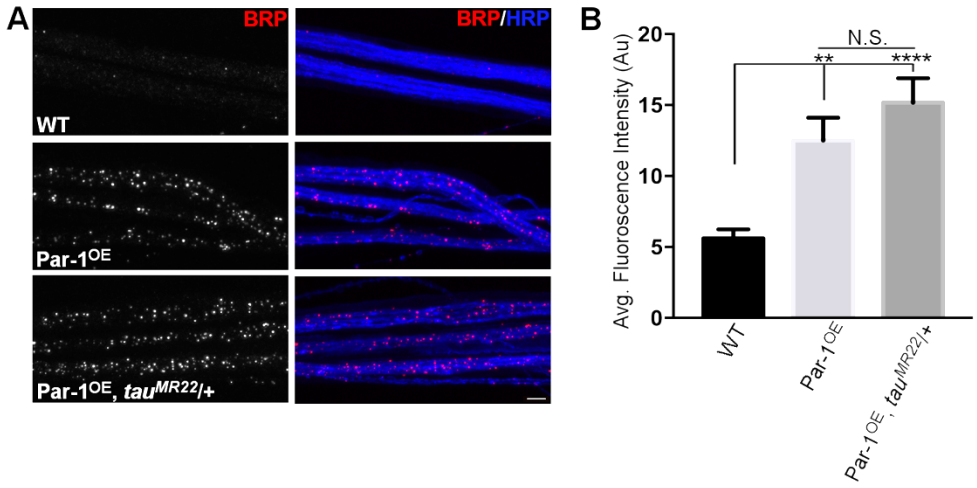

Figure 3.15 Accumulation of BRP within axons is not mediated by dTau

A) Representative third instar larvae stained with antibodies against anti-BRP (Red) and anti-HRP (Blue) from the following genotypes: WT, Par-1^{OE}, Par-1^{OE}, *tau*^{MR22}/+. **B**) Quantification of BRP intensity in the axons from the genotypes. N=15, **=p<0.001, ****=p<0.0001. Scale bar=10µm. Error bars represent S.E.M.

To test this, I stained WT, Par-1^{OE} and Par-1^{OE}, *tau*^{MR22}/+ fly NMJs with antibodies against BRP. As expected, Par-1^{OE} showed elevated levels of BRP in axons as compared to WT (Figure 3.15 A, B). However, the levels of BRP protein in the axons of Par-1^{OE} and *tau*^{MR22}/+ flies were quantitatively similar, demonstrating that dTau is unlikely to be the substrate of Par-1 that mediates the axonal transport deficits elicited by elevated levels of Par-1. Finally, I confirmed that BRP transport was unaffected in *tau*^{MR22} transheterozygotes as well as dtau^{KO} flies (Figure 3.16 A-D). Together, these data strongly support the idea that BRP accumulations observed within the axons for Par-1 overexpressing flies are independent of Tau.

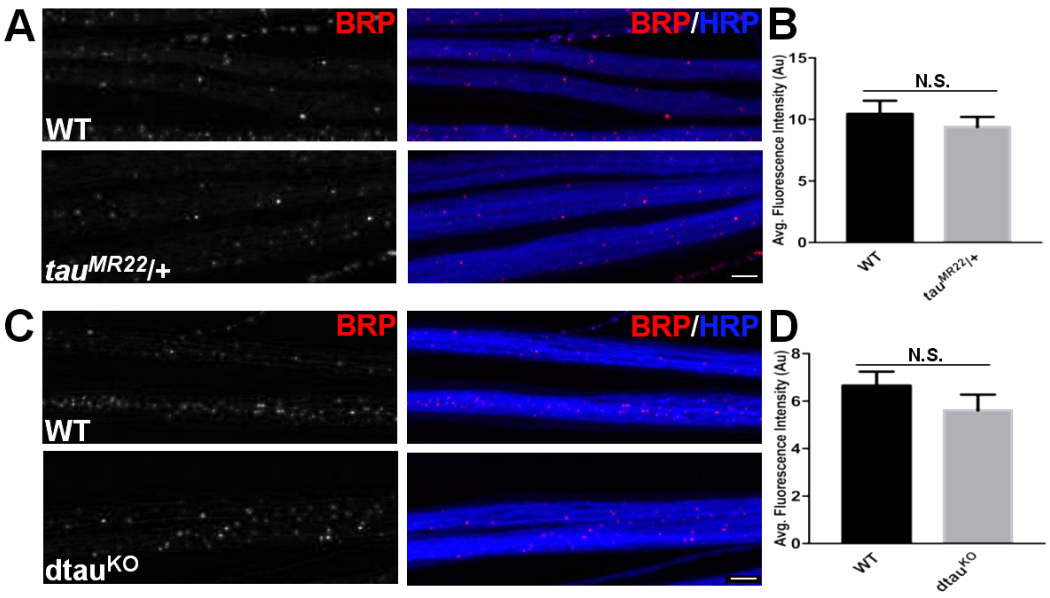

Figure 3.16 Reduction of dTau does not lead to accumulation of BRP in axons

A) Representative images from WT and *tau*^{MR22}/+flies showing axons stained against BRP (Red) and HRP (Blue). **B**) Quantification of BRP intensity in axons. N=8, p=0.4309. Scale bar=10µm. **C**) Representative images from WT and dtau^{KO}flies showing axons stained against BRP (Red) and HRP (Blue). **D**) Quantification of BRP intensity in axons. N=8, p=0.24. Scale bar=10µm. Error bars represent S.E.M.

CHAPTER 4: LEVELS OF PAR-1 KINASE DETERMINE THE LOCALIZATION OF BRUCHPILOT AT THE *DROSOPHILA* NEUROMUSCULAR JUNCTION SYNAPSES

Adapted from Barber, Hruska, Bush, Martinez, Fei, Levitan, Davla, Wairkar 2018
"Levels of Par-1 kinase determine the localization of Bruchpilot at the *Drosophila* neuromuscular junction synapses"
Published October 2018 in Scientific Reports, DOI: 10.1038/s41598-018-34250-9

INTRODUCTION

Assembly of active zones on the presynaptic side of a synapse is one of the earliest steps in the formation of nascent synaptic communication networks (Friedman et al., 2000, Sudhof, 2012). Initiation of presynaptic assembly is accomplished, in part, by the transport of synaptic vesicle precursors (SVPs) and Piccolo-Bassoon transport vesicles (PTVs) that carry the components of active zones (Shapira et al., 2003, Sudhof, 2012). Interestingly, active zone density is maintained after its formation and decreases only later with aging (Chen et al., 2012). Indeed, many synapses are thought to be stable for long periods of time after they are established (Lin and Koleske, 2010). Therefore, mechanisms must exist that maintain the presynaptic components such as active zones and postsynaptic density for their long-term stability. One way presynaptic components are maintained at the synapse is by active replenishment of synaptic proteins via axonal transport (Millecamps and Julien, 2013). Although such mechanisms are relatively well studied for synaptic vesicles and mitochondria(Holzbaur and Scherer, 2011, Maday et al.,

2014, Stowers et al., 2002), little is known about how cargo destined for active zones is transported and how the transport is regulated.

Par-1 kinase is a *Drosophila* homolog of Microtubule affinity regulating kinase (MARK), which is elevated in many diseases (Chin et al., 2000, Liu et al., 2016, Beghini et al., 2003) including, neurodevelopmental and neurodegenerative disorders(Chin et al., 2000, Seshadri et al., 2010, Lund et al., 2014, Maussion et al., 2008). At the synapse, Par-1, a cell polarity kinase(Doerflinger et al., 2003), has been previously implicated in regulating the postsynaptic glutamate receptor localization(Zhang et al., 2007). Interestingly, it was also noted that Par-1 is present in the presynaptic compartment albeit at very low levels(Zhang et al., 2007), suggesting that Par-1 may also have a role in the presynaptic compartment. In the previous chapter, I demonstrated that elevated levels of presynaptic Par-1 lead to selective localization defects of BRP, with a significant accumulation of BRP within the axons and a corresponding decrease of BRP from the active zones (Barber et al., 2017). While it is clear that the effect of increased Par-1 on localization of BRP is independent of Tau-a microtubule associated protein (MAP) and a well-studied substrate of Par-1 (Barber et al., 2017, Yu et al., 2012, Wang et al., 2007, Trinczek et al., 2004), it is unclear whether other microtubule binding proteins such as Futsch (a MAP1B homolog)(Hummel et al., 2000), which has been proposed to be a likely substrate of Par-1(Doerflinger et al., 2003), might be involved. Also, it is unclear whether increased localization of BRP to the axons is a cause of the decreased BRP at the active zones. This is important because while the disruption of axonal transport has been implicated in many neurodegenerative diseases, it has been difficult to tease out whether

axonal transport is a cause or consequence of synaptic demise(Millecamps and Julien, 2013).

In this chapter, using temporal expression of Par-1, I show that BRP accumulation precedes decreased BRP at the synapse and that it is independent on Futsch-the neuron specific MAP(Hummel et al., 2000). Interestingly, I found that increased levels of BRP in axons are accompanied by decrease in synapse function followed by an increase in "floating" T-bars- a electron dense structure present at active zones of invertebrates as well as vertebrates(Zhai et al., 2001, Zhai and Bellen, 2004), suggesting that active zones of these flies may be unstable. Finally, I show that BRP and Par-1 are present in the same complex raising the interesting possibility that presynaptic Par-1 may regulate the localization of BRP by interacting with it.

RESULTS

Levels of presynaptic Par-1 are important in determining the proper localization of BRP

My previous chapter (Barber et al., 2017) revealed that elevated levels of presynaptic Par-1 lead to a selective accumulation of BRP in the axons concomitant with loss of BRP from the synapses. Since this study largely used overexpression of Par-1 as a means to increase its levels, I wondered whether physiological manipulations that lead to increased Par-1 levels would also show selective axonal accumulations of BRP. To test this, I used well-characterized mutations in E3 ubiquitin ligase, Slimb (Slmb), which is known to increase the levels of Par-1 (Lee et al., 2012). Consistent with my hypothesis, mutations in *Slmb* led to a selective increase in the levels of BRP within the axons

(Figure 1 A-C). Thus, the overexpression model of Par-1 has the same effect as physiologically increasing the levels of Par-1 by mutations in *Slmb*. Although it is important to note that the accumulation of BRP in *Slmb* mutants could be due to other possible downstream affects, the combination of increase in Par-1 levels in *Slmb* mutants(Lee et al., 2012), and the selective increase in BRP suggests the possibility that increased Par-1 levels in *Slmb* mutants cause increased BRP accumulation within the axons.

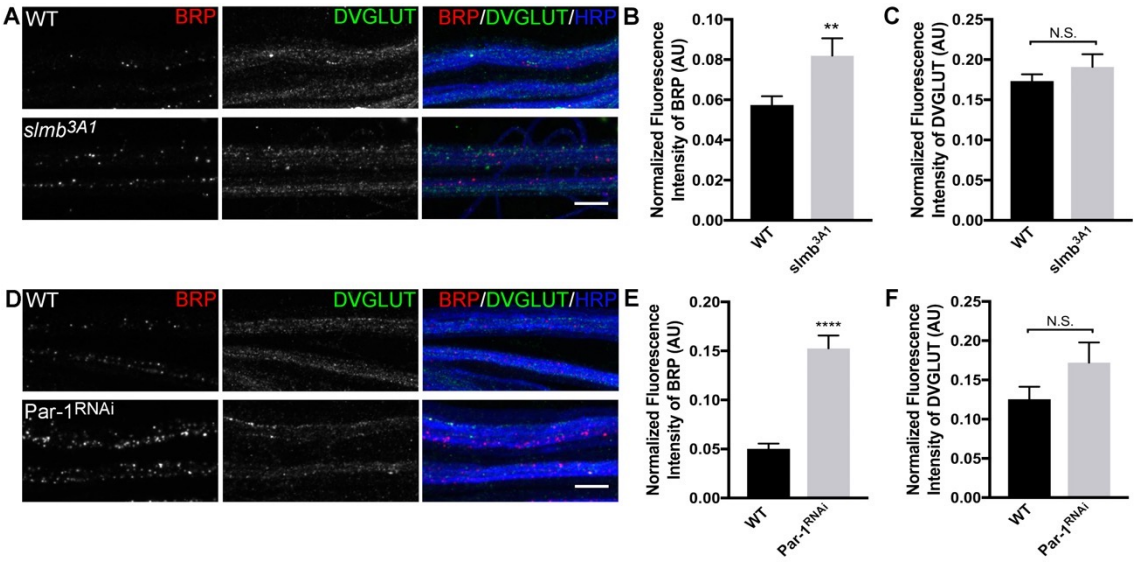

Figure 4.1 Precise levels of Par-1 are required for BRP localization

(A) Representative confocal stacks showing axon bundles from third instar larvae of WT and *Slmb* mutant (*slmb*^{3A1}). Axon bundles are stained with antibodies against BRP (Red), DVGLUT (Green) and HRP (Blue), n>10, Scale bar = 10µm. **(B)** Mean fluorescent intensity of BRP (BRP fluorescence normalized to HRP) in axon bundles represented in A. **(C)** Mean fluorescence intensity of DVGLUT normalized to HRP intensity **(D)** Representative confocal stacks showing axon bundles from third instar larvae of WT and Par-1^{RNAi}. Axon bundles are stained with antibodies against BRP (Red), DVGLUT (Green) and HRP (Blue), n>10, Scale bar = 10µm. **(E)** Mean fluorescence intensity of BRP normalized to HRP intensity. **(F)** Mean fluorescent intensity of DVGLUT normalized to HRP intensity. Error bars represent S.E.M. N.S.=p>0.05, **=p≤0.01, ****=p≤0.0001.

Since increased levels of Par-1 caused increase in BRP accumulation in axons, I hypothesized that decrease in the levels of Par-1 would lead to a decrease in BRP levels in axons. To test this hypothesis, I knocked down Par-1 presynaptically using a previously characterized Par-1 RNAi line(Zhang et al., 2007) using the presynaptic driver BG380-Gal4(Budnik et al., 1996). Surprisingly, decrease in the presynaptic Par-1 also led to an increase in selective accumulation of BRP (Figure 4.1 D-F). RNAi knockdown of

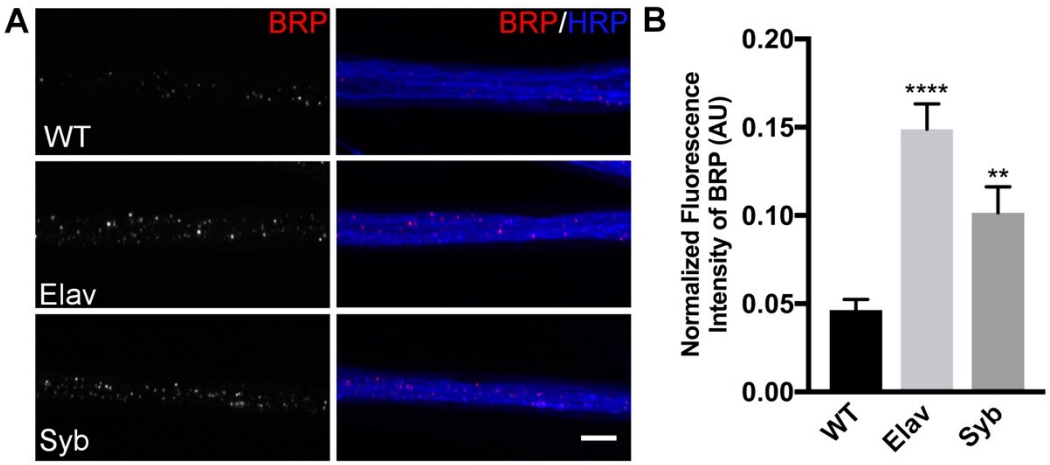

Par-1 with multiple presynaptic drivers yielded the same results (Figure 4.2 A, B). These data indicate that not only does Par-1 have a physiological role in regulating the localization of BRP but also that its fine balance is required for the its precise localization.

Figure 4.2 Knockdown of Par-1 using multiple presynaptic drivers show accumulations of BRP

(A) Representative confocal stacks showing axons from third instar larvae of WT and Par-1^{RNAi} third instar larvae using different presynaptic Gal-4 drivers (indicated on figure). Axons are stained with antibodies against BRP (Red), and HRP (Blue). Scale bar = 10μm **(B)** Mean fluorescence intensity of BRP normalized to HRP. Error bars represent S.E.M. **=p≤0.01, ****=p≤0.0001.

Accumulation of BRP precedes its decrease from synapses.

There are at least two possible reasons why BRP might accumulate within the axons. First, levels of neuronal Par-1 may determine proper transport BRP to the active zones. Second, precise levels of Par-1 may be required at the synapses to stabilize BRP at the active zones and breakdown of either of these processes may lead to BRP accumulating in the axons. If transport of BRP were the primary issue, I expect to find accumulation of BRP in axons to precede its reduction at the synapses. To test these possibilities, I took advantage of the GeneSwitch-Gal4 system (Osterwalder et al., 2001). This system allows the temporal expression of a transgene by feeding the larvae with a progesterone homolog, RU-486. In these experiments, I expressed the Par-1 transgene for a given period of time and then tested the effect of its expression on BRP accumulation within the axons and its loss from the synapses. Flies were allowed to lay eggs and develop on normal food and were transferred to food containing RU-486 at or just before the early third instar stage. Transfer onto the RU-486 containing food should turn "ON" the expression of Par-1 transgene. I systematically stained the larvae with antibodies against Par-1, BRP and HRP after 0, 9, 12, 24, 48 and 72 hours exposure to RU-486 and tested the expression of Par-1 transgene and the localization of BRP.

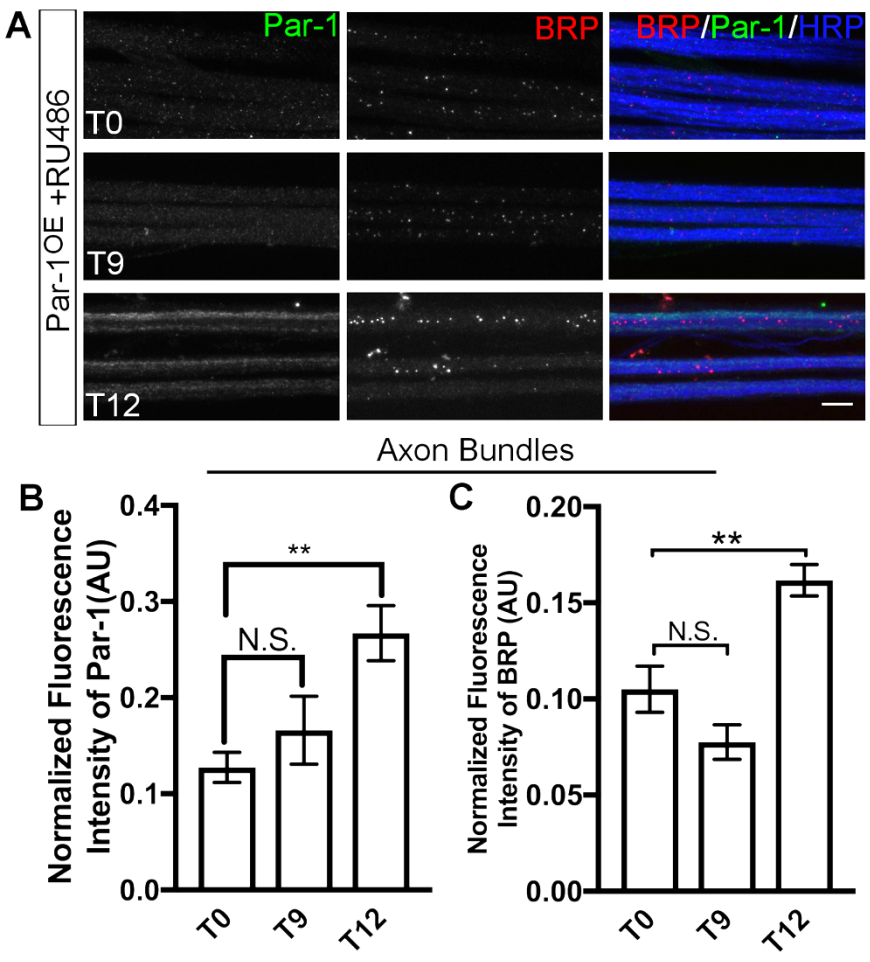

Figure 4.3 No change is noticeable in the intensity of axonal BRP until 12 hours of Par-1 induction

(A) Representative confocal stacks from larvae overexpressing Par-1 induced using GeneSwitch-ElavGal4 from T_0, T_9, and T_{12}. Axons are stained with antibodies against Par-1 (Green), BRP (Red) and HRP (Blue). Mean fluorescence intensity of Par-1 (**B**) and BRP (**C**) normalized to HRP in axon bundles from T_0, T_9, and T_{12}. N=12. Error bars represent S.E.M. N.S.=$p>0.05$, **=$p\leq0.01$, ***= $p\leq0.001$, ****=$p\leq0.0001$.

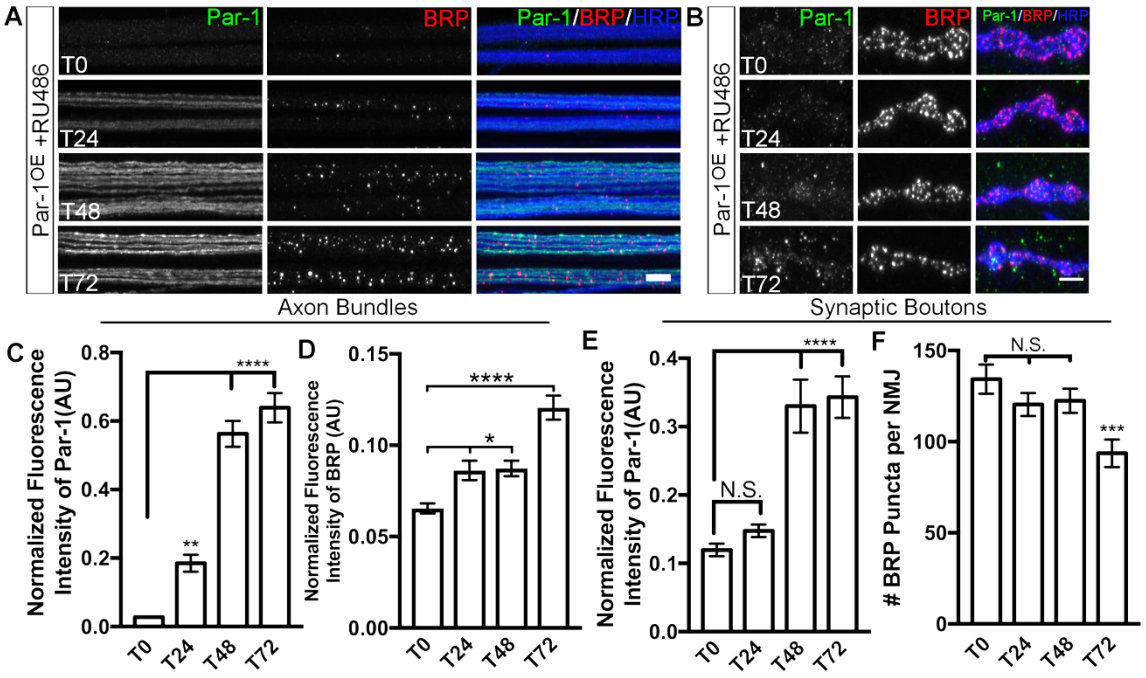

Figure 4.4 Accumulation of BRP in axons precedes its loss from synapses

(A-B) Representative axon bundles from larvae overexpressing Par-1 using GeneSwitch-Elav-Gal4. Time (T) represents time after exposure to RU-486 (T_0, T_{24}, T_{48}, and T_{72}) containing food. Axon bundles **(A)** are stained with antibodies against Par-1 (Green), BRP (Red) and HRP (Blue). Scale bar = 10µm. Synaptic boutons **(B)** are stained with identical antibodies as A. Scale bar = 5µm. **(C)** Mean Par-1 intensity normalized to HRP intensity within axons bundles **(D)** and mean BRP intensity normalized to HRP intensity in axon bundles **(D)** from same series of time points as A. n>20. **(E)** Mean Par-1 intensity from synaptic boutons normalized to HRP **(F)** and quantification of the number of active zones (BRP puncta) per NMJ from same time points as B. n≥15. Error bars represent S.E.M. N.S.=p>0.05, *=p≤0.05, **=p≤0.01, ***= p≤0.001, ****=p≤0.0001.

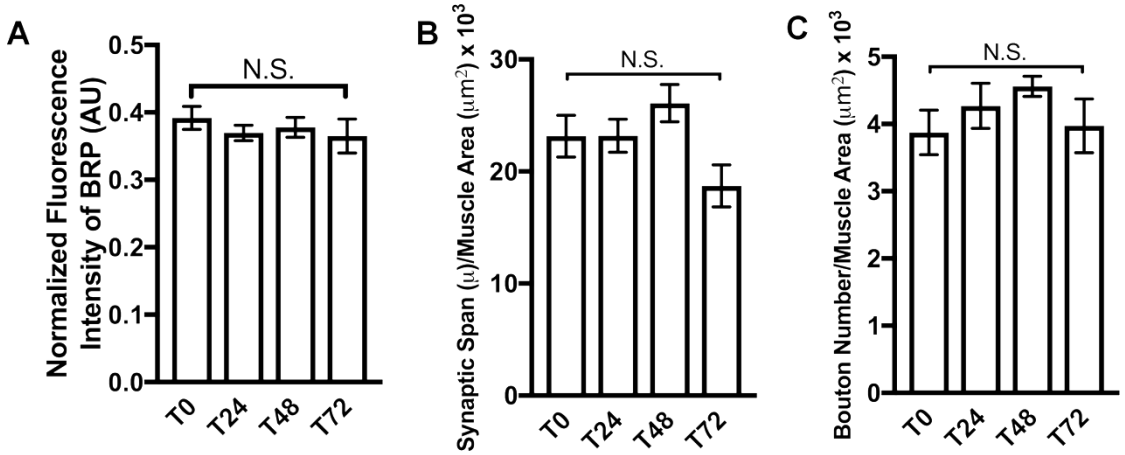

Figure 4.5 Additional quantification pertaining to Figure 2

(A) Mean fluorescence intensity of BRP normalized to HRP from synaptic boutons, across the NMJ arbor from larvae overexpressing Par-1 using GeneSwitch-Elav-Gal4. Time (T) represents time after exposing late second instar larvae to the RU-486 (T_0, T_{24}, T_{48}, and T_{72}). **(B-C)** Quantification of synaptic span **(B)** and average number of boutons per NMJ **(C)** from identical genotypes and normalized to mean muscle area. N≥20, N.S.=p>0.05.

Little to no detectable Par-1 was observed within axons from 0-9 hours (Figure 4.3 A,B). The BRP intensity within the axons remained similar to the zero time point after the exposure to RU-486 (Figure 4.3 A,C). I started to detect a significant increase in Par-1 within the axons at 12 hours (Supplemental Figure 2 A, B), along with a small but significant increase in the levels of BRP within the axons (Figure 4.3 A, C). At 48 hours, the levels of Par-1 within the axons increased further (Figure 4.4 A, C) along with a significant increase in Par-1 levels at the NMJs (Figure 4.4 B,E). However, the number of BRP per NMJ area at 48 hours was unaltered (Figure 4.4 B, F); indicating that accumulation of BRP within axons precedes the detectable reductions of BRP from the synapses. Consistent with this idea, at 72 hours after induction of Par-1 I observed a significant reduction in the average number of BRP puncta at the NMJs (Figure 4.4 B,F). I also measured average synaptic span, and bouton numbers normalized to muscle area in the same larvae (Figure 4.5 B, C) and found no change in these parameters to the control group. The intensity of BRP within the axons and at the number of BRP at the synapses were unaltered in the group that were exposed to RU-486 for the same time period as the experimental group but did not contain Par-1 transgene (Figure 4.6 A-D). These data indicate that there was no "leaky" expression of Par-1 in the experimental group. Together, these data indicate that BRP accumulation precedes the loss of BRP at the

synapses and thus points to the possibility that Par-1 may primarily regulate the transport of BRP.

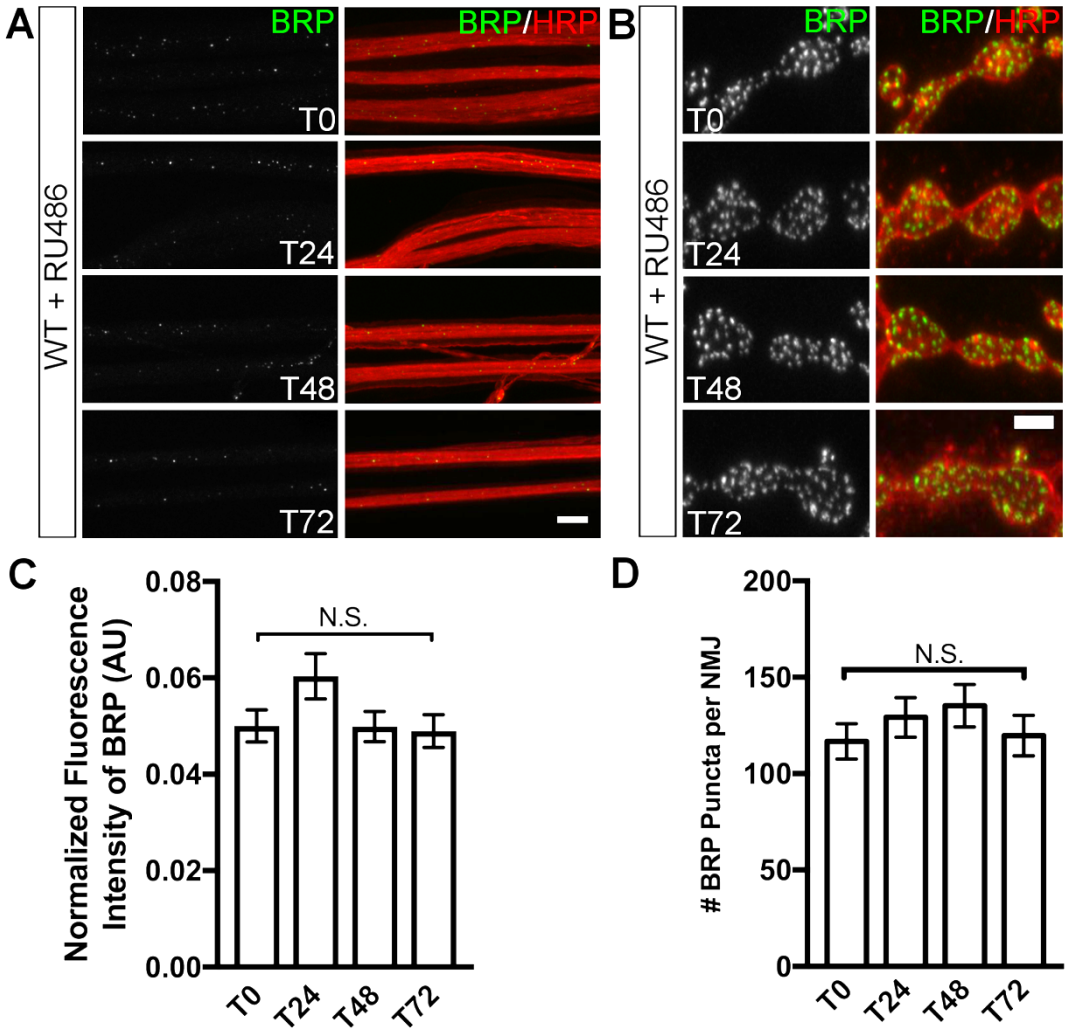

Figure 4.6 RU486 alone does not lead to BRP accumulation or loss of BRP at synapses

(A-B) Representative confocal stacks from WT larvae. Time (T) represents time after exposing the early third instar larvae to the RU-486 containing food (T0, T24, T48, and T72). Axons (A) and synaptic boutons (B) are stained with antibodies against BRP (Green) and HRP (Red). (C-D) Mean fluorescence intensity of BRP normalized to HRP (C) and BRP puncta count per NMJ (D) from identical genotypes in A-B. N=12. Error bars represent S.E.M. N.S.=p>0.05.

Synaptic function is altered before the loss of BRP from active zones.

To test whether decreased synaptic transmission (Barber et al., 2017) was an early consequence of increased accumulation of BRP within axons, I performed intracellular recordings from larvae that had just begun to accumulate BRP (~24 Hours post induction of Par-1 transgene) and time points in between until the synapses started to show a significant decrease in BRP (~72 Hours). I found that at 0 hours when accumulation of BRP within the axons is not increased significantly, the synaptic transmission (mEJP amplitude, frequency and EJP amplitudes) (Figure 4.7 A-F) is indistinguishable from the controls (WT larvae raised on RU-486) (Figure 4.8 A-F). Similarly, at 24 hours after the induction of Par-1 transgene although there was a significant increase in BRP levels within the axons, there was no change in the synaptic transmission. However, at 48 hours after the induction of Par-1 transgene, I began to observe a significant decrease in the EJP amplitudes and mini frequency while the mEJP amplitudes were unchanged (Figure 4.7 A-E). Interestingly, of note, at this time point there is a significant increase in the levels of Par-1 at the NMJs (Figure 4.4 B,E). However, the number of BRP puncta at the synapses were unaltered at this time point (Figure 4.4 B,F). At 72 hours after the induction of Par-1, there was a further decrease in EJP amplitudes while the mini EJP amplitudes remained unaltered (Figure 4.7 A-D), consistent with the previous observation that neither apposition nor the intensity of DGluRIII were significantly altered in lines overexpressing Par-1(Barber et al., 2017). It is important to note while there were some effects of the drug RU-486 on mEJP amplitudes and frequency (Figure 4.6 B,D,E), the EJP amplitudes and the quantal content remained unaltered (Figure 4.8 C,F). These data show that disruption of synaptic transmission is an early consequence of increased BRP accumulation in axons.

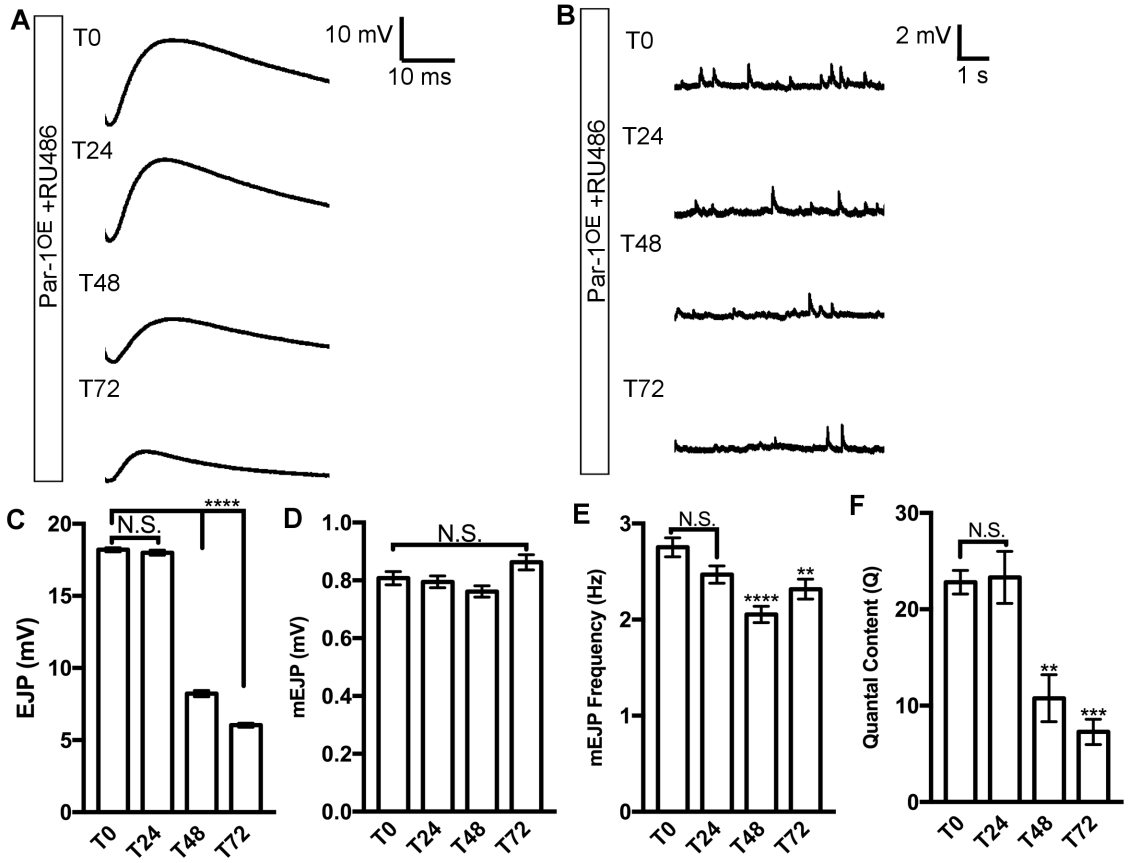

Figure 4.7 Functional deficits precede detectable decrease in BRP at synapses of flies overexpressing Par-1

(A-B) Representative traces of EJPs **(A)** and mEJPs **(B)** from larvae overexpressing Par-1 using GeneSwitch-Elav-Gal4. Time (T) represents time after exposing larvae to the RU-486 (T_0, T_{24}, T_{48}, and T_{72}). **(C-F)** Quantification of EJPs **(C)** and mEJP amplitudes **(D)**, frequency **(E)**, and quantal content **(F)** N=8. Error bars represent S.E.M. N.S.=p>0.05, **=p≤0.01, ***= p≤0.001, ****=p≤0.0001.

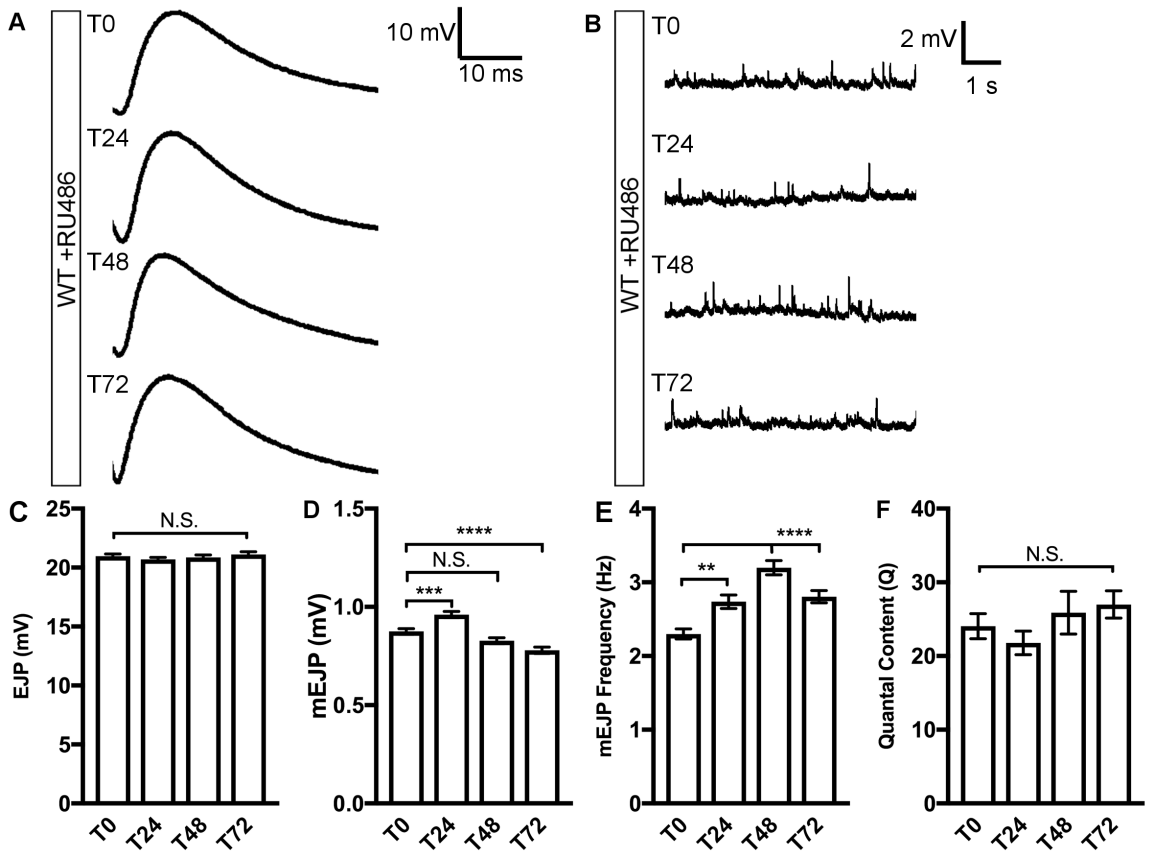

Figure 4.8 RU486 alone does not lead to functional deficits

(A-B) Representative traces of EJPs **(A)** and mEJPs **(B)** from WT larvae raised on RU486. Time (T) represents time after exposure to the RU-486 (T_0, T_{24}, T_{48}, and T_{72}). **(C-F)** Quantification of EJP amplitudes **(C)** and mEJP amplitudes **(D)**, frequency **(E)**, and quantal content **(F)** N=7. Error bars represent S.E.M. N.S.=p>0.05, **=p≤0.01, ***= p≤0.001, ****=p≤0.0001.

High axonal accumulation of BRP causes active zones to be unstable

So far, my data indicate that decreased BRP at the synapses might be a consequence of axonal accumulation of BRP. If WT Par-1 levels are required for the proper localization of BRP to the active zones, increase in BRP within axons could cause active zones to be unstable by "starving" the active zones of "fresh" BRP. This could possibly compromise active zone integrity and make them unstable. Instability of synapses in *Drosophila* is often associated with a loss of microtubule binding protein

Futsch(Eaton and Davis, 2003). Interestingly, a previous report has found that loss of Futsch leads to decrease in BRP density at the synapses and that Futsch interacts with BRP *in situ* at synapses (Lepicard et al., 2014). Finally, Futsch has KXGS motif that can potentially be phosphorylated by Par-1 kinase (Doerflinger et al., 2003). Therefore, changes in the levels of Par-1 could alter the levels and/or localization of Futsch. To test these possibilities I stained the NMJ preparations from WT and Par-1 overexpressing flies with anti-Futsch antibodies. I observed no change in the intensity of Futsch within axons of flies overexpressing WT Par-1 (Figure 4.9 A,B). Interestingly, however, there was a significant reduction in the intensity of synaptic Futsch (Figure 4.10 A,B). Importantly, such reductions were not apparent in Par-1^{T408A} expressing flies, indicating that the defect was not a result of secondary affect of Par-1 overexpression (Figure 4.10 A,B). To test whether the loss of Futsch might mediate affects of Par-1 overexpression, I tested whether *futsch* mutants accumulated BRP within their axons. Consistent with the previous report(Lepicard et al., 2014), I did not observe axonal accumulation of BRP within the axons of *futsch* mutants (Figure 4.9 C,D), indicating that Futsch may not mediate the affects of Par-1 overexpression. Finally, in the Gene Switch experiments (even at ~72 hrs post-induction of Par-1 transgene), I did not observe any alterations in the levels of synaptic Futsch (Figure 4.10 C,D) while there was a significant reductions of synaptic BRP (Figure 4.4 B,F). Although I cannot rule out the role of Futsch and/or cytoskeleton at later stages, these data indicate that Futsch, similar to tau(Barber et al., 2017) is not required for the increase in BRP accumulation within axons at the initial time points.

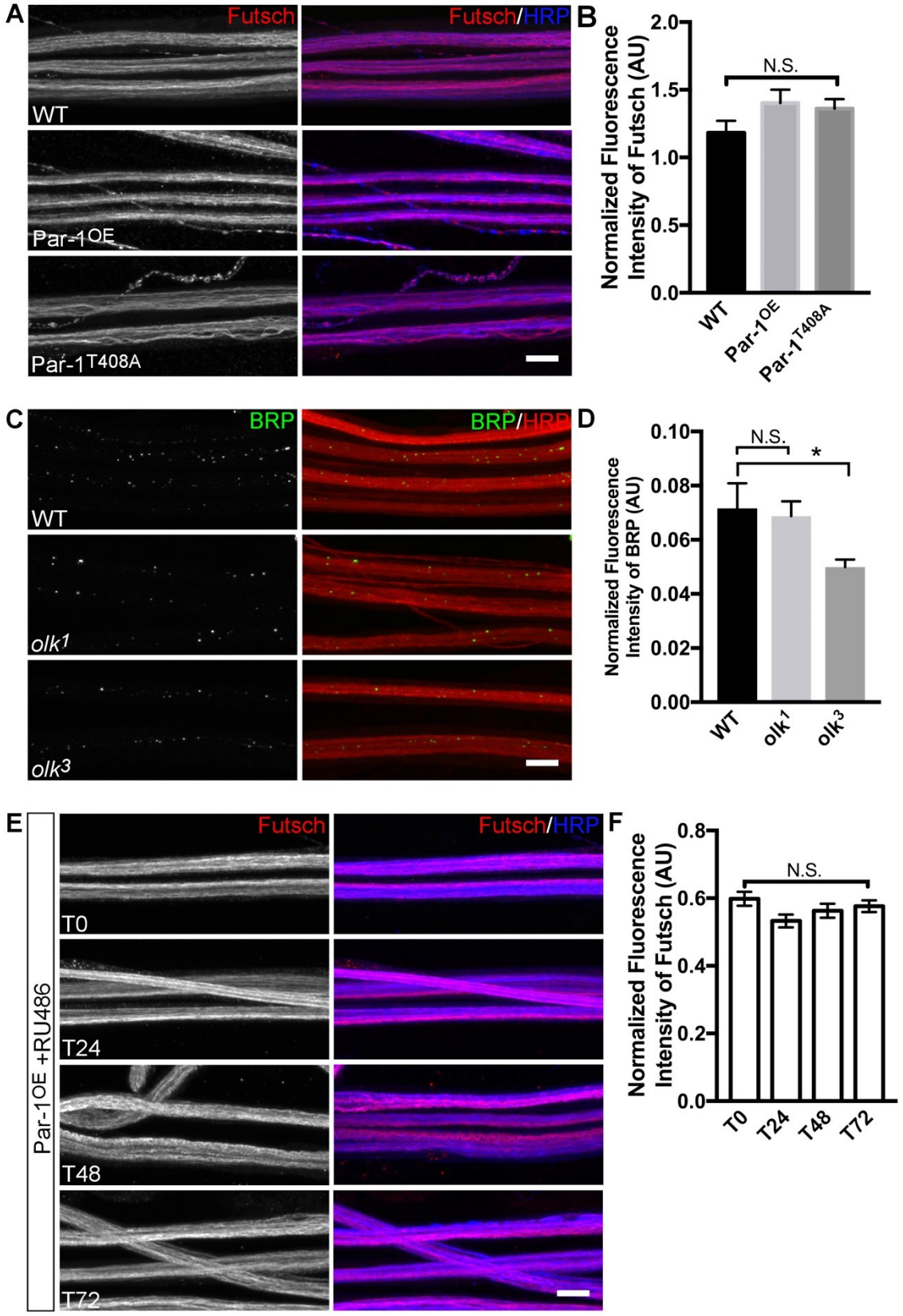
A
Futsch
Futsch/HRP
WT
Par-1OE
Par-1T408A
B
Normalized Fluorescence Intensity of Futsch (AU)
2.0
1.5
1.0
0.5
0.0
N.S.
WT
Par-1OE
Par-1T408A
C
BRP
BRP/HRP
WT
olk1
olk3
D
Normalized Fluorescence Intensity of BRP (AU)
0.10
0.08
0.06
0.04
0.02
0.00
N.S.
*
WT
olk1
olk3
E
Par-1OE +RU486
Futsch
Futsch/HRP
T0
T24
T48
T72
F
Normalized Fluorescence Intensity of Futsch (AU)
0.8
0.6
0.4
0.2
0.0
N.S.
T0
T24
T48
T72

Figure 4.9 Futsch may not mediate the effects of elevated neuronal Par-1

(A) Representative confocal image stacks showing axon bundles from WT, Par-1OE and Par-1T408A third instar larvae stained with antibodies against Futsch (Red) and HRP (Blue). (B) Normalized Futsch fluorescent intensity (A.U.) within axon bundles is not significantly different. N=10. (C) Representative confocal stacks showing axons from WT, olk1, and olk3 stained with antibodies against BRP (Green) and HRP (Red). (D) Mean fluorescence intensity of BRP from identical genotypes normalized to HRP. N=12. (E) Representative confocal stacks from larvae overexpressing Par-1 using GeneSwitch-ElavGal4 from T0, T24, T48, and T72. First column shows axons stained with an antibody against Futsch (Red) and second column with Merge of Futsch (Red) and HRP (Blue). (F) Mean Futsch fluorescence normalized to HRP levels within axons bundles. N=12. Error bars represent S.E.M. N.S.=$p>0.05$, *=$p\leq0.05$.

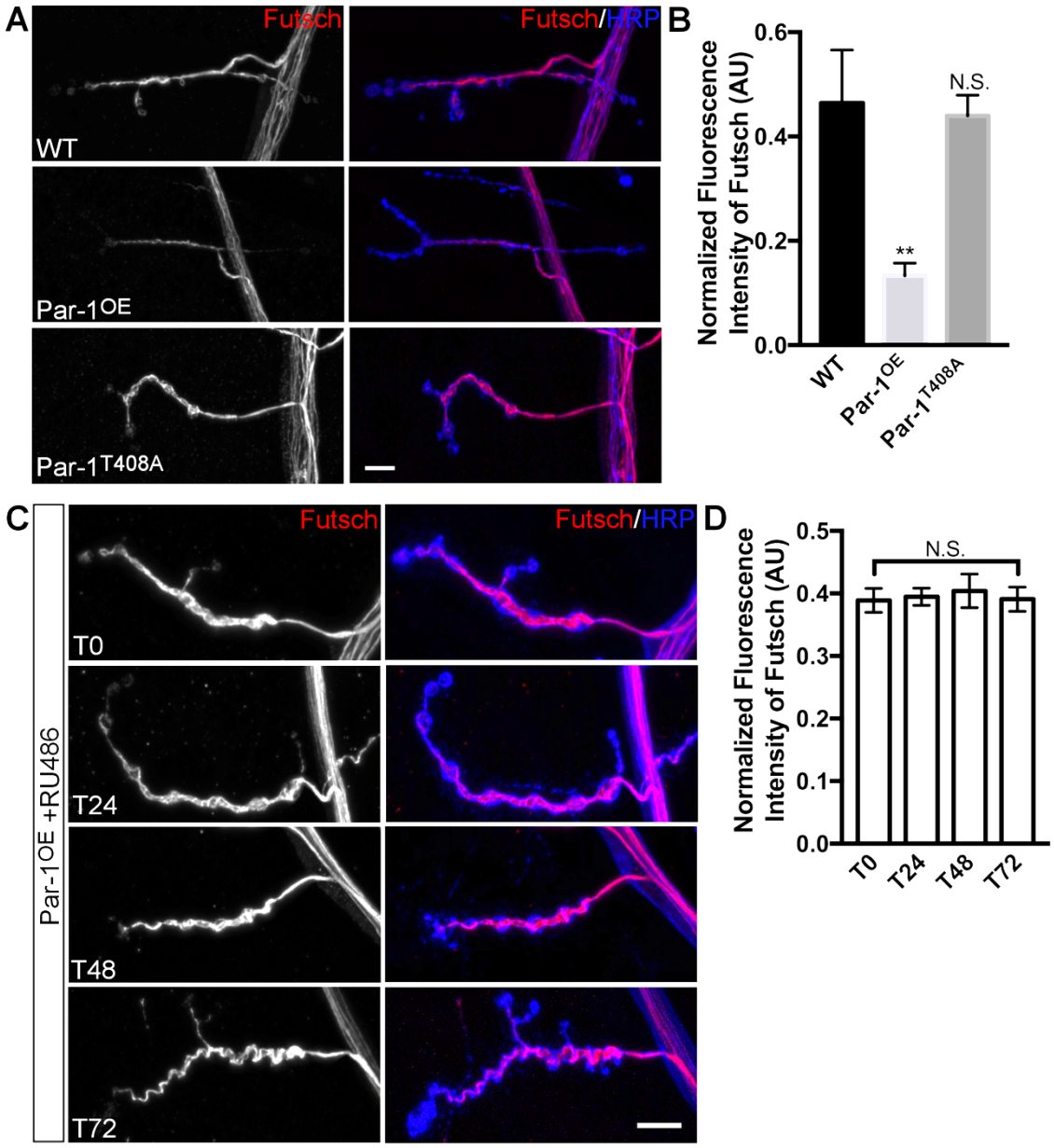

Figure 4.10 Futsch does not mediate accumulation of BRP within axons

(A) Representative confocal image stacks showing NMJ synapses from WT, Par-1^{OE} and Par-1^{T408A} third instar larvae stained with anti-Futsch (Red) and anti-HRP (Blue) antibodies. **(B)** Mean Futsch fluorescence intensity (A.U.) normalized to HRP intensity from entire NMJ arbor. n≥10. **(C)** Representative confocal stacks from larvae overexpressing Par-1 using GeneSwitch-ElavGal4 at T_0, T_{24}, T_{48}, and T_{72}. NMJ synapses are stained with anti-Futsch (Red) and anti-HRP (Blue) antibodies. **(D)** Mean Futsch fluorescent intensity (A.U.) normalized to HRP intensity from entire NMJ arbor. n>20. Error bars represent S.E.M. N.S.=p>0.05, **=p≤0.01.

Next, I reasoned that perhaps, the first signs of changes in active zone structure might manifest as subtle changes in the structure of T-bars. To test this possibility, I utilized simulated emission depletion microscopy (STED). When viewed using STED microscopy, BRP generally appears as a "doughnut" shaped structure at the active zones(Kittel et al., 2006). Subtle changes to this structure have previously been reported and are thought to be one of the early signs of active zone disassembly in a fly model of ALS(Shahidullah et al., 2013), perhaps by causing active zone instability. To test whether elevated levels of Par-1 lead to structural disruption of BRP doughnut structure, I performed STED on third instar larvae from WT, Par-1^{OE} and Par-1^{T408A} synapses. As expected, most BRP at the WT synapses showed the typical "doughnut" like structure, which was indistinguishable from larvae expressing Par-1^{T408A}. However, Par-1 overexpressing active zones showed significant reductions in visible BRP doughnuts (Figure 4.11 A-D). These data indicate that synapses in Par-1 overexpressing flies might be unstable. It is interesting to note that although *futsch* mutants have decreased BRP density, the doughnut structure of BRP is indistinguishable from WT(Lepicard et al., 2014) further supporting the idea that reductions in Futsch may not be the primary reason for the accumulation of BRP within axons.

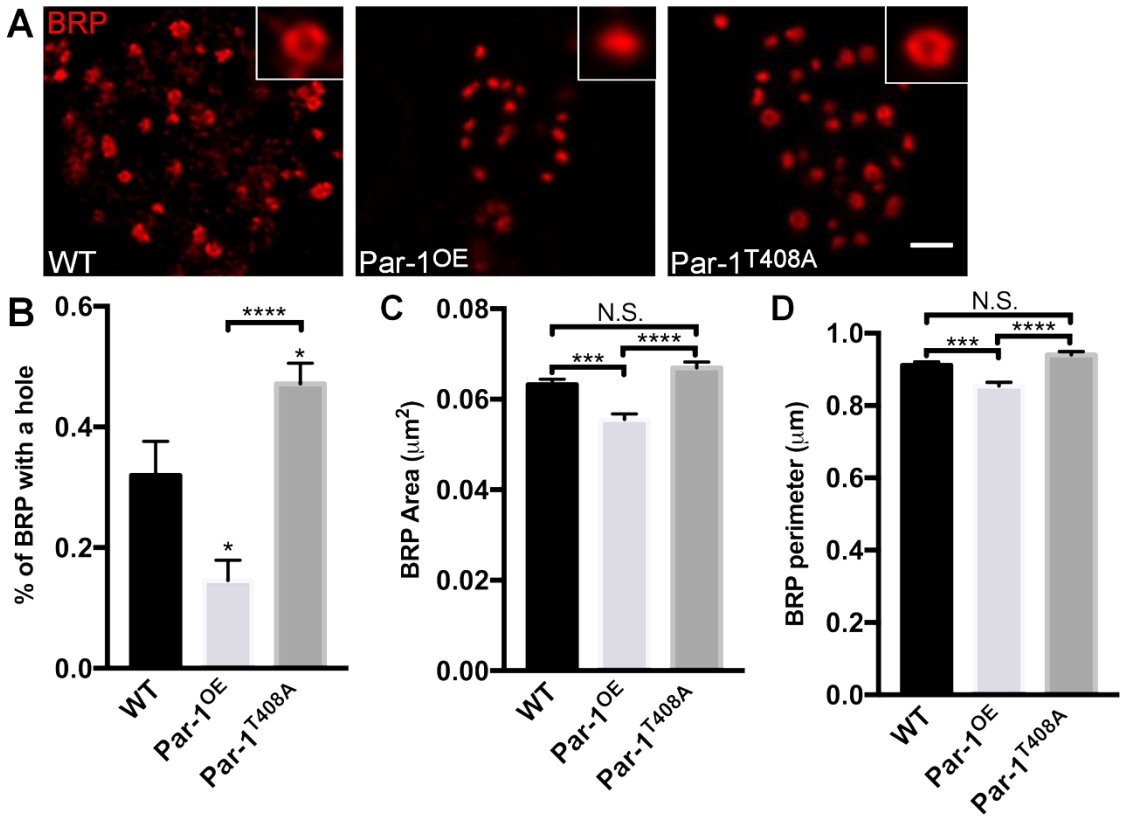

Figure 4.11 Elevated levels of Par-1 lead to alterations in BRP doughnuts

(A) Representative STED images showing BRP doughnuts at synapses from WT, Par-1^{OE} and Par-1^{T408A} third instar larvae stained against BRP. Scale bar = 1μm. Insets highlight a representative BRP structure at boutons of the respective genotype. **(B-D)** Quantification of the percent BRP with doughnut structure **(B)**, area of BRP puncta **(C)**, and perimeter of BRP puncta **(D)**. n>700 BRP puncta count. Error bars represent S.E.M. N.S.=p>0.05, *=p≤0.05, ***= p≤0.001, ****=p≤0.0001.

Since the STED data suggest that active zones in Par-1 expressing neurons might be unstable, I decided to test this directly by performing transmission electron microscopic analysis of active zones. An unstable active zone has previously been described at the ultrastructural level as diffuse and having long active zones with increased frequency of floating T-bars(Eaton and Davis, 2003). I found a significant increase in all these criteria in neurons expressing WT Par-1 (Figure 4.12 A-G). The length of active zones at Par-1^{OE} synapses as compared to WT was significantly increased.

Furthermore, the electron-dense active zone regions in Par-1^{OE} flies were significantly more diffuse/wider than WT active zones, which were more tightly packed (Figure 4.12 D-F). Finally, I observed there was a strong positive relationship between increased Par-1 and increase in the frequency of detached or floating T-bars (p=009) (Figure 4.12 G). Together, these data indicate that synapses in Par-1 overexpressing flies are unstable.

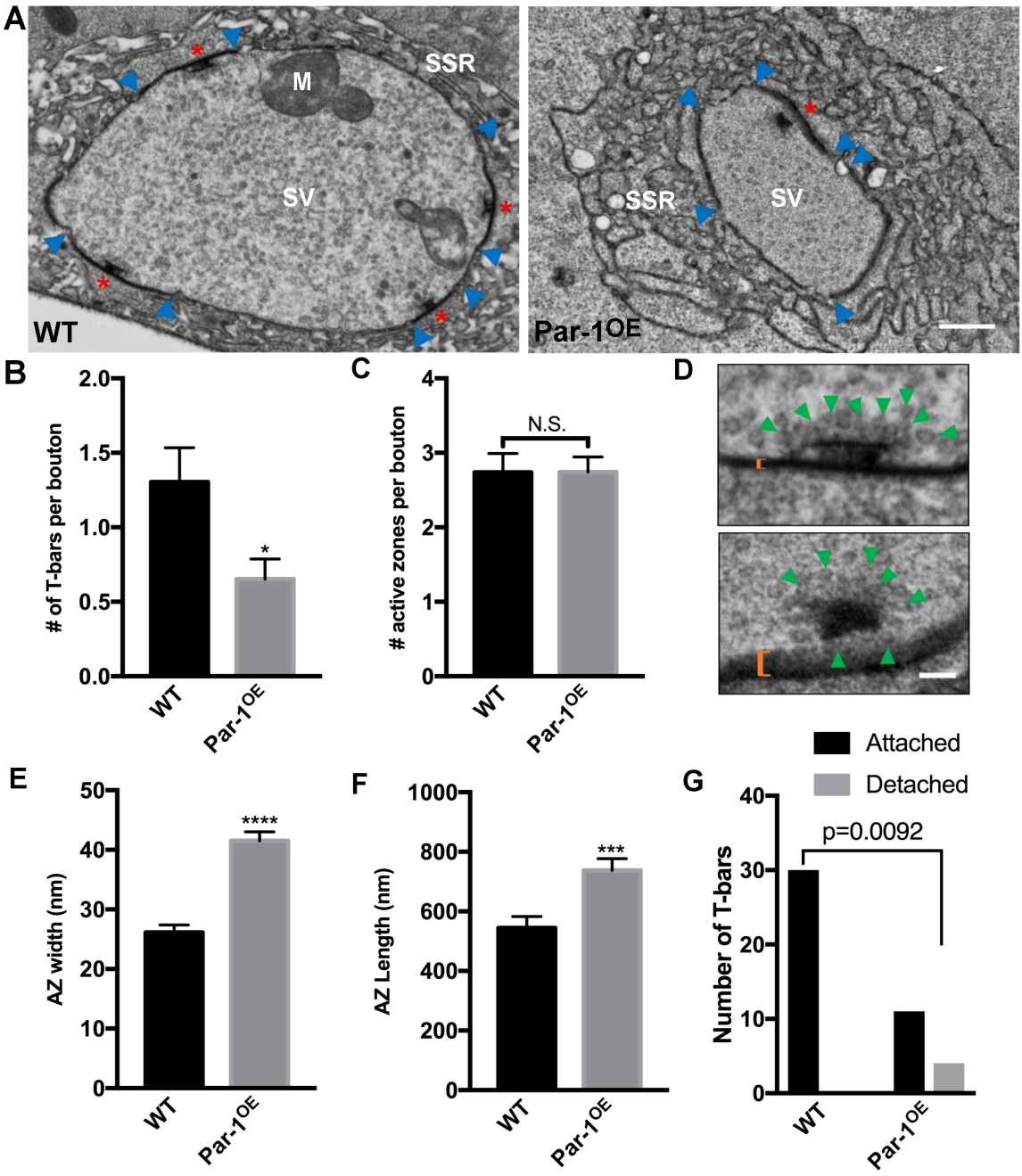

Figure 4.12 Elevated levels of Par-1 lead to disruption of active zone structure

(A) Representative electron micrographs from WT and Par-1^{OE} third instar larvae showing T-bars (red asterisks), synaptic vesicles (SV) and sub-synaptic reticulum (SSR). Scale Bar=500 nm. **(B)** Mean number of T-bars per bouton **(C)** and AZ's per boutons. **(D)** Representative T-bars with electron dense Active Zones (orange bracket), and synaptic vesicles (green arrows) from WT and Par-1^{OE}. Scale bar=100nm. AZ width **(E)**, and AZ length **(F)**, from WT and Par-1^{OE} larvae. N=20. **(G)** Quantification of detached T-bars in WT and Par-1^{OE}. Par-1^{OE} larvae show a significant increase in detached T-bars.

Error bars represent S.E.M. N.S.=$p>0.05$, *=$p\leq0.05$, ***= $p\leq0.001$, ****=$p\leq0.0001$.

Par-1 associates with BRP in a complex.

What might be the mechanism of action of Par-1? I have already explored two possible substrates of Par-1. Both these substrates of Par-1-Tau (Barber et al., 2017) and Futsch (this study) do not seem to mediate the affect of Par-1 overexpression. Because BRP selectively accumulates in Par-1 expressing flies, I wondered whether one way Par-1 could selectively regulate BRP localization could be by interacting with it. To test this possibility, I first tested whether overexpressed Par-1 and BRP co-localized. Indeed, overexpressed Par-1 and BRP partially co-localized with each other in the axons and at the NMJs (Figure 7A). However, co-localization is not a proof of interaction. Also, co-localization can be attributed to the overexpression of Par-1, which saturates the axons and the synapses. Therefore, I went back to the geneswitch experiments where there was little to no detectable Par-1 at zero hours of Par-1 transgene induction (Figure 4.4 A-C,E), and performed the proximity ligation assay (PLA, (Lepicard et al., 2014)). PLA signal relies on proximity of two proteins to each other (<40nm apart) such that the secondary antibodies that are conjugated to fluorescent oligonucleotides can be ligated giving rise to a bright fluorescent signal(Soderberg et al., 2006). I used anti-BRP and anti-Par-1

antibodies to perform the PLA assays. At zero hours of Par-1 transgene induction I detected little to no PLA signal in axons or synapses consistent with the data that at zero hours I detect little to no of Par-1 expression (Figure 4.13 C,E). I detected a significant increase in PLA signal in axons at 24-72 hours (Figure 4.13 C,E). This is consistent with the increase in Par-1 intensity in the axons for these time points (Figure 4.4 A,C). Interestingly, I also detected significant increases in the PLA signal at the synapse at 24 hours when the expression of Par-1 transgene was not detectably increased (Figure 4.13 D,F). This could be because PLA leads to a significant amplification of signal(Bellucci et al., 2014). These data suggest that Par-1 is in a complex with BRP *in situ*. To further test this interaction under endogenous conditions, I performed co-immunoprecipitation assay with anti-BRP antibody. Protein extracts from the fly heads were used to test this interaction. BRP successfully immunoprecipitated Par-1 from WT heads indicating that Par-1 and BRP are present in the same protein complex (Figure 4.13 B). BRP also immunoprecipitated overexpressed Par-1 and surprisingly, overexpressed Par-1^{T408A}. These data indicate that even inactive Par-1 can interact with BRP and show that Par-1 and BRP are in the same molecular complex (Figure 7B). There was no signal in the beads only control (Figure 4.13 B). Together, these data indicate that Par-1 and BRP are in the same complex and that Par-1 and BRP may share a functional relationship.

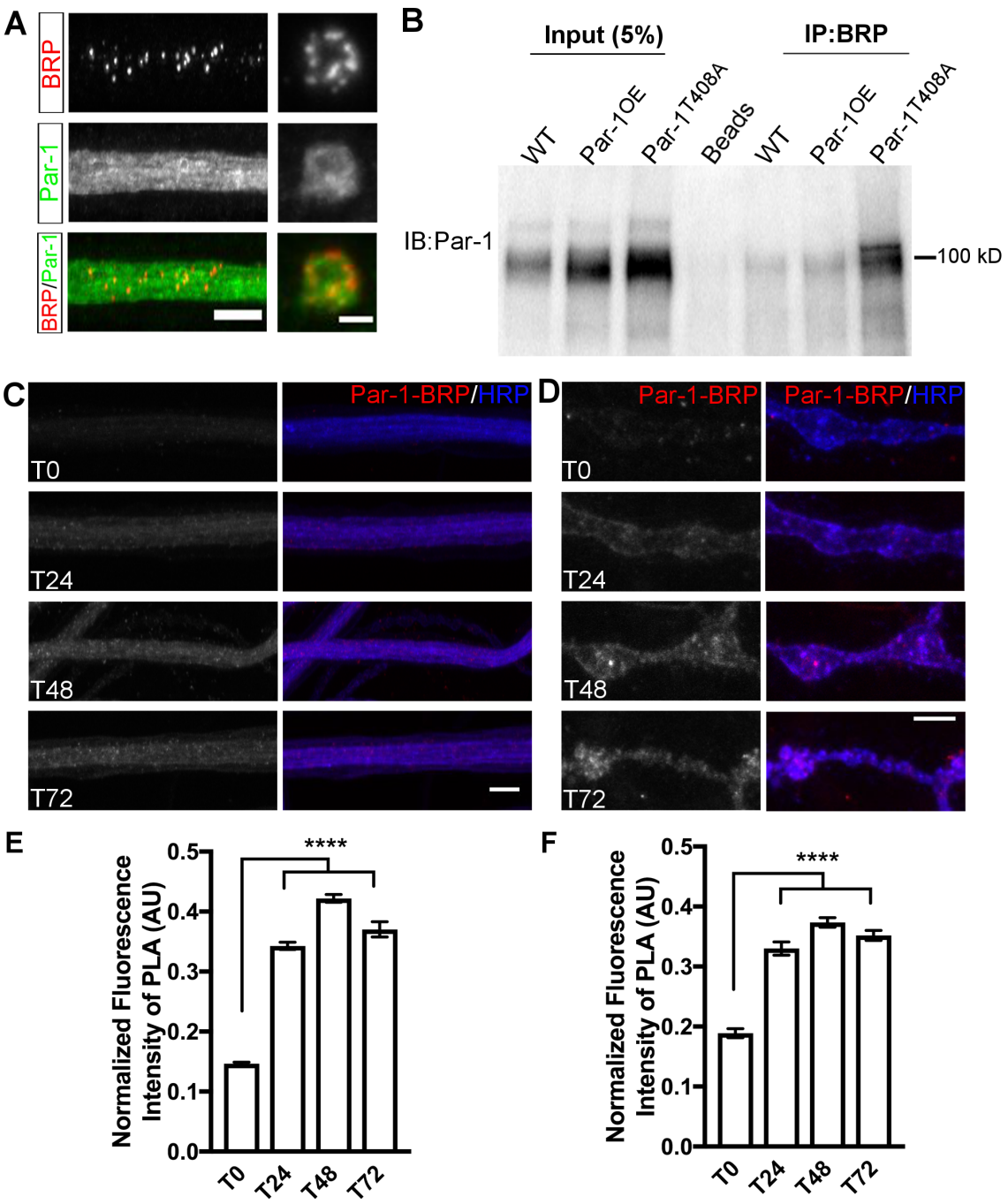

Figure 4.13 Par-1 and BRP are present within the same molecular complex

(A) Representative confocal stacks showing co-localization of Par-1 and BRP in the axons and boutons from third instar larvae of Par-1^{OE}. Axons (Scale bar = 10µm) and synaptic boutons (Scale bar = 5µm) are stained with antibodies against BRP (Red), and Par-1 (Green). **(B)** Representative Western blot of proteins pulled down using the anti-BRP antibody and probed using anti-Par-1 antibody. Both the input and the IP were performed in the same blot and loaded on the same gel (different lanes). Beads only

control shows no signal **(C-D)** Representative PLA signal (red) from larvae overexpressing Par-1 using GeneSwitch-ElavGal4 at T_0, T_{24}, T_{48}, and T_{72} from axon bundles **(C)** and synaptic boutons **(D)**. HRP marks presynaptic membrane boundary (blue). **(E-F)** Average PLA fluorescent intensity (A.U.) normalized to HRP intensity in axons bundles **(E)** and synaptic boutons **(F)**. (n>10). Error bars represent S.E.M. ****=p≤0.0001.

CHAPTER 5: DISCUSSION

SUMMARY

Par-1 is an evolutionarily conserved serine-threonine kinase that has many diverse roles, including essential roles in regulating cell polarity and regulating microtubule stability(Drewes et al., 1998, Doerflinger et al., 2003). I have contributed to this knowledge by adding an important role for Par-1 in mediating the transport of an essential AZ protein, BRP. My data show that elevated levels of Par-1 have a strong effect on the transport of BRP, leading to defects in synaptic transmission. Furthermore, the data seems to suggest that of all the tested markers BRP might be the only protein that Par-1 may be involved in trafficking. These data may have important implications for neurodevelopmental disorders like ASDs and neurodegenerative diseases where Par-1/MARK levels are elevated(Carayol et al., 2011, Maussion et al., 2008, Hu et al., 2009, Chin et al., 2000, Lee et al., 2012, Nishimura et al., 2004). While deficits in axon transport have been implicated in neurodegenerative disease, most studies have focused on transport defects that block many cargoes, this dramatic reduction in axonal transport is devastating for neurons and can undoubtedly be responsible for the widespread neuronal death observed in neurodegenerative diseases. However, it might not be able to explain the slow progression observed in many neurodegenerative diseases, and a selective transport deficit may be a more practically possible scenario. My data support this hypothesis and suggest that a selective accumulation of AZ protein BRP can first trigger synapse instability and then lead to synapse loss.

How would the disruption of BRP transport lead to the demise of the synapse? At the *Drosophila* NMJ synapses, active zones can be rapidly modified to induce homeostatic synaptic changes, which are partly dependent on BRP(Weyhersmuller et al., 2011). Interestingly, in a *Drosophila* model of ALS, disruption of shape and size of T-bars, which consists primarily of BRP, precedes synapse degeneration(Shahidullah et al., 2013). These data suggest that disruption of T-bars might be an early marker for synapse breakdown(Shahidullah et al., 2013). My data support this hypothesis because I find that the doughnut shape of T-bars is dramatically altered in flies overexpressing Par-1 and this happens before the decrease in the number of AZs marked by BRP. Finally, I posit that the loss of BRP from synapses could lead to a failure of synaptic homeostasis because BRP plays an essential role in synaptic vesicle release(Kittel et al., 2006). Interestingly, loss of synaptic homeostasis has been implicated in early phases of neurodegeneration (Small, 2004) and, restoring synaptic homeostasis can restore synaptic strength in a *Drosophila* model of ALS,(Perry et al., 2017). Thus, gradual loss of BRP from synapse may impair the ability of a synapse to efficaciously respond to changes that perturb synaptic homeostasis leading to catastrophic failure of neural networks(Palop and Mucke, 2016).

IMPLICATIONS FOR THE TRANSPORT OF ACTIVE ZONE PROTEINS DURING DEVELOPMENT

PTVs have been shown to carry AZ components(Zhai et al., 2001) in mammalian cell culture studies. However, some of the main components of PTVs for example, Bassoon have no homologs in invertebrates(Wagh et al., 2006). Recent studies in flies

and *C. elegans* have shed some light on the mechanisms of AZ transport. For example, mutants in imac (kinesin 3 homolog in flies) have severe reductions in BRP protein at the synapses(Pack-Chung et al., 2007). However, these flies also have a reduction in synaptic vesicles(Pack-Chung et al., 2007), suggesting that imac may transport both synaptic vesicles and AZ components. Supporting this argument, studies in *C. elegans* show that synaptic vesicles and active zone components are transported together(Klassen et al., 2010). However, a recent study in flies suggests that AZ components could be transported in distinct vesicles (Siebert et al., 2015). This study found that BRP and RIM-binding protein (RBP) can be co-transported (Siebert et al., 2015). Intriguingly, RBP and BRP transport could be uncoupled (Siebert et al., 2015). Indeed, my data support such an idea and suggests the possibility that BRP could be transported via a distinct mechanism. Overexpression of Par-1 leads to specific accumulation of BRP (Figure 3.1) while mitochondria, markers for synaptic vesicles, and other active zone proteins do not accumulate (Figure 3.3). Moreover, my data also demonstrate that this process is not mediated Tau (Figure 3.15).

It is less clear exactly how AZ proteins, such as BRP, are transported. However, PTVs and synaptic vesicles are transported via kinesin superfamily motors (KIFs) and are likely attached by to KIFs via adaptor proteins(Schlager and Hoogenraad, 2009, Hirokawa et al., 2009). Hence, making KIFs via an adapter a likely carrier of other BRP containing cargoes. To test whether KIFs involved in the transport of BRP I performed a candidate screen of kinesins looking for a specific accumulation of BRP within the axon bundles of the *Drosophila* NMJ. I found that knockdown of kinesin heavy chain 3 family motor (Khc-73)(Li et al., 1997, Huckaba et al., 2011, Yoshimura et al., 2010) leads to a

selective increase in BRP accumulations within the axons (Figure 5.1). While other axonal cargo such as, synaptic vesicles that utilize a different kinesin(Hirokawa et al., 2009, Goldstein et al., 2008, Pack-Chung et al., 2007, Okada et al., 1995), do not accumulate in axons (Figure 5.1). Interestingly, Khc-73 mammalian homolog GAKIN is known bind Par-1 homolog, MARK 2 (Yoshimura et al., 2010), indicating there could be an evolutionarily conserved relationship between Par-1/MARK and Khc-73/GAKIN. I hypothesize that BRP might be a cargo of Khc-73 and as it reaches the synapses, Par-1 (which is typically found only at the synapses at very low levels under normal physiological conditions(Zhang et al., 2007) could help localize BRP to the AZs of synapses by regulating the interaction between BRP and Khc-73 (possibly by disengaging BRP from Khc-73). Future experiments are needed to confirm this hypothesis and verify the actual relationship between Par-1 and Khc-73.

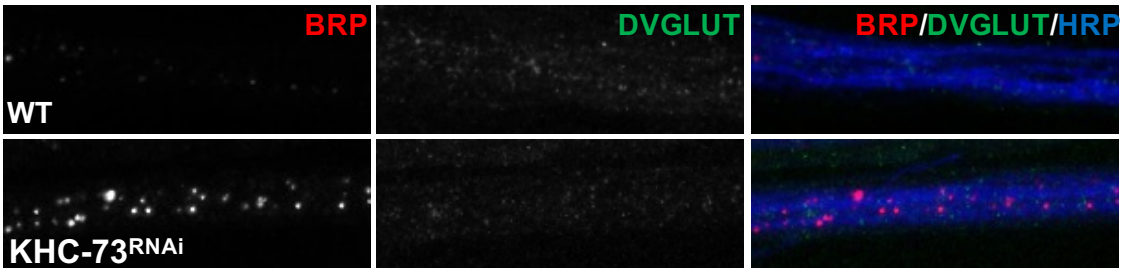

Figure 5.1. Knockdown of KCH-73 leads to a selective accumulation of BRP within axons.

Representative confocal image stacks showing axons from WT and KCH-73^{RNAi} third instar larvae stained with antibodies against BRP (Green), DVGLUT (Red) and HRP (Blue). N=10, p=0.002.

IMPLICATIONS FOR NEURODEVELOPMENTAL DISORDERS

Par-1/MARK is an essential gene that is required for cell polarity(Doerflinger et al., 2003, Doerflinger et al., 2006, Huynh et al., 2001) and therefore, is essential for proper embryogenesis and is also enriched in neurons and has been shown to have important neuronal developmental roles (Tabler et al., 2010, Ossipova et al., 2009). Elegant studies in *C. elegans* have shown that SYD2 and Liprin-α- two active zone proteins- are important in synapse assembly and maturation(Zhen and Jin, 1999, Dai et al., 2006, Taru and Jin, 2011). Interestingly, while SYD2/ Liprin-α can interact with (Rab3 interacting molecule) RIM/Unc10(Stigloher et al., 2011) respectively these interactions are dispensable for AZ maturation(Dai et al., 2006). The maturation of AZs instead depends on the interaction with BRP homolog ELKS, both in *C. elegans* and mice(Dai et al., 2006, Chia et al., 2013). Since my data shows that axonal transport of BRP is deficient in Par-1 overexpressing flies (Figure 3.1), this may affect the development or maturation of AZ, which may, in turn, have functional consequences as suggested by my data that show reduced synaptic transmission in flies overexpressing Par-1 (Figure 3.8). A decrease in the number of T-bars in Par-1 overexpression flies (Figure 3.7) is not accompanied by a change in apposition of AZs and PSDs (Figure 3.6) suggesting a developmental defect, and such a defect could arise due to the synaptic instability(Eaton and Davis, 2003, Eaton et al., 2002). Finally, MARK levels are increased in postmortem brains of children diagnosed with ASD(Maussion et al., 2008). Importantly, the increase in MARK is specific to the pre-frontal cortex in ASD, a region of the brain most affected in ASDs(Maussion et al., 2008). My data would suggest that an increase in Par-1/MARK might lead to defects in active zone formation or maturation in these areas. These questions need to be addressed by future studies.

IMPLICATIONS FOR NEURODEGENERATIVE DISEASES

Role of Par-1 kinase independent of Tau

It was discovered more than a decade ago that MARK was strongly associated with tau tangles (Chin et al., 2000, Lund et al., 2014) in AD patients. Since then many elegant studies have implicated MARK in phosphorylating tau(Mandelkow et al., 2004, Trinczek et al., 2004, Yu et al., 2012), including a study that shows that MARK is the kinase that initiates the cascade of tau hyperphosphorylation(Nishimura et al., 2004). Hyperphosphorylation of Tau has been hypothesized to be the underlying cause of neurodegeneration(Braak and Del Tredici, 2015). Par-1/MARK can phosphorylate Tau at serine 262(Drewes et al., 1995), which has also been shown to be hyperphosphorylated in postmortem AD patient brains(Gu et al., 2013) and it has been demonstrated that Par-1/MARK can function as an "initiator kinase"(Nishimura et al., 2004) for the cascade that hyperphosphorylates Tau. *In vitro*, hyperphosphorylation of Tau can cause its detachment from microtubules leading to their destabilization(Drewes et al., 1997). Microtubules serve as "highways" on which the transport of synaptic cargo is dependent. Thus, overexpression of Par-1 could lead to hyperphosphorylation of Tau and could cause axonal transport deficits. My data suggest that selective axonal transport defects caused due to Par-1 overexpression are independent of endogenous *Drosophila* Tau (dTau). Although *Drosophila* Par-1 can phosphorylate Tau *in vitro*(Nishimura et al., 2004), previous studies have shown that it can act independently of Tau *in vivo* (Doerflinger et al., 2003), suggesting additional substrates of Par-1 could regulate the selective transport of BRP. Furthermore, many studies suggest that axonal transport is likely to precede

overt neurodegeneration(Bilsland et al., 2010, Tang et al., 2012, Milde et al., 2015, Millecamps and Julien, 2013). It is tempting to speculate that one possibility is that transport of active zone proteins could be an initial event that leads to synaptic dysfunction, another symptom that precedes neuronal degeneration(Yoshiyama et al., 2007). Thus, although the hyperphosphorylation of Tau could drive the ultimate neuronal degeneration, other proteins may play a role in setting the stage for Tau pathology. Indeed, *in vivo* observation of axonal transport in a mouse model of neurodegeneration suggests that axonal transport deficits can occur early in the neuronal pathology and is likely not driven by Tau(Majid et al., 2014).

Increased levels of MARK trigger synapse instability in AD

Genome-wide association studies have implicated Par-1/MARK in AD(Seshadri et al., 2010). While accumulations of Aβ and tau are implicated in the widespread neuronal death found in late stages of AD(Braak and Del Trecidi, 2015), synapse instability is often associated with early stages during the progression of AD(Purro et al., 2014, Scheff et al., 2013). However, both the role of MARK in synapse stability and the role of synapse instability in neurodegenerative diseases are poorly understood. Indeed, animal models of tauopathy show an increase in synapse instability that precedes overt neurodegeneration (Jackson et al., 2017). Therefore, I propose that synapse instability might be one of the early events in neurodegenerative diseases like AD and that increase in Par-1/ MARK could facilitate the instability and hasten the demise of synapses.

My data show that increases in the levels of MARK within a neuron may destabilize its synapses by depriving the synapse of essential AZ components. Moreover, while increased MARK levels have been shown in AD patients(Chin et al., 2000, Lund et

al., 2014), its association with aMCI has not been reported. For the first time, my data reveal increases in MARK in aMCI patients (Figure 1.4), indicating that MARK may play a novel role in early stages of synapse pathology. Interestingly, our preliminary data also show that similar to age-matched controls, MARK is undetectable in NDAN individuals (Figure 1.4) whose synapses resist the binding of toxic Aβ aggregates and remain functional(Bjorklund et al., 2012). Importantly, the increases in MARK that were observed in human post-mortem samples were specific to the entorhinal cortex, a region of the brain that is affected early during disease pathology(Braak and Del Trecidi, 2015). This is consistent with my hypothesis that MARK might function early during the process of synapse degeneration, suggesting that MARK overexpression might be one of the early and necessary contributors for the cognitive impairments observed in AD patients.

Role of Par-1 in regulating synapse maintenance

Synaptic plasticity is determined by its ability to modulate its response to stimulation(Frank, 2014). Generally, activity leads to the strengthening of synapses, which is a more significant response to stimulation(Tessier and Broadie, 2009). Therefore, maintenance of synapses is essential in maintaining the synaptic networks, which are disrupted in both neurodevelopmental and neurodegenerative diseases(Palop and Mucke, 2016, Ben-David and Shifman, 2012, Shepherd and Katz, 2011). Indeed, mutations in cysteine string protein (CSP), which plays an important role in synaptic maintenance, causes a progressive motor neuron disorder characterized by neurodegeneration(Sharma et al., 2012). Thus, maintaining stable synapses might be important to avoid the failure of synaptic networks.

One of the vital functions performed by axonal transport is to maintain steady-state levels of synaptic proteins required for the efficacious release of neurotransmitter release(Goldstein et al., 2008, Nirschl et al., 2017). Disruption of axonal transport has been implicated in neurodegenerative diseases(Chevalier-Larsen and Holzbaur, 2006, Morfini et al., 2009, Millecamps and Julien, 2013). Indeed, mutations that affect axonal transport lead to neurodegenerative diseases(Hafezparast et al., 2003, Puls et al., 2003, Ishihara et al., 1999, Pigino et al., 2003, Lazarov et al., 2007, Zhang et al., 2004). A recent study suggests that active zone density is maintained during the developmental stages but is significantly decreased with aging (Chen et al., 2012). Interestingly, axonal transport also declines with aging (Milde et al., 2015) suggesting that a combination of decreased axonal transport of active zone proteins along with aging may lead to a gradual decrease in the maintenance of active zones and may eventually lead to a failure to maintain synaptic function and ultimately lead to synapse degeneration. While this hypothesis is generally accepted, it has proven difficult to determine whether axonal transport is a cause or consequence of synapse loss. My temporal analysis suggests that following sequence of events (Figure 4.4): Par-1 localizes to the axons followed by BRP accumulation in axons likely leading to the decreased synaptic function and finally the reduction of BRP from synaptic AZs likely leading to synapse instability. Together, these findings suggest that axonal accumulation of BRP precedes synapse instability, and this mislocalization of BRP is sufficient to trigger progressive synapse instability.

PAR-1 REGULATES THE SHAPE OF T-BARS AT THE AZ

BRP is an AZ scaffolding protein in *Drosophila*, which plays a critical role in AZ assembly(Kittel et al., 2006, Wagh et al., 2006). Reduction in BRP levels in *Drosophila* motoneurons leads to nearly a complete loss of electron-dense bodies (aka T-bars)(Wagh et al., 2006), indicating that BRP is essential for the development of T-bars. While it is not clear how BRP protein is targeted to nascent AZs, recent studies suggest that BRP may be transported from the motoneuron cell bodies to synapses via active transport, packaged into vesicles that are distinct from those of synaptic vesicles and other organelles(Siebert et al., 2015, Barber et al., 2017). Using super-resolution imaging has revealed that BRP forms "donut" shaped structure at the AZ (Fouquet et al., 2009) and is formed by approximately ~140 molecules of BRP per T-bar (Fouquet et al., 2009, Van Vactor and Sigrist, 2017). Furthermore, it has been shown that BRP molecules, just like postsynaptic glutamate receptors, cluster and grow as synapses mature(Fouquet et al., 2009). After maturation, BRP can also be rapidly modified to induce synaptic homeostatic changes(Weyhersmuller et al., 2011). Due to the dynamic nature of BRP at the AZ, it requires highly regulated maintenance. If issues in maintenance arise, it should manifest as subtle changes in T-bars and likely manifest as a loss of "donut" shaped BRP in super-resolution microscopy without the overt loss of BRP at the synapses. In fact, in a *Drosophila* model of ALS, disruption of shape and size of BRP precedes synapse degeneration(Shahidullah et al., 2013). These data suggest that BRP can be an excellent diagnostic marker of synapse maintenance (Shahidullah et al., 2013) acting as an indicator of impending synapse loss. Furthermore, my data show that Par-1 overexpression but not those overexpressing inactive Par-1 (Figure 4.11) disrupts BRP donuts at the AZ. Together, these data indicate that overexpression of Par-1 can result in synapse instability and that low levels of presynaptic Par-1 are needed to maintain T-bar structures at the AZ.

Another intriguing possibility is that that Par-1 may play a role in the dis-assembly and re-assembly of BRP within individual AZ structures and in doing so might be important in

redistributing BRP in between AZs. *Rab3* is a small GTPase, and *rab3* mutants show unequal distribution of BRP with some AZs having more BRP than WT AZs while the others are devoid of any BRP(Graf et al., 2009). However, BRP distribution can be rapidly normalized after acute induction of Rab3 expression in *rab3* mutant neurons. These data suggest that the BRP can be redistributed from AZs where it is present at high levels to those AZs that are devoid of BRP. Future studies will need to examine the relation between *Rab3* and Par-1 to determine if the synapse instability induced by Par-1 is required for the distribution of BRP within AZs.

WHAT ARE THE UPSTREAM REGULATORS OF PAR-1?

LKB1 activates Par-1 by phosphorylating it on the threonine 408(Wang et al., 2007). My data suggest that Threonine 408 is necessary for the manifestation of BRP transport phenotype. Overexpression of inactive Par-1 (Par-1T^{408A}) does not lead to BRP accumulation within axons, suggesting that inactive Par-1 cannot induce the accumulation of BRP within the axons. However, overexpression of LKB1 in neurons is unable to induce accumulation of BRP within axons (Figure 5.2) suggesting that while activation of Par-1 by LKB1 might be indeed important in other functions of Par-1 (Lee et al., 2012), it may not be necessary to induce BRP accumulation in the axons. This raises the possibility of a novel upstream regulator of Par-1 kinase that might be important in regulating the transport of BRP within axons.

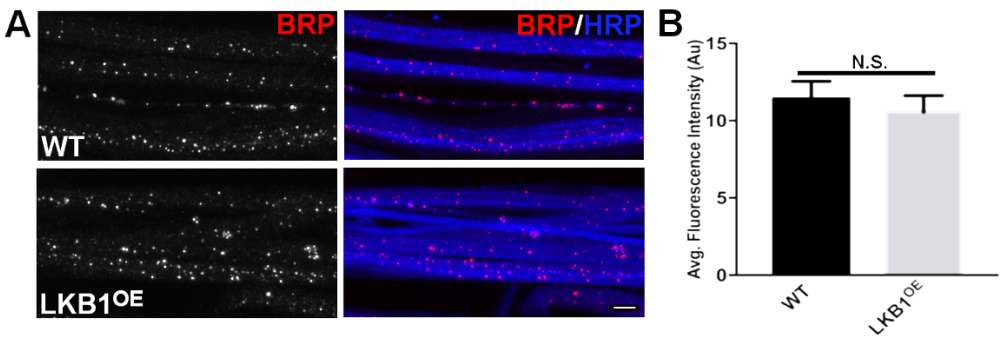

Figure 5.2. Overexpression of LKB1 does lead to accumulation of BRP in axons

(**A**) Representative images from WT and presynaptic overexpression of LKB1 ($LKB1^{OE}$) flies driven using BG380-Gal4 showing axons stained against BRP (Red) and HRP (Blue). (**B**) Quantification of BRP intensity in axons. N=8, p=0.58. Scale bar=10μm. Error bars represent S.E.M.

Thus, my current study demonstrates that distinct mechanisms exist to transport components of AZs like BRP and that availability of these components is likely regulated tightly by kinases such as Par-1 kinase.

HOW DOES PAR-1 REGULATE LOCALIZATION OF BRP?

While so far, we do not precisely understand how active zone scaffold proteins like BRP are localized, based on my data I can speculate that phosphorylation of Par-1 substrate may be important in determining the localization of BRP. This is because while the expression of WT Par-1 causes accumulation of BRP within axons, expression of inactive Par-1 does not lead to show any aberrant localization of BRP (Figure 3.1). My data suggest that defects in BRP localization are not mediated either by tau (Figure 3.15) or Futsch (Figure 4.10), but BRP may be a possible substrate of Par-1. This is because my data indicate that BRP and Par-1 may be in the same molecular complex (Figure 4.13) and similar to Futsch and tau, BRP has a KXGS motif that is present at its

conserved N-terminus. Interestingly, Dlg, a homolog of PSD-95(Budnik et al., 1996) is also phosphorylated by Par-1 kinase(Zhang et al., 2007) and Dlg also contains only one KXGS motif that can be phosphorylated, suggesting that the presence of a single KXGS motif might be enough for Par-1 to phosphorylate a protein. Previous studies have shown that BRP can be acetylated and that this posttranslational modification is important in regulating the structure of T-bars(Miskiewicz et al., 2011) but whether BRP can be phosphorylated and whether phosphorylation of BRP is required for its localization, remains to be studied.

Finally, my data indicate that presynaptic Par-1 levels are important in determining BRP localization because Par-1 knockdown also results in the accumulation of BRP within the axons (Figure 4.1). Thus, Par-1 not only has a vital role in the postsynaptic compartment (Zhang et al., 2007) but also has a novel function on the presynaptic side.

Overall Summary

AZs are vital components of neurons and are essential for maintaining communication links between a neuron and their targets. While there is strong evidence suggesting AZs in many neurodevelopmental and neurodegenerative diseases, the mechanisms behind how AZs are formed and how they are maintained is poorly understood. By understanding the basic mechanisms of how protein components of the AZ localize via axonal transport and how they are maintained, will provide critical insights into what may happen early in these disease conditions. My dissertation suggests that presynaptic levels of Par-1 kinase may determine the selective transport of the components of the AZ (Figure 3.1) and that this is likely via a distinct mechanism from

other presynaptic cargoes, like synaptic vesicles and mitochondria (Figure 3.3). Furthermore, this process occurs independently of tau (Figure 3.15), one of the best-studied substrates of Par-1. Importantly, a temporal analysis revealed that accumulation of AZ proteins could trigger synapse instability and cause synapse loss (Figure 4.4) – a precursor to neuronal degeneration(Jackson et al., 2017, Eaton et al., 2002, Shahidullah et al., 2013). Thus, my dissertation shows: **1** - AZ proteins have a distinct mechanisms for the transport of their cargo (Figure 3.1, Figure 3.3), **2** - Par-1, a polarity gene(Doerflinger et al., 2006, Doerflinger et al., 2003, Huynh et al., 2001) has a presynaptic role in regulating the transport of the protein components of AZs (Figure 4.1), **3** - axonal transport could lead to defects in synaptic function and eventual synapse loss (Figure 4.4) -filling the long standing-gap of whether axonal transport leads to synapse loss or synapse loss causes accumulation of synaptic materials in axons and finally, **4** - provides a possible mechanisms of synapses might be disassembled in AD and how the increase in Par-1/MARK might be an important event in the progression of AD (Figure 1.4).

Bibliography

1997. Consensus recommendations for the postmortem diagnosis of Alzheimer's disease. The National Institute on Aging, and Reagan Institute Working Group on Diagnostic Criteria for the Neuropathological Assessment of Alzheimer's Disease. *Neurobiol Aging,* 18**,** S1-2.

ACKERMANN, F., WAITES, C. L. & GARNER, C. C. 2015. Presynaptic active zones in invertebrates and vertebrates. *EMBO Rep,* 16**,** 923-38.

ADAMS, S. J., CROOK, R. J., DETURE, M., RANDLE, S. J., INNES, A. E., YU, X. Z., LIN, W. L., DUGGER, B. N., MCBRIDE, M., HUTTON, M., DICKSON, D. W. & MCGOWAN, E. 2009. Overexpression of wild-type murine tau results in progressive tauopathy and neurodegeneration. *Am J Pathol,* 175**,** 1598-609.

ANDORFER, C., KRESS, Y., ESPINOZA, M., DE SILVA, R., TUCKER, K. L., BARDE, Y. A., DUFF, K. & DAVIES, P. 2003. Hyperphosphorylation and aggregation of tau in mice expressing normal human tau isoforms. *J Neurochem,* 86**,** 582-90.

ARENDT, T. 2009. Synaptic degeneration in Alzheimer's disease. *Acta Neuropathol,* 118**,** 167-79.

ATWOOD, H. L., GOVIND, C. K. & WU, C. F. 1993. Differential ultrastructure of synaptic terminals on ventral longitudinal abdominal muscles in Drosophila larvae. *J Neurobiol,* 24**,** 1008-24.

AUGUSTINACK, J. C., SCHNEIDER, A., MANDELKOW, E. M. & HYMAN, B. T. 2002. Specific tau phosphorylation sites correlate with severity of neuronal cytopathology in Alzheimer's disease. *Acta Neuropathol,* 103**,** 26-35.

BAE, J. R. & KIM, S. H. 2017. Synapses in neurodegenerative diseases. *BMB Rep,* 50**,** 237-246.

BARBER, K. R., TANQUARY, J., BUSH, K., SHAW, A., WOODSON, M., SHERMAN, M. & WAIRKAR, Y. P. 2017. Active zone proteins are transported via distinct mechanisms regulated by Par-1 kinase. *PLoS Genet,* 13**,** e1006621.

BARNETT, J. H., LEWIS, L., BLACKWELL, A. D. & TAYLOR, M. 2014. Early intervention in Alzheimer's disease: a health economic study of the effects of diagnostic timing. *BMC Neurol,* 14**,** 101.

BEGHINI, A., MAGNANI, I., ROVERSI, G., PIEPOLI, T., DI TERLIZZI, S., MORONI, R. F., POLLO, B., FUHRMAN CONTI, A. M., COWELL, J. K., FINOCCHIARO, G. & LARIZZA, L. 2003. The neural progenitor-restricted

isoform of the MARK4 gene in 19q13.2 is upregulated in human gliomas and overexpressed in a subset of glioblastoma cell lines. *Oncogene,* 22**,** 2581-91.

BELLEN, H. J., TONG, C. & TSUDA, H. 2010. 100 years of Drosophila research and its impact on vertebrate neuroscience: a history lesson for the future. *Nat Rev Neurosci,* 11**,** 514-22.

BELLUCCI, A., FIORENTINI, C., ZALTIERI, M., MISSALE, C. & SPANO, P. 2014. The "in situ" proximity ligation assay to probe protein-protein interactions in intact tissues. *Methods Mol Biol,* 1174**,** 397-405.

BEN-DAVID, E. & SHIFMAN, S. 2012. Networks of neuronal genes affected by common and rare variants in autism spectrum disorders. *PLoS Genet,* 8**,** e1002556.

BETTENCOURT DA CRUZ, A., SCHWARZEL, M., SCHULZE, S., NIYYATI, M., HEISENBERG, M. & KRETZSCHMAR, D. 2005. Disruption of the MAP1B-related protein FUTSCH leads to changes in the neuronal cytoskeleton, axonal transport defects, and progressive neurodegeneration in Drosophila. *Mol Biol Cell,* 16**,** 2433-42.

BIERNAT, J., GUSTKE, N., DREWES, G., MANDELKOW, E. M. & MANDELKOW, E. 1993. Phosphorylation of Ser262 strongly reduces binding of tau to microtubules: distinction between PHF-like immunoreactivity and microtubule binding. *Neuron,* 11**,** 153-63.

BILSLAND, L. G., SAHAI, E., KELLY, G., GOLDING, M., GREENSMITH, L. & SCHIAVO, G. 2010. Deficits in axonal transport precede ALS symptoms in vivo. *Proc Natl Acad Sci U S A,* 107**,** 20523-8.

BJORKLUND, N. L., REESE, L. C., SADAGOPARAMANUJAM, V. M., GHIRARDI, V., WOLTJER, R. L. & TAGLIALATELA, G. 2012. Absence of amyloid beta oligomers at the postsynapse and regulated synaptic Zn2+ in cognitively intact aged individuals with Alzheimer's disease neuropathology. *Mol Neurodegener,* 7**,** 23.

BOLKAN, B. J. & KRETZSCHMAR, D. 2014. Loss of Tau results in defects in photoreceptor development and progressive neuronal degeneration in Drosophila. *Dev Neurobiol,* 74**,** 1210-25.

BOURGERON, T. 2009. A synaptic trek to autism. *Curr Opin Neurobiol,* 19**,** 231-4.

BRAAK, H. & DEL TRECIDI, K. 2015. Neuroanatomy and pathology of sporadic Alzheimer's disease. *Adv Anat Embryol Cell Biol,* 215**,** 1-162.

BRAAK, H. & DEL TREDICI, K. 2011. The pathological process underlying Alzheimer's disease in individuals under thirty. *Acta Neuropathol,* 121**,** 171-81.

BRAAK, H. & DEL TREDICI, K. 2015. The preclinical phase of the pathological process underlying sporadic Alzheimer's disease. *Brain*.

BRAAK, H., THAL, D. R., GHEBREMEDHIN, E. & DEL TREDICI, K. 2011. Stages of the pathologic process in Alzheimer disease: age categories from 1 to 100 years. *J Neuropathol Exp Neurol,* 70**,** 960-9.

BRAND, A. H. & PERRIMON, N. 1993. Targeted gene expression as a means of altering cell fates and generating dominant phenotypes. *Development,* 118**,** 401-15.

BROSE, N., HOFMANN, K., HATA, Y. & SUDHOF, T. C. 1995. Mammalian homologues of Caenorhabditis elegans unc-13 gene define novel family of C2-domain proteins. *J Biol Chem,* 270**,** 25273-80.

BRUCKNER, J. J., GRATZ, S. J., SLIND, J. K., GESKE, R. R., CUMMINGS, A. M., GALINDO, S. E., DONOHUE, L. K. & O'CONNOR-GILES, K. M. 2012. Fife, a Drosophila Piccolo-RIM homolog, promotes active zone organization and neurotransmitter release. *J Neurosci,* 32**,** 17048-58.

BUDNIK, V., KOH, Y. H., GUAN, B., HARTMANN, B., HOUGH, C., WOODS, D. & GORCZYCA, M. 1996. Regulation of synapse structure and function by the Drosophila tumor suppressor gene dlg. *Neuron,* 17**,** 627-40.

BURGESS, R. W., DEITCHER, D. L. & SCHWARZ, T. L. 1997. The synaptic protein syntaxin1 is required for cellularization of Drosophila embryos. *J Cell Biol,* 138**,** 861-75.

BURNOUF, S., GRONKE, S., AUGUSTIN, H., DOLS, J., GORSKY, M. K., WERNER, J., KERR, F., ALIC, N., MARTINEZ, P. & PARTRIDGE, L. 2016. Deletion of endogenous Tau proteins is not detrimental in Drosophila. *Sci Rep,* 6**,** 23102.

CALISSANO, P., MATRONE, C. & AMADORO, G. 2010. Nerve growth factor as a paradigm of neurotrophins related to Alzheimer's disease. *Dev Neurobiol,* 70**,** 372-83.

CAPSONI, S., UGOLINI, G., COMPARINI, A., RUBERTI, F., BERARDI, N. & CATTANEO, A. 2000. Alzheimer-like neurodegeneration in aged antinerve growth factor transgenic mice. *Proc Natl Acad Sci U S A,* 97**,** 6826-31.

CARAYOL, J., SCHELLENBERG, G. D., DOMBROSKI, B., GENIN, E., ROUSSEAU, F. & DAWSON, G. 2011. Autism risk assessment in siblings of affected children using sex-specific genetic scores. *Mol Autism,* 2**,** 17.

CASTELLO, M. A., JEPPSON, J. D. & SORIANO, S. 2014. Moving beyond anti-amyloid therapy for the prevention and treatment of Alzheimer's disease. *BMC Neurol,* 14**,** 169.

CATTERALL, W. A. 1998. Structure and function of neuronal Ca2+ channels and their role in neurotransmitter release. *Cell Calcium,* 24**,** 307-23.

CAVISTON, J. P. & HOLZBAUR, E. L. 2006. Microtubule motors at the intersection of trafficking and transport. *Trends Cell Biol,* 16**,** 530-7.

CHEN, J., MIZUSHIGE, T. & NISHIMUNE, H. 2012. Active zone density is conserved during synaptic growth but impaired in aged mice. *J Comp Neurol,* 520**,** 434-52.

CHEVALIER-LARSEN, E. & HOLZBAUR, E. L. 2006. Axonal transport and neurodegenerative disease. *Biochim Biophys Acta,* 1762**,** 1094-108.

CHIA, P. H., LI, P. & SHEN, K. 2013. Cell biology in neuroscience: cellular and molecular mechanisms underlying presynapse formation. *J Cell Biol,* 203**,** 11-22.

CHIN, J. Y., KNOWLES, R. B., SCHNEIDER, A., DREWES, G., MANDELKOW, E. M. & HYMAN, B. T. 2000. Microtubule-affinity regulating kinase (MARK) is tightly associated with neurofibrillary tangles in Alzheimer brain: a fluorescence resonance energy transfer study. *J Neuropathol Exp Neurol,* 59**,** 966-71.

COLLINS, C. A. & DIANTONIO, A. 2007. Synaptic development: insights from Drosophila. *Curr Opin Neurobiol,* 17**,** 35-42.

DAI, Y., TARU, H., DEKEN, S. L., GRILL, B., ACKLEY, B., NONET, M. L. & JIN, Y. 2006. SYD-2 Liprin-alpha organizes presynaptic active zone formation through ELKS. *Nat Neurosci,* 9**,** 1479-87.

DAMULEWICZ, M., MAZZOTTA, G. M., SARTORI, E., ROSATO, E., COSTA, R. & PYZA, E. M. 2017. Cryptochrome Is a Regulator of Synaptic Plasticity in the Visual System of Drosophila melanogaster. *Front Mol Neurosci,* 10**,** 165.

DANIELS, R. W., COLLINS, C. A., GELFAND, M. V., DANT, J., BROOKS, E. S., KRANTZ, D. E. & DIANTONIO, A. 2004. Increased expression of the Drosophila vesicular glutamate transporter leads to excess glutamate release and a compensatory decrease in quantal content. *J Neurosci,* 24**,** 10466-74.

DAVIS, G. W. & MULLER, M. 2015. Homeostatic control of presynaptic neurotransmitter release. *Annu Rev Physiol,* 77**,** 251-70.

DE GOIS, S., SCHAFER, M. K., DEFAMIE, N., CHEN, C., RICCI, A., WEIHE, E., VAROQUI, H. & ERICKSON, J. D. 2005. Homeostatic scaling of vesicular glutamate and GABA transporter expression in rat neocortical circuits. *J Neurosci,* 25**,** 7121-33.

DEKOSKY, S. 2003. Early intervention is key to successful management of Alzheimer disease. *Alzheimer Dis Assoc Disord,* 17 Suppl 4**,** S99-104.

DEKOSKY, S. T. & SCHEFF, S. W. 1990. Synapse loss in frontal cortex biopsies in Alzheimer's disease: correlation with cognitive severity. *Ann Neurol,* 27**,** 457-64.

DOERFLINGER, H., BENTON, R., SHULMAN, J. M. & ST JOHNSTON, D. 2003. The role of PAR-1 in regulating the polarised microtubule cytoskeleton in the Drosophila follicular epithelium. *Development,* 130**,** 3965-75.

DOERFLINGER, H., BENTON, R., TORRES, I. L., ZWART, M. F. & ST JOHNSTON, D. 2006. Drosophila anterior-posterior polarity requires actin-dependent PAR-1 recruitment to the oocyte posterior. *Curr Biol,* 16**,** 1090-5.

DREWES, G. 2004. MARKing tau for tangles and toxicity. *Trends Biochem Sci,* 29**,** 548-55.

DREWES, G., EBNETH, A. & MANDELKOW, E. M. 1998. MAPs, MARKs and microtubule dynamics. *Trends Biochem Sci,* 23**,** 307-11.

DREWES, G., EBNETH, A., PREUSS, U., MANDELKOW, E. M. & MANDELKOW, E. 1997. MARK, a novel family of protein kinases that phosphorylate microtubule-associated proteins and trigger microtubule disruption. *Cell,* 89**,** 297-308.

DREWES, G., TRINCZEK, B., ILLENBERGER, S., BIERNAT, J., SCHMITT-ULMS, G., MEYER, H. E., MANDELKOW, E. M. & MANDELKOW, E. 1995. Microtubule-associated protein/microtubule affinity-regulating kinase (p110mark). A novel protein kinase that regulates tau-microtubule interactions and dynamic instability by phosphorylation at the Alzheimer-specific site serine 262. *J Biol Chem,* 270**,** 7679-88.

EATON, B. A. & DAVIS, G. W. 2003. Synapse disassembly. *Genes Dev,* 17**,** 2075-82.

EATON, B. A., FETTER, R. D. & DAVIS, G. W. 2002. Dynactin is necessary for synapse stabilization. *Neuron,* 34**,** 729-41.

EBNETH, A., GODEMANN, R., STAMER, K., ILLENBERGER, S., TRINCZEK, B. & MANDELKOW, E. 1998. Overexpression of tau protein inhibits kinesin-dependent trafficking of vesicles, mitochondria, and endoplasmic reticulum: implications for Alzheimer's disease. *J Cell Biol,* 143**,** 777-94.

EHMANN, N., SAUER, M. & KITTEL, R. J. 2015. Super-resolution microscopy of the synaptic active zone. *Front Cell Neurosci,* 9**,** 7.

EHMANN, N., VAN DE LINDE, S., ALON, A., LJASCHENKO, D., KEUNG, X. Z., HOLM, T., RINGS, A., DIANTONIO, A., HALLERMANN, S., ASHERY, U., HECKMANN, M., SAUER, M. & KITTEL, R. J. 2014. Quantitative super-resolution imaging of Bruchpilot distinguishes active zone states. *Nat Commun,* 5**,** 4650.

FENSTER, S. D., CHUNG, W. J., ZHAI, R., CASES-LANGHOFF, C., VOSS, B., GARNER, A. M., KAEMPF, U., KINDLER, S., GUNDELFINGER, E. D. & GARNER, C. C. 2000. Piccolo, a presynaptic zinc finger protein structurally related to bassoon. *Neuron,* 25**,** 203-14.

FORTINI, M. E. 2004. PAR-1 for the course of neurodegeneration. *Cell,* 116**,** 631-2.

FOUQUET, W., OWALD, D., WICHMANN, C., MERTEL, S., DEPNER, H., DYBA, M., HALLERMANN, S., KITTEL, R. J., EIMER, S. & SIGRIST, S. J. 2009. Maturation of active zone assembly by Drosophila Bruchpilot. *J Cell Biol,* 186**,** 129-45.

FRANK, C. A. 2014. Homeostatic plasticity at the Drosophila neuromuscular junction. *Neuropharmacology,* 78**,** 63-74.

FRANK, C. A., KENNEDY, M. J., GOOLD, C. P., MAREK, K. W. & DAVIS, G. W. 2006. Mechanisms underlying the rapid induction and sustained expression of synaptic homeostasis. *Neuron,* 52**,** 663-77.

FRIEDMAN, H. V., BRESLER, T., GARNER, C. C. & ZIV, N. E. 2000. Assembly of new individual excitatory synapses: time course and temporal order of synaptic molecule recruitment. *Neuron,* 27**,** 57-69.

GALLIO, M., OFSTAD, T. A., MACPHERSON, L. J., WANG, J. W. & ZUKER, C. S. 2011. The coding of temperature in the Drosophila brain. *Cell,* 144**,** 614-24.

GASPARINI, S., KASYANOV, A. M., PIETROBON, D., VORONIN, L. L. & CHERUBINI, E. 2001. Presynaptic R-type calcium channels contribute to fast excitatory synaptic transmission in the rat hippocampus. *J Neurosci,* 21**,** 8715-21.

GHANNAD-REZAIE, M., WANG, X., MISHRA, B., COLLINS, C. & CHRONIS, N. 2012. Microfluidic chips for in vivo imaging of cellular responses to neural injury in Drosophila larvae. *PLoS One,* 7**,** e29869.

GLATER, E. E., MEGEATH, L. J., STOWERS, R. S. & SCHWARZ, T. L. 2006. Axonal transport of mitochondria requires milton to recruit kinesin heavy chain and is light chain independent. *J Cell Biol,* 173**,** 545-57.

GOLDSTEIN, A. Y., WANG, X. & SCHWARZ, T. L. 2008. Axonal transport and the delivery of pre-synaptic components. *Curr Opin Neurobiol,* 18**,** 495-503.

GORSKA-ANDRZEJAK, J., MAKUCH, R., STEFAN, J., GORLICH, A., SEMIK, D. & PYZA, E. 2013. Circadian expression of the presynaptic active zone protein Bruchpilot in the lamina of Drosophila melanogaster. *Dev Neurobiol,* 73**,** 14-26.

GORSKA-ANDRZEJAK, J., SALVATERRA, P. M., MEINERTZHAGEN, I. A., KRZEPTOWSKI, W., GORLICH, A. & PYZA, E. 2009. Cyclical expression of

Na+/K+-ATPase in the visual system of Drosophila melanogaster. *J Insect Physiol,* 55**,** 459-68.

GRAF, E. R., DANIELS, R. W., BURGESS, R. W., SCHWARZ, T. L. & DIANTONIO, A. 2009. Rab3 dynamically controls protein composition at active zones. *Neuron,* 64**,** 663-77.

GRAF, E. R., HEERSSEN, H. M., WRIGHT, C. M., DAVIS, G. W. & DIANTONIO, A. 2011. Stathmin is required for stability of the Drosophila neuromuscular junction. *J Neurosci,* 31**,** 15026-34.

GU, G. J., WU, D., LUND, H., SUNNEMARK, D., KVIST, A. J., MILNER, R., ECKERSLEY, S., NILSSON, L. N., AGERMAN, K., LANDEGREN, U. & KAMALI-MOGHADDAM, M. 2013. Elevated MARK2-dependent phosphorylation of Tau in Alzheimer's disease. *J Alzheimers Dis,* 33**,** 699-713.

GUNDELFINGER, E. D. & FEJTOVA, A. 2012. Molecular organization and plasticity of the cytomatrix at the active zone. *Curr Opin Neurobiol,* 22**,** 423-30.

HAFEZPARAST, M., KLOCKE, R., RUHRBERG, C., MARQUARDT, A., AHMAD-ANNUAR, A., BOWEN, S., LALLI, G., WITHERDEN, A. S., HUMMERICH, H., NICHOLSON, S., MORGAN, P. J., OOZAGEER, R., PRIESTLEY, J. V., AVERILL, S., KING, V. R., BALL, S., PETERS, J., TODA, T., YAMAMOTO, A., HIRAOKA, Y., AUGUSTIN, M., KORTHAUS, D., WATTLER, S., WABNITZ, P., DICKNEITE, C., LAMPEL, S., BOEHME, F., PERAUS, G., POPP, A., RUDELIUS, M., SCHLEGEL, J., FUCHS, H., HRABE DE ANGELIS, M., SCHIAVO, G., SHIMA, D. T., RUSS, A. P., STUMM, G., MARTIN, J. E. & FISHER, E. M. 2003. Mutations in dynein link motor neuron degeneration to defects in retrograde transport. *Science,* 300**,** 808-12.

HARRIS, K. P. & LITTLETON, J. T. 2015. Transmission, Development, and Plasticity of Synapses. *Genetics,* 201**,** 345-75.

HEBERT, L. E., WEUVE, J., SCHERR, P. A. & EVANS, D. A. 2013. Alzheimer disease in the United States (2010-2050) estimated using the 2010 census. *Neurology,* 80**,** 1778-83.

HENDERSON, M. X., CHUNG, C. H., RIDDLE, D. M., ZHANG, B., GATHAGAN, R. J., SEEHOLZER, S. H., TROJANOWSKI, J. Q. & LEE, V. M. Y. 2017. Unbiased proteomics of early Lewy body formation model implicates active microtubule affinity-regulating kinases (MARKs) in synucleinopathies. *J Neurosci*.

HERRUP, K. 2015. The case for rejecting the amyloid cascade hypothesis. *Nat Neurosci,* 18**,** 794-9.

HIDA, Y. & OHTSUKA, T. 2010. CAST and ELKS proteins: structural and functional determinants of the presynaptic active zone. *J Biochem,* 148**,** 131-7.

HIROKAWA, N., NODA, Y., TANAKA, Y. & NIWA, S. 2009. Kinesin superfamily motor proteins and intracellular transport. *Nat Rev Mol Cell Biol,* 10**,** 682-96.

HOLZBAUR, E. L. & SCHERER, S. S. 2011. Microtubules, axonal transport, and neuropathy. *N Engl J Med,* 365**,** 2330-2.

HU, V. W., SARACHANA, T., KIM, K. S., NGUYEN, A., KULKARNI, S., STEINBERG, M. E., LUU, T., LAI, Y. & LEE, N. H. 2009. Gene expression profiling differentiates autism case-controls and phenotypic variants of autism spectrum disorders: evidence for circadian rhythm dysfunction in severe autism. *Autism Res,* 2**,** 78-97.

HUCKABA, T. M., GENNERICH, A., WILHELM, J. E., CHISHTI, A. H. & VALE, R. D. 2011. Kinesin-73 is a processive motor that localizes to Rab5-containing organelles. *J Biol Chem,* 286**,** 7457-67.

HUMMEL, T., KRUKKERT, K., ROOS, J., DAVIS, G. & KLAMBT, C. 2000. Drosophila Futsch/22C10 is a MAP1B-like protein required for dendritic and axonal development. *Neuron,* 26**,** 357-70.

HUYNH, J. R., SHULMAN, J. M., BENTON, R. & ST JOHNSTON, D. 2001. PAR-1 is required for the maintenance of oocyte fate in Drosophila. *Development,* 128**,** 1201-9.

IIJIMA-ANDO, K., SEKIYA, M., MARUKO-OTAKE, A., OHTAKE, Y., SUZUKI, E., LU, B. & IIJIMA, K. M. 2012. Loss of axonal mitochondria promotes tau-mediated neurodegeneration and Alzheimer's disease-related tau phosphorylation via PAR-1. *PLoS Genet,* 8**,** e1002918.

ISHIHARA, T., HONG, M., ZHANG, B., NAKAGAWA, Y., LEE, M. K., TROJANOWSKI, J. Q. & LEE, V. M. 1999. Age-dependent emergence and progression of a tauopathy in transgenic mice overexpressing the shortest human tau isoform. *Neuron,* 24**,** 751-62.

JACKSON, J. S., WITTON, J., JOHNSON, J. D., AHMED, Z., WARD, M., RANDALL, A. D., HUTTON, M. L., ISAAC, J. T., O'NEILL, M. J. & ASHBY, M. C. 2017. Altered Synapse Stability in the Early Stages of Tauopathy. *Cell Rep,* 18**,** 3063-3068.

JALEEL, M., VILLA, F., DEAK, M., TOTH, R., PRESCOTT, A. R., VAN AALTEN, D. M. & ALESSI, D. R. 2006. The ubiquitin-associated domain of AMPK-related kinases regulates conformation and LKB1-mediated phosphorylation and activation. *Biochem J,* 394**,** 545-55.

JAN, L. Y. & JAN, Y. N. 1982. Antibodies to horseradish peroxidase as specific neuronal markers in Drosophila and in grasshopper embryos. *Proc Natl Acad Sci U S A,* 79**,** 2700-4.

KAESER, P. S., DENG, L., CHAVEZ, A. E., LIU, X., CASTILLO, P. E. & SUDHOF, T. C. 2009. ELKS2alpha/CAST deletion selectively increases neurotransmitter release at inhibitory synapses. *Neuron,* 64**,** 227-39.

KAUFMANN, N., DEPROTO, J., RANJAN, R., WAN, H. & VAN VACTOR, D. 2002. Drosophila liprin-alpha and the receptor phosphatase Dlar control synapse morphogenesis. *Neuron,* 34**,** 27-38.

KAWASAKI, F., IYER, J., POSEY, L. L., SUN, C. E., MAMMEN, S. E., YAN, H. & ORDWAY, R. W. 2011. The DISABLED protein functions in CLATHRIN-mediated synaptic vesicle endocytosis and exoendocytic coupling at the active zone. *Proc Natl Acad Sci U S A,* 108**,** E222-9.

KAWASAKI, F., ZOU, B., XU, X. & ORDWAY, R. W. 2004. Active zone localization of presynaptic calcium channels encoded by the cacophony locus of Drosophila. *J Neurosci,* 24**,** 282-5.

KEMPHUES, K. J., PRIESS, J. R., MORTON, D. G. & CHENG, N. S. 1988. Identification of genes required for cytoplasmic localization in early C. elegans embryos. *Cell,* 52**,** 311-20.

KESHISHIAN, H., BROADIE, K., CHIBA, A. & BATE, M. 1996. The drosophila neuromuscular junction: a model system for studying synaptic development and function. *Annu Rev Neurosci,* 19**,** 545-75.

KITTEL, R. J., WICHMANN, C., RASSE, T. M., FOUQUET, W., SCHMIDT, M., SCHMID, A., WAGH, D. A., PAWLU, C., KELLNER, R. R., WILLIG, K. I., HELL, S. W., BUCHNER, E., HECKMANN, M. & SIGRIST, S. J. 2006. Bruchpilot promotes active zone assembly, Ca2+ channel clustering, and vesicle release. *Science,* 312**,** 1051-4.

KLASSEN, M. P., WU, Y. E., MAEDER, C. I., NAKAE, I., CUEVA, J. G., LEHRMAN, E. K., TADA, M., GENGYO-ANDO, K., WANG, G. J., GOODMAN, M., MITANI, S., KONTANI, K., KATADA, T. & SHEN, K. 2010. An Arf-like small G protein, ARL-8, promotes the axonal transport of presynaptic cargoes by suppressing vesicle aggregation. *Neuron,* 66**,** 710-23.

KLEIN, W. L. 2002. Abeta toxicity in Alzheimer's disease: globular oligomers (ADDLs) as new vaccine and drug targets. *Neurochem Int,* 41**,** 345-52.

LAZAREVIC, V., SCHONE, C., HEINE, M., GUNDELFINGER, E. D. & FEJTOVA, A. 2011. Extensive remodeling of the presynaptic cytomatrix upon homeostatic adaptation to network activity silencing. *J Neurosci,* 31**,** 10189-200.

LAZAROV, O., MORFINI, G. A., PIGINO, G., GADADHAR, A., CHEN, X., ROBINSON, J., HO, H., BRADY, S. T. & SISODIA, S. S. 2007. Impairments in fast axonal transport and motor neuron deficits in transgenic mice expressing familial Alzheimer's disease-linked mutant presenilin 1. *J Neurosci,* 27**,** 7011-20.

LEE, S., WANG, J. W., YU, W. & LU, B. 2012. Phospho-dependent ubiquitination and degradation of PAR-1 regulates synaptic morphology and tau-mediated Abeta toxicity in Drosophila. *Nat Commun,* 3**,** 1312.

LEPICARD, S., FRANCO, B., DE BOCK, F. & PARMENTIER, M. L. 2014. A presynaptic role of microtubule-associated protein 1/Futsch in Drosophila: regulation of active zone number and neurotransmitter release. *J Neurosci,* 34**,** 6759-71.

LI, H. P., LIU, Z. M. & NIRENBERG, M. 1997. Kinesin-73 in the nervous system of Drosophila embryos. *Proc Natl Acad Sci U S A,* 94**,** 1086-91.

LI, L., BISCHOFBERGER, J. & JONAS, P. 2007. Differential gating and recruitment of P/Q-, N-, and R-type Ca2+ channels in hippocampal mossy fiber boutons. *J Neurosci,* 27**,** 13420-9.

LI, S., HONG, S., SHEPARDSON, N. E., WALSH, D. M., SHANKAR, G. M. & SELKOE, D. 2009. Soluble oligomers of amyloid Beta protein facilitate hippocampal long-term depression by disrupting neuronal glutamate uptake. *Neuron,* 62**,** 788-801.

LIN, Y. C. & KOLESKE, A. J. 2010. Mechanisms of synapse and dendrite maintenance and their disruption in psychiatric and neurodegenerative disorders. *Annu Rev Neurosci,* 33**,** 349-78.

LIU, Z., GAN, L., CHEN, Y., LUO, D., ZHANG, Z., CAO, W., ZHOU, Z., LIN, X. & SUN, C. 2016. Mark4 promotes oxidative stress and inflammation via binding to PPARgamma and activating NF-kappaB pathway in mice adipocytes. *Sci Rep,* 6**,** 21382.

LUND, H., GUSTAFSSON, E., SVENSSON, A., NILSSON, M., BERG, M., SUNNEMARK, D. & VON EULER, G. 2014. MARK4 and MARK3 associate with early tau phosphorylation in Alzheimer's disease granulovacuolar degeneration bodies. *Acta Neuropathol Commun,* 2**,** 22.

MADAY, S., TWELVETREES, A. E., MOUGHAMIAN, A. J. & HOLZBAUR, E. L. 2014. Axonal transport: cargo-specific mechanisms of motility and regulation. *Neuron,* 84**,** 292-309.

MAGLIONE, M. & SIGRIST, S. J. 2013. Seeing the forest tree by tree: super-resolution light microscopy meets the neurosciences. *Nat Neurosci,* 16**,** 790-7.

MAJID, T., ALI, Y. O., VENKITARAMANI, D. V., JANG, M. K., LU, H. C. & PAUTLER, R. G. 2014. In vivo axonal transport deficits in a mouse model of fronto-temporal dementia. *Neuroimage Clin,* 4**,** 711-7.

MANDELKOW, E. M., THIES, E., TRINCZEK, B., BIERNAT, J. & MANDELKOW, E. 2004. MARK/PAR1 kinase is a regulator of microtubule-dependent transport in axons. *J Cell Biol,* 167**,** 99-110.

MARRUS, S. B., PORTMAN, S. L., ALLEN, M. J., MOFFAT, K. G. & DIANTONIO, A. 2004. Differential localization of glutamate receptor subunits at the Drosophila neuromuscular junction. *J Neurosci,* 24**,** 1406-15.

MARX, A., NUGOOR, C., PANNEERSELVAM, S. & MANDELKOW, E. 2010. Structure and function of polarity-inducing kinase family MARK/Par-1 within the branch of AMPK/Snf1-related kinases. *FASEB J,* 24**,** 1637-48.

MATENIA, D. & MANDELKOW, E. M. 2009. The tau of MARK: a polarized view of the cytoskeleton. *Trends Biochem Sci,* 34**,** 332-42.

MATKOVIC, T., SIEBERT, M., KNOCHE, E., DEPNER, H., MERTEL, S., OWALD, D., SCHMIDT, M., THOMAS, U., SICKMANN, A., KAMIN, D., HELL, S. W., BURGER, J., HOLLMANN, C., MIELKE, T., WICHMANN, C. & SIGRIST, S. J. 2013. The Bruchpilot cytomatrix determines the size of the readily releasable pool of synaptic vesicles. *J Cell Biol,* 202**,** 667-83.

MAUSSION, G., CARAYOL, J., LEPAGNOL-BESTEL, A. M., TORES, F., LOE-MIE, Y., MILBRETA, U., ROUSSEAU, F., FONTAINE, K., RENAUD, J., MOALIC, J. M., PHILIPPI, A., CHEDOTAL, A., GORWOOD, P., RAMOZ, N., HAGER, J. & SIMONNEAU, M. 2008. Convergent evidence identifying MAP/microtubule affinity-regulating kinase 1 (MARK1) as a susceptibility gene for autism. *Hum Mol Genet,* 17**,** 2541-51.

MCDONALD, J. A. 2014. Canonical and noncanonical roles of Par-1/MARK kinases in cell migration. *Int Rev Cell Mol Biol,* 312**,** 169-99.

MILDE, S., ADALBERT, R., ELAMAN, M. H. & COLEMAN, M. P. 2015. Axonal transport declines with age in two distinct phases separated by a period of relative stability. *Neurobiol Aging,* 36**,** 971-81.

MILLECAMPS, S. & JULIEN, J. P. 2013. Axonal transport deficits and neurodegenerative diseases. *Nat Rev Neurosci,* 14**,** 161-76.

MISKIEWICZ, K., JOSE, L. E., BENTO-ABREU, A., FISLAGE, M., TAES, I., KASPROWICZ, J., SWERTS, J., SIGRIST, S., VERSEES, W., ROBBERECHT, W. & VERSTREKEN, P. 2011. ELP3 controls active zone morphology by acetylating the ELKS family member Bruchpilot. *Neuron,* 72**,** 776-88.

MORFINI, G. A., BURNS, M., BINDER, L. I., KANAAN, N. M., LAPOINTE, N., BOSCO, D. A., BROWN, R. H., JR., BROWN, H., TIWARI, A., HAYWARD, L., EDGAR, J., NAVE, K. A., GARBERRN, J., ATAGI, Y., SONG, Y., PIGINO, G. & BRADY, S. T. 2009. Axonal transport defects in neurodegenerative diseases. *J Neurosci,* 29**,** 12776-86.

MOSTANY, R., ANSTEY, J. E., CRUMP, K. L., MACO, B., KNOTT, G. & PORTERA-CAILLIAU, C. 2013. Altered synaptic dynamics during normal brain aging. *J Neurosci,* 33**,** 4094-104.

MULLEN, R. J., BUCK, C. R. & SMITH, A. M. 1992. NeuN, a neuronal specific nuclear protein in vertebrates. *Development,* 116**,** 201-11.

MURPHY, J. M., KORZHNEV, D. M., CECCARELLI, D. F., BRIANT, D. J., ZARRINE-AFSAR, A., SICHERI, F., KAY, L. E. & PAWSON, T. 2007. Conformational instability of the MARK3 UBA domain compromises ubiquitin recognition and promotes interaction with the adjacent kinase domain. *Proc Natl Acad Sci U S A,* 104**,** 14336-41.

NAKATA, T., KITAMURA, Y., SHIMIZU, K., TANAKA, S., FUJIMORI, M., YOKOYAMA, S., ITO, K. & EMI, M. 1999. Fusion of a novel gene, ELKS, to RET due to translocation t(10;12)(q11;p13) in a papillary thyroid carcinoma. *Genes Chromosomes Cancer,* 25**,** 97-103.

NATARAJAN, R., TRIVEDI-VYAS, D. & WAIRKAR, Y. P. 2013. Tuberous sclerosis complex regulates Drosophila neuromuscular junction growth via the TORC2/Akt pathway. *Hum Mol Genet,* 22**,** 2010-23.

NIRSCHL, J. J., GHIRETTI, A. E. & HOLZBAUR, E. L. F. 2017. The impact of cytoskeletal organization on the local regulation of neuronal transport. *Nat Rev Neurosci,* 18**,** 585-597.

NISHIMURA, I., YANG, Y. & LU, B. 2004. PAR-1 kinase plays an initiator role in a temporally ordered phosphorylation process that confers tau toxicity in Drosophila. *Cell,* 116**,** 671-82.

OKADA, Y., YAMAZAKI, H., SEKINE-AIZAWA, Y. & HIROKAWA, N. 1995. The neuron-specific kinesin superfamily protein KIF1A is a unique monomeric motor for anterograde axonal transport of synaptic vesicle precursors. *Cell,* 81**,** 769-80.

OSSIPOVA, O., EZAN, J. & SOKOL, S. Y. 2009. PAR-1 phosphorylates Mind bomb to promote vertebrate neurogenesis. *Dev Cell,* 17**,** 222-33.

OSTERWALDER, T., YOON, K. S., WHITE, B. H. & KESHISHIAN, H. 2001. A conditional tissue-specific transgene expression system using inducible GAL4. *Proc Natl Acad Sci U S A,* 98**,** 12596-601.

PACK-CHUNG, E., KURSHAN, P. T., DICKMAN, D. K. & SCHWARZ, T. L. 2007. A Drosophila kinesin required for synaptic bouton formation and synaptic vesicle transport. *Nat Neurosci,* 10**,** 980-9.

PALOP, J. J. & MUCKE, L. 2010a. Amyloid-beta-induced neuronal dysfunction in Alzheimer's disease: from synapses toward neural networks. *Nat Neurosci,* 13**,** 812-8.

PALOP, J. J. & MUCKE, L. 2010b. Synaptic depression and aberrant excitatory network activity in Alzheimer's disease: two faces of the same coin? *Neuromolecular Med,* 12**,** 48-55.

PALOP, J. J. & MUCKE, L. 2016. Network abnormalities and interneuron dysfunction in Alzheimer disease. *Nat Rev Neurosci,* 17**,** 777-792.

PANNEERSELVAM, S., MARX, A., MANDELKOW, E. M. & MANDELKOW, E. 2006. Structure of the catalytic and ubiquitin-associated domains of the protein kinase MARK/Par-1. *Structure,* 14**,** 173-83.

PAULI, A., ALTHOFF, F., OLIVEIRA, R. A., HEIDMANN, S., SCHULDINER, O., LEHNER, C. F., DICKSON, B. J. & NASMYTH, K. 2008. Cell-type-specific TEV protease cleavage reveals cohesin functions in Drosophila neurons. *Dev Cell,* 14**,** 239-51.

PERRY, S., HAN, Y., DAS, A. & DICKMAN, D. 2017. Homeostatic plasticity can be induced and expressed to restore synaptic strength at neuromuscular junctions undergoing ALS-related degeneration. *Hum Mol Genet*.

PETERSEN, S. A., FETTER, R. D., NOORDERMEER, J. N., GOODMAN, C. S. & DIANTONIO, A. 1997. Genetic analysis of glutamate receptors in Drosophila reveals a retrograde signal regulating presynaptic transmitter release. *Neuron,* 19**,** 1237-48.

PIGINO, G., MORFINI, G., PELSMAN, A., MATTSON, M. P., BRADY, S. T. & BUSCIGLIO, J. 2003. Alzheimer's presenilin 1 mutations impair kinesin-based axonal transport. *J Neurosci,* 23**,** 4499-508.

PILLING, A. D., HORIUCHI, D., LIVELY, C. M. & SAXTON, W. M. 2006. Kinesin-1 and Dynein are the primary motors for fast transport of mitochondria in Drosophila motor axons. *Mol Biol Cell,* 17**,** 2057-68.

PULS, I., JONNAKUTY, C., LAMONTE, B. H., HOLZBAUR, E. L., TOKITO, M., MANN, E., FLOETER, M. K., BIDUS, K., DRAYNA, D., OH, S. J., BROWN, R. H., JR., LUDLOW, C. L. & FISCHBECK, K. H. 2003. Mutant dynactin in motor neuron disease. *Nat Genet,* 33**,** 455-6.

PURRO, S. A., GALLI, S. & SALINAS, P. C. 2014. Dysfunction of Wnt signaling and synaptic disassembly in neurodegenerative diseases. *J Mol Cell Biol,* 6**,** 75-80.

ROSELLI, F., TIRARD, M., LU, J., HUTZLER, P., LAMBERTI, P., LIVREA, P., MORABITO, M. & ALMEIDA, O. F. 2005. Soluble beta-amyloid1-40 induces NMDA-dependent degradation of postsynaptic density-95 at glutamatergic synapses. *J Neurosci,* 25**,** 11061-70.

RUSSO, G. J., LOUIE, K., WELLINGTON, A., MACLEOD, G. T., HU, F., PANCHUMARTHI, S. & ZINSMAIER, K. E. 2009. Drosophila Miro is required

for both anterograde and retrograde axonal mitochondrial transport. *J Neurosci,* 29**,** 5443-55.

SAXTON, W. M. 2001. Microtubules, motors, and mRNA localization mechanisms: watching fluorescent messages move. *Cell,* 107**,** 707-10.

SAXTON, W. M. & HOLLENBECK, P. J. 2012. The axonal transport of mitochondria. *J Cell Sci,* 125**,** 2095-104.

SCHEFF, S. W., DEKOSKY, S. T. & PRICE, D. A. 1990. Quantitative assessment of cortical synaptic density in Alzheimer's disease. *Neurobiol Aging,* 11**,** 29-37.

SCHEFF, S. W., PRICE, D. A., SCHMITT, F. A., ROBERTS, K. N., IKONOMOVIC, M. D. & MUFSON, E. J. 2013. Synapse stability in the precuneus early in the progression of Alzheimer's disease. *J Alzheimers Dis,* 35**,** 599-609.

SCHINDELIN, J., ARGANDA-CARRERAS, I., FRISE, E., KAYNIG, V., LONGAIR, M., PIETZSCH, T., PREIBISCH, S., RUEDEN, C., SAALFELD, S., SCHMID, B., TINEVEZ, J. Y., WHITE, D. J., HARTENSTEIN, V., ELICEIRI, K., TOMANCAK, P. & CARDONA, A. 2012. Fiji: an open-source platform for biological-image analysis. *Nat Methods,* 9**,** 676-82.

SCHLAGER, M. A. & HOOGENRAAD, C. C. 2009. Basic mechanisms for recognition and transport of synaptic cargos. *Mol Brain,* 2**,** 25.

SELKOE, D. J. 2002. Alzheimer's disease is a synaptic failure. *Science,* 298**,** 789-91.

SERRANO-POZO, A., FROSCH, M. P., MASLIAH, E. & HYMAN, B. T. 2011. Neuropathological alterations in Alzheimer disease. *Cold Spring Harb Perspect Med,* 1**,** a006189.

SESHADRI, S., FITZPATRICK, A. L., IKRAM, M. A., DESTEFANO, A. L., GUDNASON, V., BOADA, M., BIS, J. C., SMITH, A. V., CARASSQUILLO, M. M., LAMBERT, J. C., HAROLD, D., SCHRIJVERS, E. M., RAMIREZ-LORCA, R., DEBETTE, S., LONGSTRETH, W. T., JR., JANSSENS, A. C., PANKRATZ, V. S., DARTIGUES, J. F., HOLLINGWORTH, P., ASPELUND, T., HERNANDEZ, I., BEISER, A., KULLER, L. H., KOUDSTAAL, P. J., DICKSON, D. W., TZOURIO, C., ABRAHAM, R., ANTUNEZ, C., DU, Y., ROTTER, J. I., AULCHENKO, Y. S., HARRIS, T. B., PETERSEN, R. C., BERR, C., OWEN, M. J., LOPEZ-ARRIETA, J., VARADARAJAN, B. N., BECKER, J. T., RIVADENEIRA, F., NALLS, M. A., GRAFF-RADFORD, N. R., CAMPION, D., AUERBACH, S., RICE, K., HOFMAN, A., JONSSON, P. V., SCHMIDT, H., LATHROP, M., MOSLEY, T. H., AU, R., PSATY, B. M., UITTERLINDEN, A. G., FARRER, L. A., LUMLEY, T., RUIZ, A., WILLIAMS, J., AMOUYEL, P., YOUNKIN, S. G., WOLF, P. A., LAUNER, L. J., LOPEZ, O. L., VAN DUIJN, C. M. & BRETELER, M. M. 2010. Genome-

wide analysis of genetic loci associated with Alzheimer disease. *JAMA,* 303**,** 1832-40.

SHAHIDULLAH, M., LE MARCHAND, S. J., FEI, H., ZHANG, J., PANDEY, U. B., DALVA, M. B., PASINELLI, P. & LEVITAN, I. B. 2013. Defects in synapse structure and function precede motor neuron degeneration in Drosophila models of FUS-related ALS. *J Neurosci,* 33**,** 19590-8.

SHAPIRA, M., ZHAI, R. G., DRESBACH, T., BRESLER, T., TORRES, V. I., GUNDELFINGER, E. D., ZIV, N. E. & GARNER, C. C. 2003. Unitary assembly of presynaptic active zones from Piccolo-Bassoon transport vesicles. *Neuron,* 38**,** 237-52.

SHARMA, M., BURRE, J., BRONK, P., ZHANG, Y., XU, W. & SUDHOF, T. C. 2012. CSPalpha knockout causes neurodegeneration by impairing SNAP-25 function. *EMBO J,* 31**,** 829-41.

SHEPHERD, G. M. & KATZ, D. M. 2011. Synaptic microcircuit dysfunction in genetic models of neurodevelopmental disorders: focus on Mecp2 and Met. *Curr Opin Neurobiol,* 21**,** 827-33.

SHULMAN, J. M., BENTON, R. & ST JOHNSTON, D. 2000. The Drosophila homolog of C. elegans PAR-1 organizes the oocyte cytoskeleton and directs oskar mRNA localization to the posterior pole. *Cell,* 101**,** 377-88.

SIEBERT, M., BOHME, M. A., DRILLER, J. H., BABIKIR, H., MAMPELL, M. M., REY, U., RAMESH, N., MATKOVIC, T., HOLTON, N., REDDY-ALLA, S., GOTTFERT, F., KAMIN, D., QUENTIN, C., KLINEDINST, S., ANDLAUER, T. F., HELL, S. W., COLLINS, C. A., WAHL, M. C., LOLL, B. & SIGRIST, S. J. 2015. A high affinity RIM-binding protein/Aplip1 interaction prevents the formation of ectopic axonal active zones. *Elife,* 4.

SKWAREK, L. C., WINDLER, S. L., DE VREEDE, G., ROGERS, G. C. & BILDER, D. 2014. The F-box protein Slmb restricts the activity of aPKC to polarize epithelial cells. *Development,* 141**,** 2978-83.

SMALL, D. H. 2004. Mechanisms of synaptic homeostasis in Alzheimer's disease. *Curr Alzheimer Res,* 1**,** 27-32.

SNYDER, E. M., NONG, Y., ALMEIDA, C. G., PAUL, S., MORAN, T., CHOI, E. Y., NAIRN, A. C., SALTER, M. W., LOMBROSO, P. J., GOURAS, G. K. & GREENGARD, P. 2005. Regulation of NMDA receptor trafficking by amyloid-beta. *Nat Neurosci,* 8**,** 1051-8.

SODERBERG, O., GULLBERG, M., JARVIUS, M., RIDDERSTRALE, K., LEUCHOWIUS, K. J., JARVIUS, J., WESTER, K., HYDBRING, P., BAHRAM, F., LARSSON, L. G. & LANDEGREN, U. 2006. Direct observation of individual

endogenous protein complexes in situ by proximity ligation. *Nat Methods,* 3**,** 995-1000.

SPIRES-JONES, T. L. & HYMAN, B. T. 2014. The intersection of amyloid beta and tau at synapses in Alzheimer's disease. *Neuron,* 82**,** 756-71.

STANLEY, E. F. 1997. The calcium channel and the organization of the presynaptic transmitter release face. *Trends Neurosci,* 20**,** 404-9.

STEWART, B. A., ATWOOD, H. L., RENGER, J. J., WANG, J. & WU, C. F. 1994. Improved stability of Drosophila larval neuromuscular preparations in haemolymph-like physiological solutions. *J Comp Physiol A,* 175**,** 179-91.

STIGLOHER, C., ZHAN, H., ZHEN, M., RICHMOND, J. & BESSEREAU, J. L. 2011. The presynaptic dense projection of the Caenorhabditis elegans cholinergic neuromuscular junction localizes synaptic vesicles at the active zone through SYD-2/liprin and UNC-10/RIM-dependent interactions. *J Neurosci,* 31**,** 4388-96.

STOKIN, G. B. & GOLDSTEIN, L. S. 2006. Axonal transport and Alzheimer's disease. *Annu Rev Biochem,* 75**,** 607-27.

STOKIN, G. B., LILLO, C., FALZONE, T. L., BRUSCH, R. G., ROCKENSTEIN, E., MOUNT, S. L., RAMAN, R., DAVIES, P., MASLIAH, E., WILLIAMS, D. S. & GOLDSTEIN, L. S. 2005. Axonopathy and transport deficits early in the pathogenesis of Alzheimer's disease. *Science,* 307**,** 1282-8.

STOWERS, R. S., MEGEATH, L. J., GORSKA-ANDRZEJAK, J., MEINERTZHAGEN, I. A. & SCHWARZ, T. L. 2002. Axonal transport of mitochondria to synapses depends on milton, a novel Drosophila protein. *Neuron,* 36**,** 1063-77.

SUDHOF, T. C. 2004. The synaptic vesicle cycle. *Annu Rev Neurosci,* 27**,** 509-47.

SUDHOF, T. C. 2012. The presynaptic active zone. *Neuron,* 75**,** 11-25.

TABLER, J. M., YAMANAKA, H. & GREEN, J. B. 2010. PAR-1 promotes primary neurogenesis and asymmetric cell divisions via control of spindle orientation. *Development,* 137**,** 2501-5.

TAI, H. C., SERRANO-POZO, A., HASHIMOTO, T., FROSCH, M. P., SPIRES-JONES, T. L. & HYMAN, B. T. 2012. The synaptic accumulation of hyperphosphorylated tau oligomers in Alzheimer disease is associated with dysfunction of the ubiquitin-proteasome system. *Am J Pathol,* 181**,** 1426-35.

TANG, Y., SCOTT, D. A., DAS, U., EDLAND, S. D., RADOMSKI, K., KOO, E. H. & ROY, S. 2012. Early and selective impairments in axonal transport kinetics of synaptic cargoes induced by soluble amyloid beta-protein oligomers. *Traffic,* 13**,** 681-93.

TARU, H. & JIN, Y. 2011. The Liprin homology domain is essential for the homomeric interaction of SYD-2/Liprin-alpha protein in presynaptic assembly. *J Neurosci,* 31**,** 16261-8.

TERRY, R. D., MASLIAH, E., SALMON, D. P., BUTTERS, N., DETERESA, R., HILL, R., HANSEN, L. A. & KATZMAN, R. 1991. Physical basis of cognitive alterations in Alzheimer's disease: synapse loss is the major correlate of cognitive impairment. *Ann Neurol,* 30**,** 572-80.

TESSIER, C. R. & BROADIE, K. 2009. Activity-dependent modulation of neural circuit synaptic connectivity. *Front Mol Neurosci,* 2**,** 8.

TIMM, T., MARX, A., PANNEERSELVAM, S., MANDELKOW, E. & MANDELKOW, E. M. 2008. Structure and regulation of MARK, a kinase involved in abnormal phosphorylation of Tau protein. *BMC Neurosci,* 9 Suppl 2**,** S9.

TOM DIECK, S., SANMARTI-VILA, L., LANGNAESE, K., RICHTER, K., KINDLER, S., SOYKE, A., WEX, H., SMALLA, K. H., KAMPF, U., FRANZER, J. T., STUMM, M., GARNER, C. C. & GUNDELFINGER, E. D. 1998. Bassoon, a novel zinc-finger CAG/glutamine-repeat protein selectively localized at the active zone of presynaptic nerve terminals. *J Cell Biol,* 142**,** 499-509.

TRINCZEK, B., BRAJENOVIC, M., EBNETH, A. & DREWES, G. 2004. MARK4 is a novel microtubule-associated proteins/microtubule affinity-regulating kinase that binds to the cellular microtubule network and to centrosomes. *J Biol Chem,* 279**,** 5915-23.

UCHIDA, N., HONJO, Y., JOHNSON, K. R., WHEELOCK, M. J. & TAKEICHI, M. 1996. The catenin/cadherin adhesion system is localized in synaptic junctions bordering transmitter release zones. *J Cell Biol,* 135**,** 767-79.

VAN SPRONSEN, M. & HOOGENRAAD, C. C. 2010. Synapse pathology in psychiatric and neurologic disease. *Curr Neurol Neurosci Rep,* 10**,** 207-14.

VAN VACTOR, D. & SIGRIST, S. J. 2017. Presynaptic morphogenesis, active zone organization and structural plasticity in Drosophila. *Curr Opin Neurobiol,* 43**,** 119-129.

WAGH, D. A., RASSE, T. M., ASAN, E., HOFBAUER, A., SCHWENKERT, I., DURRBECK, H., BUCHNER, S., DABAUVALLE, M. C., SCHMIDT, M., QIN, G., WICHMANN, C., KITTEL, R., SIGRIST, S. J. & BUCHNER, E. 2006. Bruchpilot, a protein with homology to ELKS/CAST, is required for structural integrity and function of synaptic active zones in Drosophila. *Neuron,* 49**,** 833-44.

WAIRKAR, Y. P., TODA, H., MOCHIZUKI, H., FURUKUBO-TOKUNAGA, K., TOMODA, T. & DIANTONIO, A. 2009. Unc-51 controls active zone density and protein composition by downregulating ERK signaling. *J Neurosci,* 29**,** 517-28.

WAIRKAR, Y. P., TRIVEDI, D., NATARAJAN, R., BARNES, K., DOLORES, L. & CHO, P. 2013. CK2alpha regulates the transcription of BRP in Drosophila. *Dev Biol,* 384**,** 53-64.

WANG, J. W., IMAI, Y. & LU, B. 2007. Activation of PAR-1 kinase and stimulation of tau phosphorylation by diverse signals require the tumor suppressor protein LKB1. *J Neurosci,* 27**,** 574-81.

WANG, S., YOO, S., KIM, H. Y., WANG, M., ZHENG, C., PARKHOUSE, W., KRIEGER, C. & HARDEN, N. 2015. Detection of in situ protein-protein complexes at the Drosophila larval neuromuscular junction using proximity ligation assay. *J Vis Exp***,** 52139.

WANG, X., KIBSCHULL, M., LAUE, M. M., LICHTE, B., PETRASCH-PARWEZ, E. & KILIMANN, M. W. 1999. Aczonin, a 550-kD putative scaffolding protein of presynaptic active zones, shares homology regions with Rim and Bassoon and binds profilin. *J Cell Biol,* 147**,** 151-62.

WANG, Y., LIU, X., BIEDERER, T. & SUDHOF, T. C. 2002. A family of RIM-binding proteins regulated by alternative splicing: Implications for the genesis of synaptic active zones. *Proc Natl Acad Sci U S A,* 99**,** 14464-9.

WANG, Y., OKAMOTO, M., SCHMITZ, F., HOFMANN, K. & SUDHOF, T. C. 1997. Rim is a putative Rab3 effector in regulating synaptic-vesicle fusion. *Nature,* 388**,** 593-8.

WEYHERSMULLER, A., HALLERMANN, S., WAGNER, N. & EILERS, J. 2011. Rapid active zone remodeling during synaptic plasticity. *J Neurosci,* 31**,** 6041-52.

WICHMANN, C. & SIGRIST, S. J. 2010. The active zone T-bar--a plasticity module? *J Neurogenet,* 24**,** 133-45.

WILSON, R. S., LEURGANS, S. E., BOYLE, P. A. & BENNETT, D. A. 2011. Cognitive decline in prodromal Alzheimer disease and mild cognitive impairment. *Arch Neurol,* 68**,** 351-6.

WOLF, N., REGAN, C. L. & FULLER, M. T. 1988. Temporal and spatial pattern of differences in microtubule behaviour during Drosophila embryogenesis revealed by distribution of a tubulin isoform. *Development,* 102**,** 311-24.

WU, Y. & GRIFFIN, E. E. 2017. Regulation of Cell Polarity by PAR-1/MARK Kinase. *Curr Top Dev Biol,* 123**,** 365-397.

YAO, K. M. & WHITE, K. 1994. Neural specificity of elav expression: defining a Drosophila promoter for directing expression to the nervous system. *J Neurochem,* 63**,** 41-51.

YOSHIMURA, Y., TERABAYASHI, T. & MIKI, H. 2010. Par1b/MARK2 phosphorylates kinesin-like motor protein GAKIN/KIF13B to regulate axon formation. *Mol Cell Biol,* 30**,** 2206-19.

YOSHIYAMA, Y., HIGUCHI, M., ZHANG, B., HUANG, S. M., IWATA, N., SAIDO, T. C., MAEDA, J., SUHARA, T., TROJANOWSKI, J. Q. & LEE, V. M. 2007. Synapse loss and microglial activation precede tangles in a P301S tauopathy mouse model. *Neuron,* 53**,** 337-51.

YU, W., POLEPALLI, J., WAGH, D., RAJADAS, J., MALENKA, R. & LU, B. 2012. A critical role for the PAR-1/MARK-tau axis in mediating the toxic effects of Abeta on synapses and dendritic spines. *Hum Mol Genet,* 21**,** 1384-90.

ZHAI, R. G. & BELLEN, H. J. 2004. The architecture of the active zone in the presynaptic nerve terminal. *Physiology (Bethesda),* 19**,** 262-70.

ZHAI, R. G., VARDINON-FRIEDMAN, H., CASES-LANGHOFF, C., BECKER, B., GUNDELFINGER, E. D., ZIV, N. E. & GARNER, C. C. 2001. Assembling the presynaptic active zone: a characterization of an active one precursor vesicle. *Neuron,* 29**,** 131-43.

ZHANG, B., HIGUCHI, M., YOSHIYAMA, Y., ISHIHARA, T., FORMAN, M. S., MARTINEZ, D., JOYCE, S., TROJANOWSKI, J. Q. & LEE, V. M. 2004. Retarded axonal transport of R406W mutant tau in transgenic mice with a neurodegenerative tauopathy. *J Neurosci,* 24**,** 4657-67.

ZHANG, Y., GUO, H., KWAN, H., WANG, J. W., KOSEK, J. & LU, B. 2007. PAR-1 kinase phosphorylates Dlg and regulates its postsynaptic targeting at the Drosophila neuromuscular junction. *Neuron,* 53**,** 201-15.

ZHANG, Y. Q., BAILEY, A. M., MATTHIES, H. J., RENDEN, R. B., SMITH, M. A., SPEESE, S. D., RUBIN, G. M. & BROADIE, K. 2001. Drosophila fragile X-related gene regulates the MAP1B homolog Futsch to control synaptic structure and function. *Cell,* 107**,** 591-603.

ZHEN, M. & JIN, Y. 1999. The liprin protein SYD-2 regulates the differentiation of presynaptic termini in C. elegans. *Nature,* 401**,** 371-5.

ZOGHBI, H. Y. & BEAR, M. F. 2012. Synaptic dysfunction in neurodevelopmental disorders associated with autism and intellectual disabilities. *Cold Spring Harb Perspect Biol,* 4.

Vita

Kara Rachelle Barber was born December 11, 1985, in Oklahoma City, OK. She is the daughter of Kevin Wayne Barber and Karen Elaine Seeberger. At the age of four, her family relocated from Oklahoma City, OK to Kansas City, MO and she would complete high school at Blue Ridge Christian School in Kansas City, MO in 2004. She then attended college at Drury University in Springfield, MO from 2004-2007. Due to hardships she had to leave Drury University and transferred to West Texas A&M University (WTAMU) in Canyon, TX from 2012-2014. She finally earned her Bachelor of Science degree in Biology with a certificate in Neuroscience from WTAMU in May 2014. In August of 2014, she joined the Neuroscience Graduate Program at the University of Texas Medical Branch (UTMB) in Galveston, TX. At UTMB, she joined the laboratory of Dr. Yogesh Wairkar in January of 2015. Her final oral defense and examination commenced August 24, 2018.

Permanent address: Kara R. Barber
3750 E Via Palomita Apt 18202
Tucson, AZ 85718-3360

This dissertation was typed by Kara Rachelle Barber between July and August 2018.